

---

# SLOW EXTRACTION FROM SYNCHROTRONS FOR CANCER THERAPY

*Informal Meeting held*

*February 13th and 14th 1996*

*PS, CERN*

This meeting was organised within the framework of the TERA and AUSTRON medical studies. The ultimate aim of these studies is to design a dual-species synchrotron (protons and light ions) for cancer therapy treatment and research.

The slides collected in this volume were produced quickly to ensure a full circulation of information. Consequently, it has not been possible for the authors to provide the same degree of rigour in checking that a full publication would receive. Since these notes do not constitute a publication please consider them as confidential.

The talks entitled *Simple theory of slow extraction from a synchrotron, Hardt condition for superposition of separatrices, Achromatic transfer from electrostatic septum to magnetic septum, Emittance of the slow-extracted beam, General transverse strategy, Lattice considerations and Feasibility of a phase-displacement acceleration system and a micro-bucket transfer system for 'feeding' the resonance* were the products of much discussion and common effort between the members of the TERA and AUSTRON groups. The deeper thought in the Hardt Condition and the lattice is thanks to M. Benedikt.

The TERA and AUSTRON teams would like to thank the invited speakers who contributed their special expertise and knowledge to this information meeting.

P.J. Bryant.

---

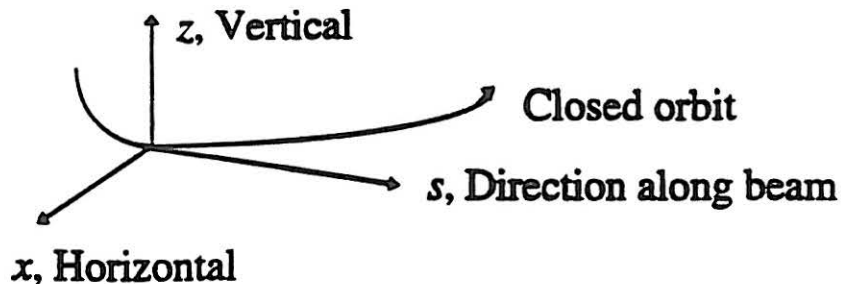
---

## BIBLIOGRAPHY

- P. Strolin, *Third order resonance slow extraction from alternating gradient synchrotrons*, ISR/TH/66-40, (1966).
  - M. Barton, *Beam extraction from synchrotrons*, Proc. VIII th Int. Conf. on High Energy Accelerators, CERN, Geneva, (1971), p85-87.
  - R. Cappi, C. Steinbach, *Improvement of the low frequency duty factor of slow extraction by rf phase displacement*, CERN/PS/OP 80-10, (1980).
  - W. Hardt, *Ultraslow extraction out of LEAR*, PS/DL/LEAR Note 81-6, (1981).
  - C. Steinbach, H. Stucki, M Thivent, *The new slow extraction system of the CERN PS*, CERN/PS 93-28 (OP).
  - C. Steinbach, *Beam optics at resonant extraction septa*, CERN/PS 92-22 (OP).
  - M. Gyr, *Low frequency fluctuations of spill rates during slow resonant extraction*, CERN SPS/89-21 (ABT), (1989).
  - G. Cesari, P. Lefèvre, D. Vandeplassche, *Feasibility study of a synchrotron for the European light-ion medical accelerator*, CERN/PS/91-08(DI) (1991).
  - C. Wuzhong, *Design of a light ion medical synchrotron*, GSI Report 92-24 (1992).
  - P. Bryant, M. Regler, M. Schuster eds, *The AUSTRON Feasibility Study*, Technische Universität, Wien,(1994).
  - U. Amaldi, M. Silari eds, *The TERA project and centre for oncological hadron therapy*, vols I & II, INFN, (2nd edition 1995).
-

## NOMENCLATURE

- Right-handed, curvilinear coordinate system  $(x,s,z)$  for the beam:



{ $y$  = the general transverse coordinate, i.e.  $x$  or  $z$ }.

- Subscript  $_0$  denotes a parameter evaluated at the origin, on the central orbit or at rest.
- $\Delta$  (0 - 1%),  $\delta$  (0 - few ‰), 'd' (infinitesimal changes).
- $\langle \dots \rangle$  denotes an average over a distribution.
- $(X, X')$  and  $(Z, Z')$  [ $\text{m}^{1/2}$ ] normalised coordinates.
- $A_x, A_z$  normalised particle amplitude ( $= \sqrt{(Y^2 + Y'^2)}$ )
- $E_x, E_z$  geometric emittance ( $1\sigma$ )  $\pi$  [m rad].
- $\epsilon_{n,x}, \epsilon_{n,z}$  normalised emittance ( $1\sigma$ )  $\pi$  [m rad].  
{ $\pi$  should always be apparent}
- $\sigma_x, \sigma_z$  standard deviation of a distribution [m]
- $E_l$  longitudinal emittance [eV s]
- $E$  total energy [eV].

- $T$  kinetic energy [eV]
- $p$  momentum [GeV/c]
- $\beta$  ( $= v/c$ ),  $\gamma$  ( $= m/m_0$ ) usual relativistic parameters.
- $e$  electronic charge [As]
- $Q_x, Q_z$  machine tune values.
- $Q'_x, Q'_z$  machine chromaticities  $(dQ_y/(dp/p))_0$
- $\beta_x, \beta_z, \alpha_x, \alpha_z, \gamma_x, \gamma_z, \mu_x, \mu_z, D_x, D_z, D'_x, D'_z$  optics parameters with their usual definitions.
- $D_{n,x}, D_{z,n}, D'_{n,x}, D'_{z,n}$  normalised dispersion functions.
- $M$  transfer matrix.
- $T_0, T_r$  revolution period [s]
- $f_0, f_r$  revolution frequency [Hz]
- $\Omega_0, \Omega_r$  angular revolution frequency [ $\text{rad s}^{-1}$ ]
- $S$  normalised sextupole strength [ $\text{m}^{-1/2}$ ].
- $l_s$  magnetic length of sextupole.
- $H$  perpendicular distance from the side to the centre of the stable triangle in normalised phase space.
- $\alpha_H$  angle of  $H$  measured anticlockwise from  $X$ -axis.
- $H$  Hamiltonian
- $B_x, B_s, B_z$  components of magnetic induction [T]
- $\rho$  radius of curvature [m]
- $B\rho$  magnetic rigidity [Tm]
- $A$  number of nucleons in an ion (mass number)

- $n$  number of charges on an ion
  - $k_{2\text{MAD}}$  normalised sextupole-gradient coefficient for the MAD optics program.
  - $\kappa$  driving term for a nonlinear resonance
  - $C$  machine circumference.
  - $Z_T$  Transverse coupling impedance.
  - ES Electrostatic septum.
  - MS Magnetic septum.
-

---

# PROGRAMME

## Tuesday, 13th February TRANSVERSE ASPECTS

### PS Auditorium

- 10.00-10.15 Introduction (P. Bryant)  
10.15-11.15 Simple theory of slow extraction from a synchrotron (S. Rossi)  
11.15-11.45 Break  
11.45-12.05 Hardt condition for superposition of separatrices (M. Pullia)  
12.05-12.30 Achromatic transfer from electrostatic septum to magnetic septum (M. Benedikt)  
12.30-14.00 Lunch

### CN Amphitheater Bldg 31, 3-005

- 14.00-14.30 Emittance of the slow-extracted beam (M. Pullia)  
14.30-15.15 General transverse strategy (P. Bryant)  
15.15-15.30 Discussion  
15.30-16.00 Break  
16.00-17.00 Lattice considerations (M. Benedikt)  
17.00-17.15 Discussion

## Wednesday, 14th February LONGITUDINAL ASPECTS

### PS Auditorium

- 09.45-10.15 Stochastic and other means of rf acceleration to 'feed' the resonance (R. Cappi)  
10.15-10.45 'Empty-bucket' stabilisation of the spill (R. Cappi)  
10.45-11.15 Break  
11.15-11.45 General longitudinal strategy. (R. Cappi)  
11.45-12.15 Phase displacement acceleration (in general) (E. Ciapala)  
12.15-12.45 Feasibility of a phase-displacement acceleration system and a micro-bucket transfer system for 'feeding' the resonance (M. Crescenti)  
12.45-14.00 Lunch

### PS Auditorium

- 14.00-14.30 Betatron acceleration into the resonance (C. Steinbach)  
14.30-15.30 SPS extraction experience and spill control (M. Gyr, K. Cornelis)  
15.30-16.00 Break  
16.00 Discussions.

\*\*\*

---

---

# CONTENTS

Bibliography	iii
Nomenclature	vi
Programme	vii
Contents	viii
1 Introduction	1
2 Simple theory of slow extraction from a synchrotron	7
3 Hardt condition for superposition of separatrices	38
4 Achromatic transfer from electrostatic septum to magnetic septum	57
5 Emittance of the slow-extracted beam	74
6 General transverse strategy	97
7 Lattice considerations	109
8 Longitudinal aspects of slow extraction (combined notes on <i>Stochastic and other means of rf acceleration to 'feed' the resonance, "Empty-bucket" stabilisation of the spill and General longitudinal strategy</i> )	127
9 Phase-displacement acceleration (in general)	149
10 Feasibility of a phase-displacement acceleration system and a micro-bucket transfer system for 'feeding' the resonance	170
11 Betatron acceleration into the resonance	184
12 SPS extraction experience and spill control	190
13 Resonant extraction in the SPS	208
14 Tentative machine parameters	222
15 Index.	225

---

## INTRODUCTION

*(slow extraction from synchrotrons  
for cancer therapy)*

presented by  
P.J. Bryant

February 13th and 14th 1996

PS, CERN

---

## AIMS

To prepare for the design of a medical synchrotron capable of delivering protons and light ions for cancer therapy. More specifically, it is hoped that the next two days will expose the problems and explore the possible design choices concerning resonant extraction using a third-order resonance.

The performance of medical synchrotrons is critically dependent on the extraction, so this is the natural place at which to start a study and from which to set criteria that will determine the rest of the design. The present programme is designed to:

- Review the underlying theory and physics of slow extraction.
  - To collect simple analytical expressions that can guide numerical computer design work
  - To identify the design choices that need to be made and the various solutions that are available.
-

### WISH LIST

Uniform spill (for precision of the delivered dose).

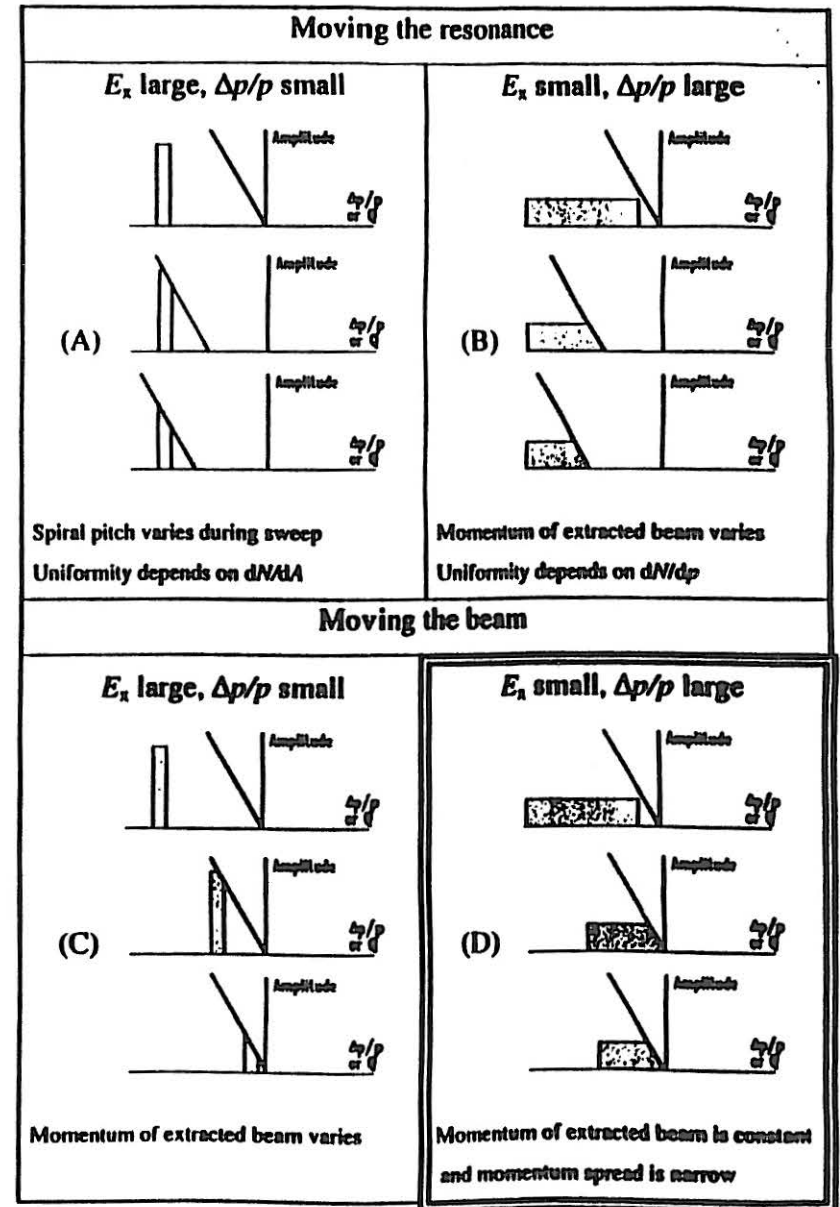
Narrow momentum spread (control of width of Bragg peak, especially in the case of a passive scanning system).

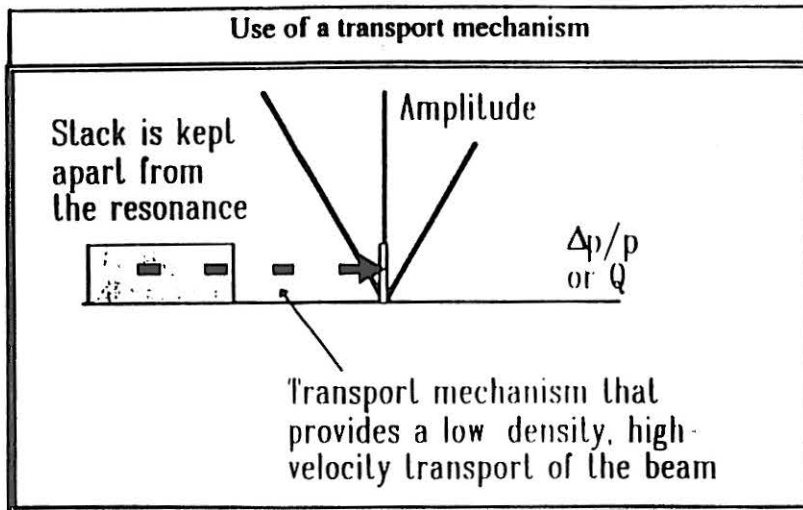
Constant momentum at extraction (for spatial stability of final beam spot, in case dispersion 'leaks' into delivery system).

Switchable spill (for economy of beam and for controlling the delivered dose).

Weakened dependency on power supply stability. Slow-extraction systems are very susceptible to power supply ripple. The resonance acts like a magnifying glass that magnifies all imperfections. Since this machine will be dual-species and the protons may require only 20-30% of the maximum field stability will be of even more importance.

Equal emittances, or a strategy for using unequal emittances (equal emittances are usually specified for gantry optics).





## TECHNIQUES

Some of the above schemes imply the need for a stack with a wide momentum spread (say 6%) and a very uniform distribution of particles in momentum space (the resonance acts like a magnifying glass that exaggerates all imperfections).

Two rf techniques will be useful to satisfy these needs: Bunch rotation on the unstable fixed point to develop the momentum spread and the application of rf noise to homogenise the stack.

## LOOKING FOR CLUES TO:

Which should move, the beam or the resonance?

How can the beam be moved?

How can the resonance be moved?

What beam transport mechanisms can be used?

What are the implications for the injection scheme?

What are the implications for the rf acceleration system?

Positions for the electrostatic & magnetic septa?

How should the sextupoles be deployed?

How should the lattice be customised?

Can the extracted emittance be adjusted?

How can the extracted current be adjusted?

## THE STARTING POINT

The advance of the separatrix over 3 turns (the so-called spiral step) at the radial position of the electrostatic septum is somewhat arbitrarily set at 10 mm.\*

\* The simple explanation for this number is that for 0.1 mm septum thickness and a 10 mm spiral step the beam loss should be close to 1%.

*Simple theory of slow extraction  
from a synchrotron*

Sandro Rossi

3rd-order resonance slow extraction for medical synchrotrons

Cern, 13-14 February 1996

## NORMALISED SYSTEM OF COORDINATES

Calculations are greatly simplified by using normalised coordinates: the betatron oscillations are represented by a circular motion in the normalised phase plane, such that their amplitude and phase can be easily evaluated. The distance along the equilibrium orbit is denoted by  $s$  and the radial or vertical component of the displacement from the reference orbit is denoted by  $x$ , the betatron oscillation is expressed by:

$$x(s) = a \sqrt{\beta(s)} \cos[\mu(s) + \delta]$$

where  $\beta(s)$  is the betatron amplitude function, and

$$\mu(s) = \int \frac{ds}{\beta(s)}$$

the betatron phase function with  $a$  and  $\delta$  arbitrary constants. This expression is reduced to a harmonic oscillation if we introduce the normalised variables:

$$X(s) = \frac{x(s)}{\sqrt{\beta(s)}}$$

$$\mu(s) = \int \frac{ds}{\beta(s)}$$

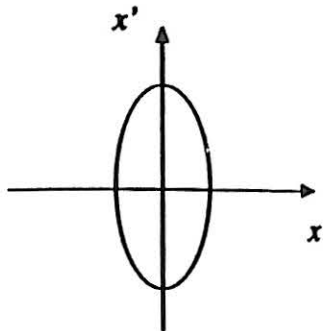
In this new system the betatron oscillation is described by:

$$X = a \cos(\mu + \delta)$$

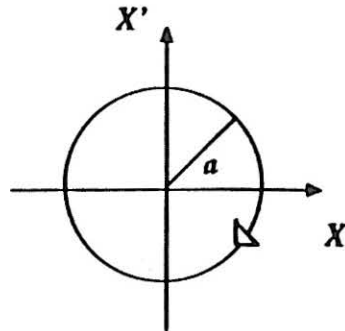
and the trajectory in phase space becomes a circle; deriving  $X$  with respect to the variable  $\mu$ :

$$X' = \frac{dX}{d\mu} = -a \sin(\mu + \delta)$$

*Real phase space*



*Normalised phase space*



The emittance is the same in both systems and is given by:

$$E_x = \frac{\epsilon^2}{\beta_x} \pi = \mathcal{E}^2 \pi$$

The normalising matrix  $N$  is expressed by:

$$N = \frac{1}{\sqrt{\beta}} \begin{pmatrix} 1 & 0 \\ \alpha & \beta \end{pmatrix}$$

while its inverse is:

$$N^{-1} = \frac{1}{\sqrt{\beta}} \begin{pmatrix} \beta & 0 \\ -\alpha & 1 \end{pmatrix}$$

The matrix for the transformation in the real phase plane  $(x, x')$  from an azimuth  $s_1$  to an azimuth  $s_2$  is:

$$M_{12} = \begin{pmatrix} \frac{\sqrt{\beta_2}(\cos\mu + \alpha_1 \sin\mu)}{\sqrt{\beta_1}} & \sqrt{\beta_1 \beta_2} \sin\mu \\ -\left( \frac{(1 + \alpha_1 \alpha_2) \sin\mu + (\alpha_2 - \alpha_1) \cos\mu}{\sqrt{\beta_1 \beta_2}} \right) & \frac{\sqrt{\beta_1}}{\sqrt{\beta_2}} (\cos\mu - \alpha_2 \sin\mu) \end{pmatrix}$$

where  $\mu = \mu(s_2) - \mu(s_1)$ ;  $\beta_1 = \beta(s_1)$ , etc. The matrix for the transformation in the normalised phase plane is:

$$\overline{M}_{12} = \begin{pmatrix} \cos\mu & \sin\mu \\ -\sin\mu & \cos\mu \end{pmatrix}$$

## FIELD IN A SEXTUPOLE

From Maxwell equations, assuming that the magnetic field has, to a good approximation, only transverse components and being interested only in the field inside the vacuum pipe, we can derive the vector potential "A" for a magnet with  $2n$  poles in Cartesian coordinates:

$$A = \sum_n A_n f_n(x, z)$$

with  $f_n$  an homogeneous function in  $x$  and  $z$  of order  $n$ :

$$f_n(x, z) = (x + iz)^n$$

The real terms correspond to regular multipoles, the imaginary ones to skew multipoles as summarised in the following table.

*Vector potential solutions in Cartesian coordinates*

Multipole	n	Regular	Skew
quadrupole	2	$x^2 - z^2$	$2xz$
sextupole	3	$x^3 - 3xz^2$	$3x^2z - z^3$
octupole	4	$x^4 - 6x^2z^2 + z^4$	$4x^3z - 4xz^3$

For our calculations, it is useful to relate  $A_n$  to the field, for example, in the median plane using the Taylor expansion:

$$B_z(z=0) = \frac{\partial A}{\partial x} = \sum_{n=1}^{\infty} n A_n x^{n-1} = \sum_{n=1}^{\infty} \frac{1}{(n-1)!} \left( \frac{d^{(n-1)} B_z}{dx^{(n-1)}} \right)_0 x^{(n-1)}$$

so that:

$$A_n = \frac{1}{n!} \left( \frac{d^{(n-1)} B_z}{dx^{(n-1)}} \right)_0$$

In particular, for a regular sextupole:

$$A = A_3(x^3 - 3xz^2)$$

so that:

$$B_z = \frac{\partial A}{\partial x} = 3A_3(x^2 - z^2) = \frac{1}{2} \left( \frac{d^2 B_z}{dx^2} \right)_0 (x^2 - z^2)$$

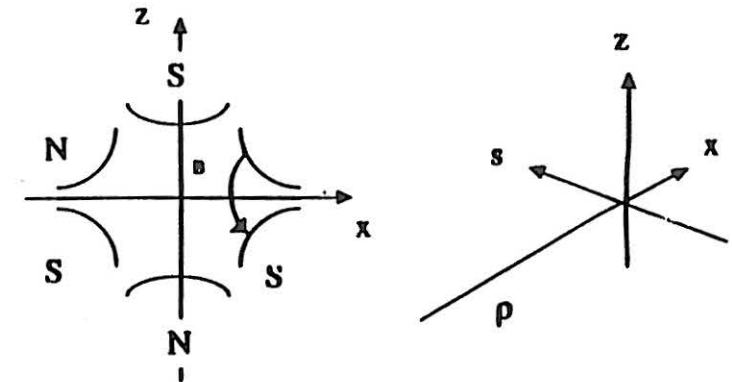
$$B_x = -\frac{\partial A}{\partial z} = 6A_3 xz = \left( \frac{d^2 B_z}{dx^2} \right)_0 xz$$

### Sign conventions

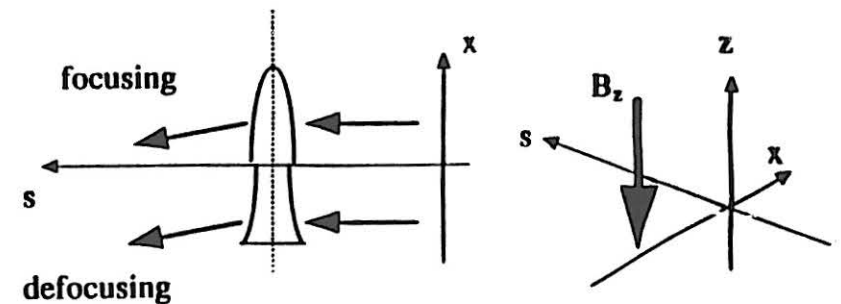
The following diagram shows the conventions adopted, i.e.:

- F-sextupole, if it focuses particle with  $x$  positive;
- D-sextupole, if it defocuses particles with  $x$  positive.

Focusing sextupole and coordinate system



F-sextupole



Let us now calculate the kick given by a focusing sextupole to a particle moving at a distance  $x$  from the central orbit on the median plane supposing the length  $\ell_s$  of the sextupole to be negligible (thin-lens approximation):

$$\Delta x' = -\frac{B_z(z=0)\ell_s}{|B_0\rho|}$$

where the minus sign is due to the fact that a particle at a positive  $x$  is bent by the  $B$  field toward the origin of axis. Substituting the expression for the field:

$$\Delta x' = -\frac{1}{2} \frac{\ell_s}{|B_0\rho|} \left( \frac{d^2 B_z}{dx^2} \right)_0 x^2$$

In normalised coordinates at the sextupole position, we have:

$$\begin{aligned} \Delta X_S' &= -\sqrt{\beta_s} \frac{1}{2} \frac{\ell_s}{|B_0\rho|} \left( \frac{d^2 B_z}{dx^2} \right)_0 (\sqrt{\beta_s} X)^2 \\ &= -\beta_s^{3/2} \frac{1}{2} \frac{\ell_s}{|B_0\rho|} \left( \frac{d^2 B_z}{dx^2} \right)_0 X^2 = S X^2 \end{aligned}$$

$$\Delta X_S' = S X^2$$

with  $S$  being the normalised sextupole strength:

$$S = -\beta_s^{3/2} \frac{1}{2} \frac{\ell_s}{|B_0\rho|} \left( \frac{d^2 B_z}{dx^2} \right)_0 = -\frac{1}{2} \beta_s^{3/2} \ell_s m_{CAS} = -\frac{1}{2} \beta_s^{3/2} \ell_s K2_{MAD}$$

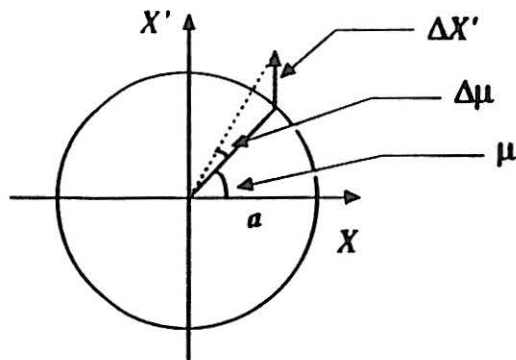
and  $K2_{MAD}$  [ $m^{-3}$ ]:

$$K2_{MAD} [m^{-3}] = \frac{1}{3.33556 \cdot p_0 [\text{GeV}/c]} \left( \frac{d^2 B_z}{dx^2} \right)_0 [\text{Tm}^{-2}].$$

## LOCKING ACTION AND ADDITION OF SEXTUPOLES

Let us go into detail analysing the effect of a sextupole treated as a thin lens. As shown in the following diagram the phase shift given by the sextupole is:

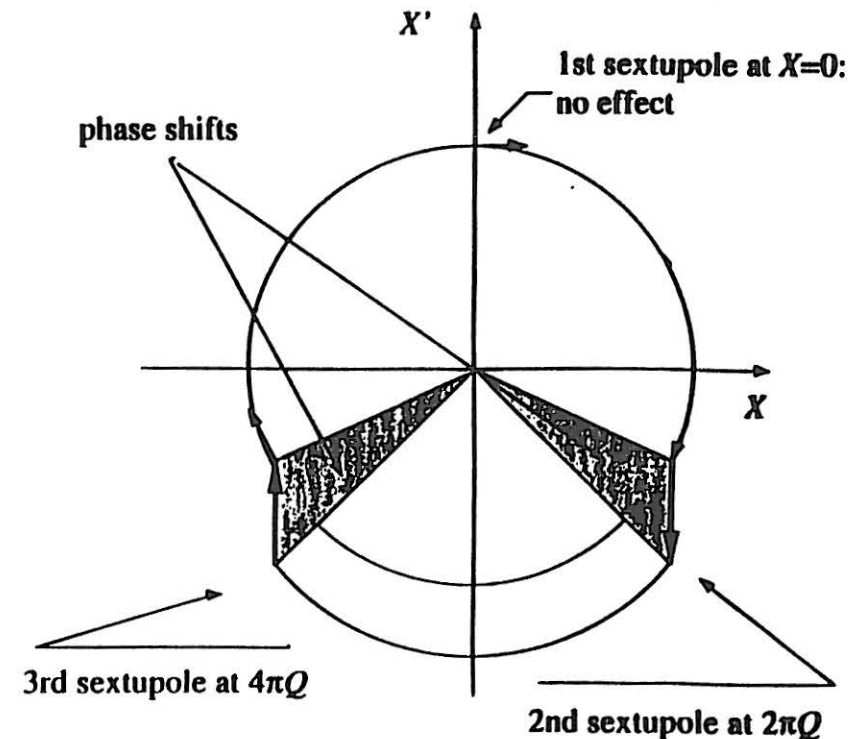
$$\Delta\mu = \frac{\Delta X'}{a} \cos\mu = \frac{S}{a} X^2 \cos\mu = Sa \cos^3 \mu = \frac{Sa}{4} (\cos 3\mu + 3\cos\mu)$$



Supposing that we are close to a third integer tune, in three turns the second term in the last equation averages zero, while the first term is constant, since its phase is an integer multiple of  $2\pi$ . From the figure it also appears that:

$$\frac{\Delta a}{a} = \frac{\Delta X'}{a} \sin\mu = \frac{S}{a} X^2 \sin\mu = Sa \cos^2 \mu \sin\mu = \frac{Sa}{4} \sin 3\mu$$

where the last equality is valid close to the resonance. When the particle is exactly on resonance, the phase advances by an integral number of  $2\pi$  and the particle 'locks' onto the resonance, repeating again and again the same trajectory in phase space. The following figure is a pictorial representation of the situation, corresponding to the "fixed points - corners" of the last stable triangle.



If we are close to resonance from the expression of phase shift, we have in the smooth approximation where  $\phi$  is the azimuthal angle:

$$\Delta\mu = 2\pi\Delta Q \approx \frac{Sa}{4}(\cos 3Q\phi)$$

smooth approx  $\Rightarrow \Delta\mu \approx \frac{2\pi Q}{2\pi} \phi = Q\phi$

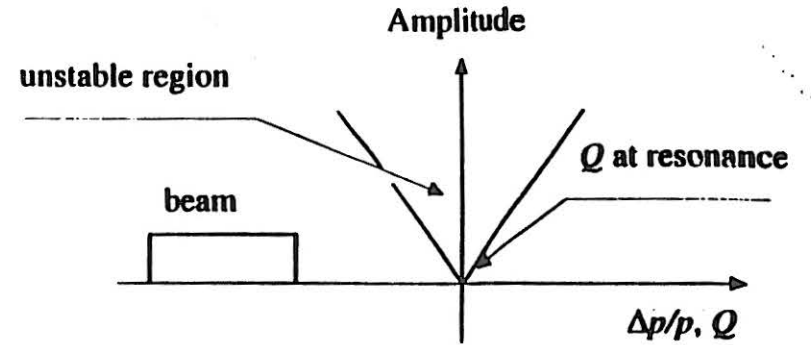
from which we deduce that the tune of the particle wanders within a band around the unperturbed tune  $Q_0$ :

$$Q_0 - \frac{Sa}{8\pi} < Q < Q_0 + \frac{Sa}{8\pi}$$

If the third integer tune value is not inside this band, the particle cannot be locked and it is stable, in other words at a "tune distance"  $\Delta Q$  from  $Q_0$  the particles with amplitude:

$$a < \frac{8\pi|\Delta Q|}{S}$$

are stable. This fact gives the phase space stable triangles that will be discussed later. Replacing the inequality by an equality, we obtain the amplitude of the unstable fixed points and figure out that in the amplitude-tune space the resonance is a straight line as shown in the following picture. The slope of the resonance line is related to the spread in momentum through the chromaticity.



Now, suppose that we have an azimuth distribution of sextupoles that can be expressed as a Fourier series in  $\phi$ :

$$S(\phi) = \sum_s S_s e^{js\phi}$$

introducing it into the equation of phase displacement and integrating around the machine circumference:

$$\Delta\mu = \sum_s \int_0^{2\pi} \frac{S_s a}{4} \cos(3Q\phi) e^{js\phi} d\phi = \sum_s \int_0^{2\pi} \frac{S_s a}{8} [e^{j(3Q+s)\phi} + e^{j(s-3Q)\phi}] d\phi \quad \text{for only } s = \pm 3Q$$

$\frac{e^{j3Q\phi} + e^{-j3Q\phi}}{2}$

we notice that the integral is large and finite if:

$$3Q = s$$

$$S_{3Q} = \int S(\phi) e^{j3Q\phi} d\phi = \sum_i S_i e^{j3\mu_i}$$

that is in the addition of the sextupoles we have to consider the third harmonic of the sextupole distribution in betatron phase around the machine. Actually, since in the expression of  $S$  it also appears as a power of the beta function, and periodicities in the lattice structure can also drive the resonance together with multipole field patterns.

Equating the sum of sextupoles to a virtual sextupole we have:

$$S_{virtual} \exp(j3\mu_{x,virtual}) = \sum_i S_i \exp(j3\mu_{x,i})$$

where  $\mu_{x,i}$  is the betatron phase location of the  $i$ -th sextupole.

By separating real and imaginary parts we obtain:

*Equivalent sextupole phase and strength*

$$\tan(3\mu_{x,virtual}) = \frac{\sum_i S_i \sin(3\mu_{x,i})}{\sum_i S_i \cos(3\mu_{x,i})} \quad (1)$$

$$S_{virtual}^2 = \left( \sum_i S_i \cos(3\mu_{x,i}) \right)^2 + \left( \sum_i S_i \sin(3\mu_{x,i}) \right)^2 \quad (2)$$

that is betatron phase and strength of a single equivalent sextupole in the ring.

### First consideration

From the previous equation (2) it is easy to show that for a distribution of sextupoles of equal strength and spaced by  $\Delta\mu$  we have:

- *cancellation* of the driving term if  $\Delta\mu = \pi/3$ ;
- *reinforcement* of the driving term if  $\Delta\mu = 2\pi/3$ .

### Second consideration

If the sextupoles are placed in a region of finite horizontal dispersion ( $D_x$ ) they also affect the chromaticity  $\Delta Q'_{x,z}$  of the machine:

$$\Delta Q'_x \equiv \frac{\partial Q'_x}{\partial \frac{\Delta p}{p}} = \frac{\ell_s}{4\pi} \left[ K2_{MAD}^{SF} \sum_{n=1}^{NF} (\beta_x D_x)_n + K2_{MAD}^{SD} \sum_{n=1}^{ND} (\beta_x D_x)_n \right] \quad (3)$$

$$\Delta Q'_z \equiv \frac{\partial Q'_z}{\partial \frac{\Delta p}{p}} = -\frac{\ell_s}{4\pi} \left[ K2_{MAD}^{SF} \sum_{n=1}^{NF} (\beta_z D_x)_n + K2_{MAD}^{SD} \sum_{n=1}^{ND} (\beta_z D_x)_n \right] \quad (4)$$

In general, it would be better to have the possibility of acting on the resonance and the chromaticity independently:

- *to drive the resonance, without affecting the chromaticity*
  - ♦ put the sextupoles in a zero dispersion region;
- *to act on the chromaticity, without driving the resonance*
  - ♦ arrange the correction sextupoles with a phase difference  $\Delta\mu = \pi/3$  between two consecutive ones.

### Third consideration

Consider a lattice with a superperiodicity of 2 and with two sextupoles with the same absolute strength ( $S$  or  $K2_{MAD}$ ), but diametrically opposing [ $\Delta\mu = Q\pi = (n \pm 1/3)\pi$ ] each other:

from (2) we have:

$$S_{virtual}^2 = (S_1 \cos(0) + S_2 \cos(3Q\pi))^2 + (S_1 \sin(0) + S_2 \sin(3Q\pi))^2$$

$$n \text{ even: } S_{virtual} = S_1 - S_2$$

$$n \text{ odd: } S_{virtual} = S_1 + S_2$$

from (3) and (4) we have:

$$\Delta Q_x^i = \frac{\ell_s}{4\pi} \beta_x D_x [ K2_{MAD}^{S1} + K2_{MAD}^{S2} ]$$

$$\Delta Q_z^i = -\frac{\ell_s}{4\pi} \beta_z D_x [ K2_{MAD}^{S1} + K2_{MAD}^{S2} ]$$

so that if  $n$  is even:

- $S_1 = -S_2 \implies$  *only driving the resonance*
- $S_1 = S_2 \implies$  *only correcting chromaticity*

no independent action is possible with  $n$  odd.

## PHASE SPACE TRAJECTORIES

Let us consider the effect of a single sextupole supposing that the unperturbed fractional tune is close to one-third of an integer and that the sextupole represents a small perturbation so that we can add up the effects turn by turn independently. We calculate the increments  $\Delta X$  and  $\Delta X'$  on three turns starting from the exit of the sextupole.

The total displacement and deflection after three turns:

$$\begin{pmatrix} \Delta X \\ \Delta X' \end{pmatrix}$$

are the sum of:

• 3 unperturbed turns plus a kick:

$$\begin{pmatrix} \cos 3\mu^* & \sin 3\mu^* \\ -\sin 3\mu^* & \cos 3\mu^* \end{pmatrix} \begin{pmatrix} X_0 \\ X_0' \end{pmatrix} + \begin{pmatrix} 0 \\ S(\cos 3\mu^* X_0 + \sin 3\mu^* X_0')^2 \end{pmatrix}$$

• 2 unperturbed turns, a kick and another turn:

$$\begin{pmatrix} \cos 2\mu^* & \sin 2\mu^* \\ -\sin 2\mu^* & \cos 2\mu^* \end{pmatrix} \begin{pmatrix} X_0 \\ X_0' \end{pmatrix} + \begin{pmatrix} 0 \\ S(\cos 2\mu^* X_0 + \sin 2\mu^* X_0')^2 \end{pmatrix} + \begin{pmatrix} \cos \mu^* & \sin \mu^* \\ -\sin \mu^* & \cos \mu^* \end{pmatrix} \begin{pmatrix} \cos 2\mu^* X_0 + \sin 2\mu^* X_0' \\ -\sin 2\mu^* X_0 + \cos 2\mu^* X_0' + S(\cos 2\mu^* X_0 + \sin 2\mu^* X_0')^2 \end{pmatrix}$$

• 1 unperturbed turn, a kick and 2 other turns:

$$\begin{pmatrix} \cos \mu^* & \sin \mu^* \\ -\sin \mu^* & \cos \mu^* \end{pmatrix} \begin{pmatrix} X_0 \\ X_0' \end{pmatrix} + \begin{pmatrix} 0 \\ S(\cos \mu^* X_0 + \sin \mu^* X_0')^2 \end{pmatrix} + \begin{pmatrix} \cos 2\mu^* & \sin 2\mu^* \\ -\sin 2\mu^* & \cos 2\mu^* \end{pmatrix} \begin{pmatrix} \cos \mu^* X_0 + \sin \mu^* X_0' \\ -\sin \mu^* X_0 + \cos \mu^* X_0' + S(\cos \mu^* X_0 + \sin \mu^* X_0')^2 \end{pmatrix}$$

Adding the contributions for:

$$\mu^* = 2\pi \left( n \pm \frac{1}{3} + \delta Q \right)$$

with  $n$  integer and  $|\delta Q| \ll \frac{1}{3}$ , we get:

*Spiral step and spiral kick*

$$\Delta X = \epsilon X_0' + \frac{3}{2} S X_0 X_0'$$

$$\Delta X' = -\epsilon X_0 + \frac{3}{4} S (X_0^2 - X_0'^2)$$

where  $\epsilon = 6\pi \delta Q$ .

Along the separatrices, for  $\epsilon = 0$ , from the above equations, we can calculate the increase in amplitude of oscillation

$R = \sqrt{(X^2 + X'^2)}$  in 3 turns:

$$\Delta R = \frac{3}{4} S R^2$$

Indicating with  $R_{ES}$  the position of the electrostatic septum along the separatrix, we find a relation that connect position of the septum, spiral step  $\Delta R$  and strength of the sextupole:

$$\frac{1}{R_{ES}} - \frac{1}{R_{ES} + \Delta R} \approx \frac{3}{4} S$$

To identify the trajectories in phase space, we deduce from the above expressions the invariant of motion choosing the time taken by a particle to make three revolutions as unit time:

$$\frac{dX}{dt} = \Delta X = \epsilon X_0' + \frac{3}{2} S X_0 X_0' = \frac{\partial H}{\partial X'} \quad (1)$$

$$\frac{dX'}{dt} = \Delta X' = -\epsilon X_0 + \frac{3}{4} S (X_0^2 - X_0'^2) = -\frac{\partial H}{\partial X} \quad (2)$$

with:

*Hamiltonian*

$$H = \frac{\epsilon}{2} (X^2 + X'^2) + \frac{S}{4} (3XX'^2 - X^3)$$

The above expressions (1) and (2) identify the invariant  $H$  as the Hamiltonian in the conjugate variables  $X$  and  $X'$ . Different values of  $H$  correspond to different trajectories in the phase space.

If  $S = 0$ :

the expression of  $H$  becomes the equation of a circle, as it should be in normalised coordinates having eliminated the source of perturbation.

If  $S \neq 0$ :

- the trajectories are symmetric with respect to the  $X$ -axis, since  $X'$  appears only in quadrature;
- for small values of  $X$  and  $X'$ , the trajectories are slightly deformed circles;
- from expression (1) and (2) equating to zero we derive the coordinates of the fixed points:
  - ♦  $O(0; 0)$  fixed point of first order (it repeats itself in one turn);

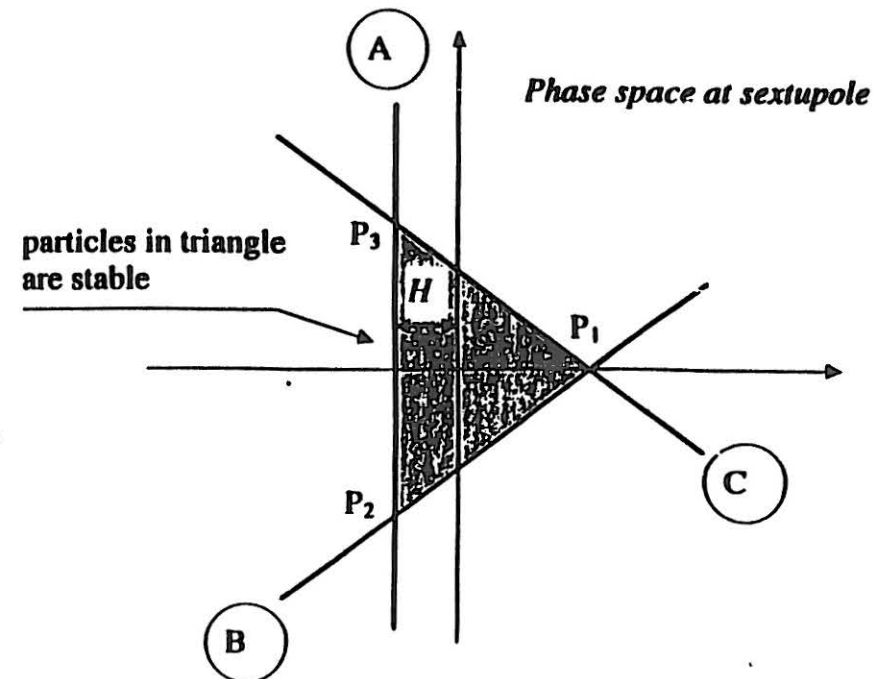
$$♦ P_1 = \left( \frac{4\epsilon}{3S}; 0 \right)$$

$$P_2 = \left( \frac{2\epsilon}{3S}; \frac{2\epsilon}{\sqrt{3}S} \right)$$

$$P_3 = \left( \frac{2\epsilon}{3S}; -\frac{2\epsilon}{\sqrt{3}S} \right)$$

fixed points of order three (repeat themselves in three turns).

The lines connecting the points  $P_i$  define a triangle that limits the stable, phase-space region (inside) from the unstable region (outside). These are called separatrices. The next figure shows the triangle for  $\epsilon/S > 0$ .



The equations of the separatrices and the area of the triangle are easily calculated for the present configuration at the sextupole position.

*Equation of separatrices*

(A)  $X = -\frac{2\epsilon}{3S}$

(B)  $X' = \frac{1}{\sqrt{3}}\left(X - \frac{4\epsilon}{3S}\right)$

(C)  $X' = \frac{1}{\sqrt{3}}\left(-X + \frac{4\epsilon}{3S}\right)$

*Distance of side of triangle to origin of axis*

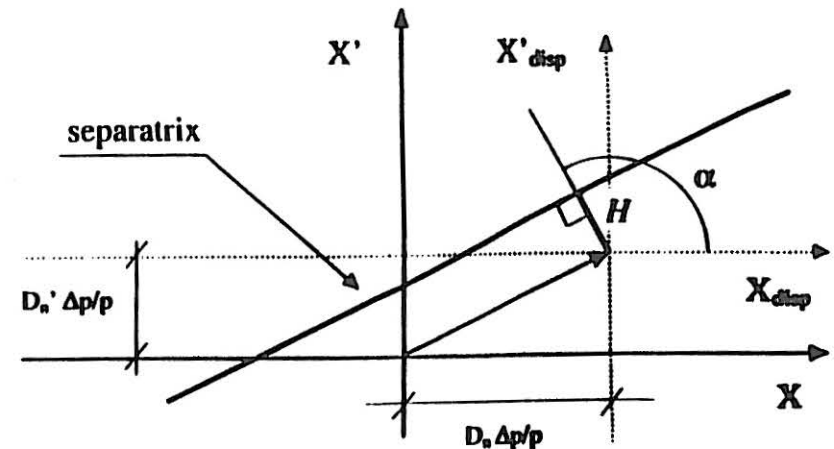
$$H = \frac{2\epsilon}{3S} = \frac{4\pi}{S} \delta Q$$

*Stable emittance = (area triangle)/ $\pi$  [ $\pi$  m rad]*

$$\frac{3\sqrt{3}}{\pi} H^2 = \frac{48\sqrt{3}\pi}{S^2} (\delta Q)^2 = \frac{48\sqrt{3}\pi}{S^2} \left(Q_s \frac{\Delta p}{p}\right)^2$$

General equation of the separatrix

The equations of the separatrices (A), (B) and (C), deduced earlier, are valid at the sextupole (single or virtual) position in the lattice. Let us generalise these equations with the help of the following picture.



The line equation is given by taking into consideration the following points:

- the anticlockwise rotation of the line by an angle  $\alpha$ ;
- the displacement of the equilibrium orbit due to the dispersion ( $D_n, D_n'$ ) in the machine and induced by the momentum deviation of the particle ( $\Delta p/p$ ).

Applying the above transformations we get the general expression of the separatrix:

$$\left(X - D_n \frac{\Delta p}{p}\right) \cos \alpha + \left(X' - D_n' \frac{\Delta p}{p}\right) \sin \alpha = H$$

It is more useful to express the equations of the separatrices (A), (B) and (C) as a function of the phase advance ( $\Delta\mu$ ) between the sextupole position and the observation point, remembering that the phase advance determines a clockwise rotation. The separatrices at the sextupole position are obtained from the preceding equation inserting:

$$\begin{aligned} \text{(A)} & \implies \alpha = 180^\circ \\ \text{(B)} & \implies \alpha = 300^\circ \\ \text{(C)} & \implies \alpha = 420^\circ \end{aligned}$$

and, rotating by  $\Delta\mu$ , we have at the observation point:

<p>(A):</p> $-\left(X - D_n \frac{\Delta p}{p}\right) \cos(\Delta\mu) + \left(X' - D_n' \frac{\Delta p}{p}\right) \sin(\Delta\mu) = H$ <p>(B):</p> $-\left(X - D_n \frac{\Delta p}{p}\right) \cos(\Delta\mu + 240^\circ) + \left(X' - D_n' \frac{\Delta p}{p}\right) \sin(\Delta\mu + 240^\circ) = H$ <p>(C):</p> $-\left(X - D_n \frac{\Delta p}{p}\right) \cos(\Delta\mu + 120^\circ) + \left(X' - D_n' \frac{\Delta p}{p}\right) \sin(\Delta\mu + 120^\circ) = H$
--

### Particle dynamics

We want to analyse the movement of the particles along the separatrices; for this purpose we substitute their expressions in the equations (1) and (2):

$$\left. \begin{aligned} X &= -\frac{2\varepsilon}{3S} \\ \frac{dX'}{dt} &= -\varepsilon X_0 + \frac{3}{4} S (X_0^2 - X_0'^2) \end{aligned} \right\} \rightarrow \frac{dX'}{dt} = -\frac{3}{4} S X'^2 + \frac{\varepsilon^2}{S}$$

$$\left. \begin{aligned} X' &= \frac{1}{\sqrt{3}} \left( X - \frac{4\varepsilon}{3S} \right) \\ \frac{dX}{dt} &= \varepsilon X_0' + \frac{3}{2} S X_0 X_0' \end{aligned} \right\} \rightarrow \frac{dX}{dt} = \frac{\sqrt{3}}{2} S X^2 - \frac{1}{\sqrt{3}} \varepsilon X - \frac{4}{3\sqrt{3}} \frac{\varepsilon^2}{S}$$

$$\left. \begin{aligned} X' &= \frac{1}{\sqrt{3}} \left( -X + \frac{4\varepsilon}{3S} \right) \\ \frac{dX}{dt} &= \varepsilon X_0' + \frac{3}{2} S X_0 X_0' \end{aligned} \right\} \rightarrow \frac{dX}{dt} = -\frac{\sqrt{3}}{2} S X^2 + \frac{1}{\sqrt{3}} \varepsilon X + \frac{4}{3\sqrt{3}} \frac{\varepsilon^2}{S}$$

### First consideration

The following figures show the sense of rotation of the particles in three turns and the direction of the outgoing separatrices at the sextupole position, depending on the sign of  $\epsilon$  and  $S$ .

At sextupole position

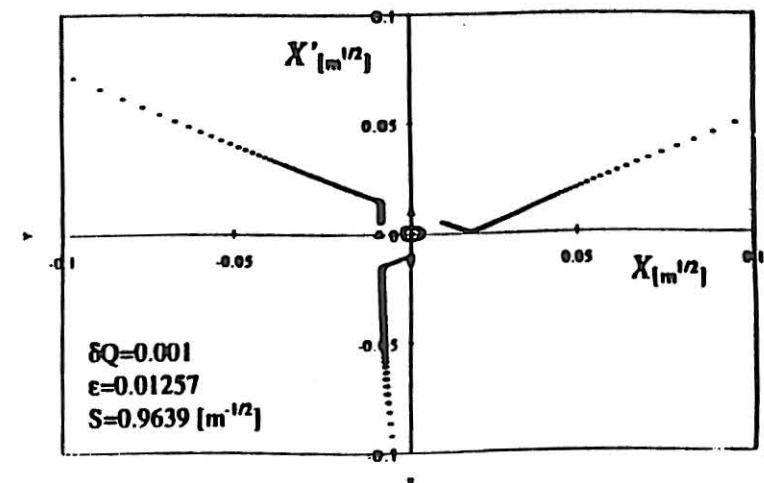
	$\delta Q > 0$ Above resonance	$\delta Q < 0$ Below resonance
$S > 0$		
$S < 0$		

### Second consideration

The parabolic expressions obtained so far become zero in correspondence to the point  $P_1$ , thus showing that they are indeed fixed points.

### Third consideration

The parabolic behaviour also shows that the movement of the particles on the separatrices in between the fixed points becomes slower and slower as we come close to them, thus giving a concentration of particles in the corners of the triangle. On the contrary, the spiral step is increasing quadratically as the particle move away from the fixed points along the separatrices, as shown in the following picture where a stable orbit and the movement on the outgoing separatrices in unit time are indicated.



## References

M.Q. Barton, Beam extraction from synchrotrons, Proc. of the VIIIth Int. Conf. on High Energy Accelerators, CERN, Geneva, 1971, p. 85.

P.J. Bryant, private communications.

D.A. Edwards, Comparison of half integer and third integer extraction for the energy doubler, TM-842 1750.000.

S. Guiducci, Chromaticity, CERN 94-01 (1994).

J. Rossbach and P. Schmüser, Basic course of accelerator optics, CERN 94-01 (1994).

Ch. Steinbach, Beam optics at resonant extraction septa, PS Report.

Ch. Steinbach, L'ejection lente, PS/OP/Note 88-25 (1988).

P. Strolin, Resonant extraction from the Cern Intersecting Storage Ring, CERN 69-6 (1969).

H. Wiedemann, Particle accelerator physics, Springer-Verlag (1993).

E.J.N. Wilson, Non-linearities and resonances, CERN 94-01 (1994).

E.J.N. Wilson, Theoretical aspects of the behaviour of beams in accelerators and storage rings, CERN 77-13 (1977).

**HARDT**

**CONDITION FOR**

**SUPERPOSITION OF**

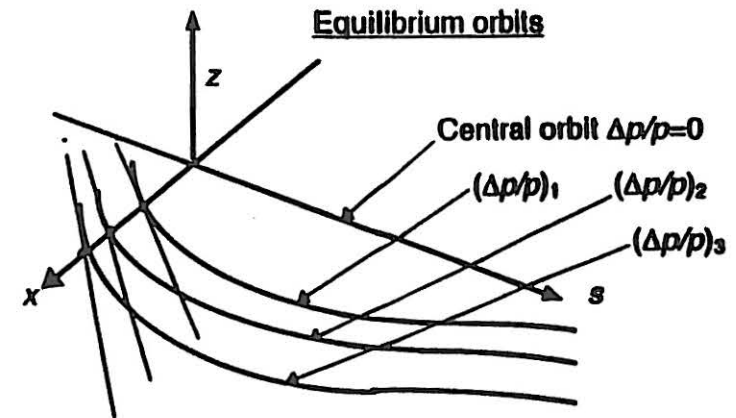
**SEPARATRICES**

presented by  
M. Pullia

February 13th and 14th 1996  
PS, CERN

## PHASE-SPACE REPRESENTATION OF A BEAM (1)

The motion in an accelerator is parameterised by defining an equilibrium orbit for each momentum and describing particle motions (betatron oscillations) about this equilibrium orbit. Equilibrium orbits for momenta different from the central orbit are parameterised by the dispersion function,  $D$ .



Positions and angles of orbits are given by

$$x(\Delta p) = D_x \frac{\Delta p}{p_0} \quad \text{and} \quad \frac{dx}{ds} = D'_x \frac{\Delta p}{p_0} \quad \text{Real phase space}$$

$$X(\Delta p) = D_{n,x} \frac{\Delta p}{p_0} \quad \text{and} \quad \frac{dX}{d\mu} = D'_{n,x} \frac{\Delta p}{p_0} \quad \text{Normalised phase space}$$

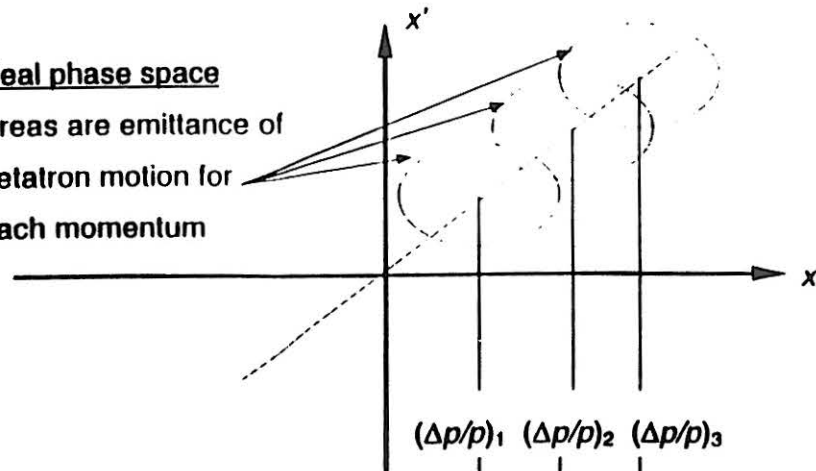
(The conversion between the normalised and real phase spaces was given in the basic lecture)

## PHASE-SPACE REPRESENTATION OF A BEAM (2)

At a given position in the machine the beam can be represented in phase space by a series of ellipses (circles in normalized phase space) centred around the dispersion vector  $(D, D) \cdot \Delta p/p$

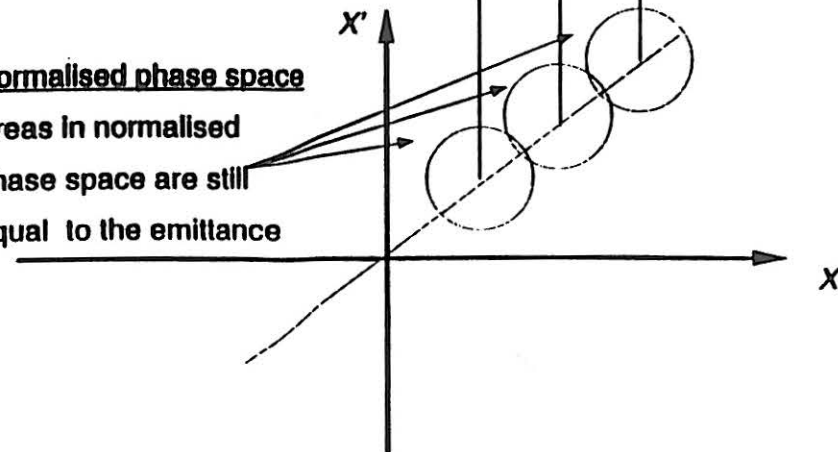
### Real phase space

Areas are emittance of betatron motion for each momentum



### Normalised phase space

Areas in normalised phase space are still equal to the emittance



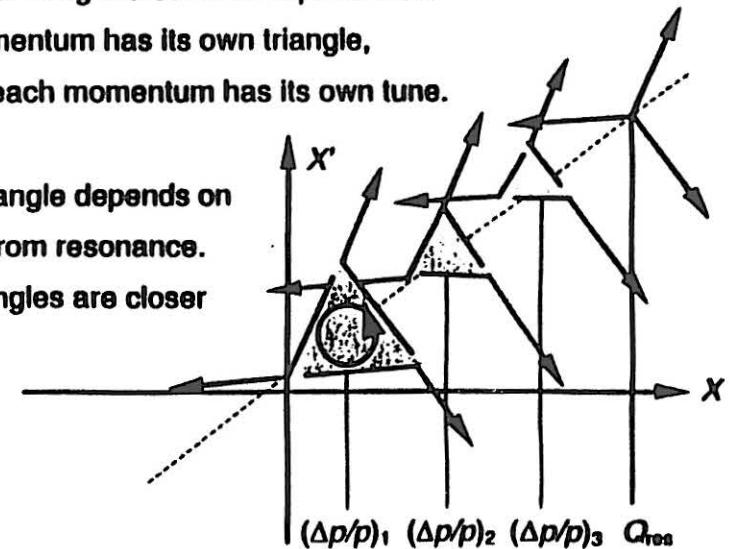
## PHASE SPACE REPRESENTATION OF THE RESONANCE (1)

The circles that represent the beam emittance in normalised phase space become triangles (of the same area) under the influence of the resonance.

The resonance for particles of each momentum is represented by a triangle corresponding to the last stable orbit and the extensions along the outward separatrices.

Each momentum has its own triangle, because each momentum has its own tune.

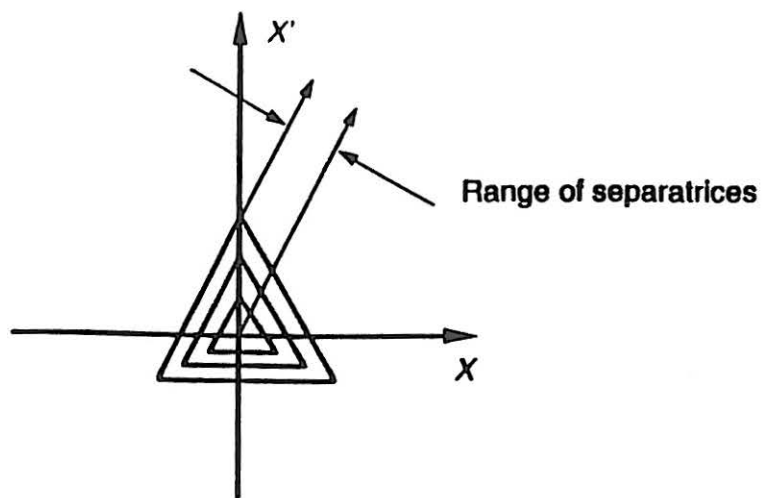
Size of triangle depends on distance from resonance. Small triangles are closer



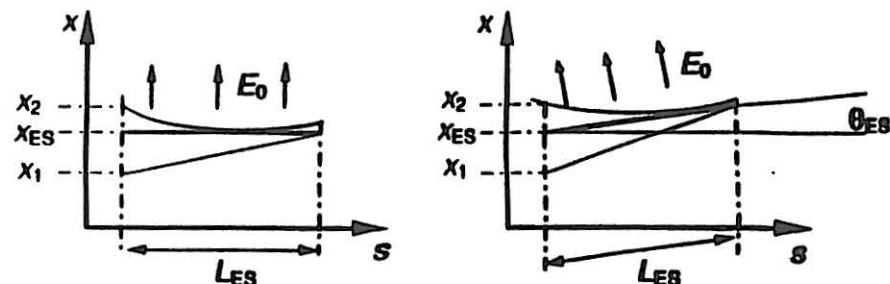
The rotation of the triangles depends on the betatron phase advance from the resonance sextupole to the observation point.

## PHASE SPACE REPRESENTATION OF THE RESONANCE (2)

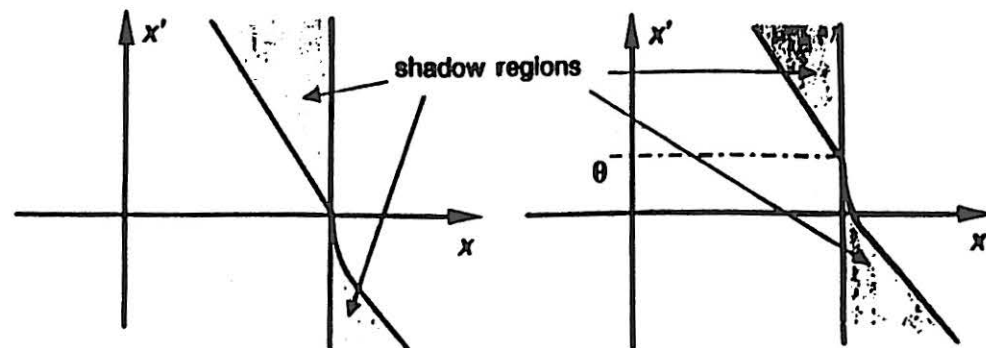
For a monoenergetic beam with increasing sextupole strength, the stable triangles shrink. The size of the stable triangles is characterised by  $H$  (see simply theory), which is proportional to  $\delta Q/S$ . By increasing the sextupole strength, particles with smaller and smaller amplitude get extracted.



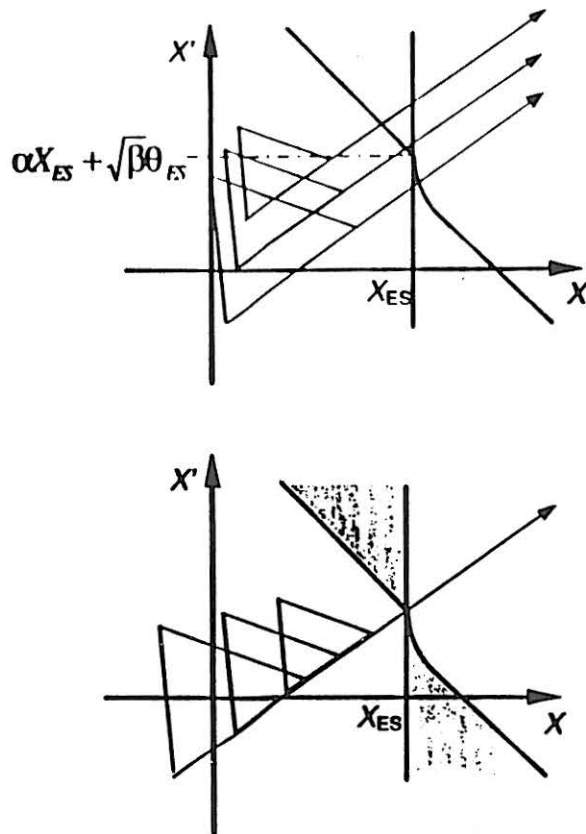
## LOSSES AT THE ELECTROSTATIC SEPTUM IN REAL PHASE SPACE



For particles starting at positions  $x_1$  and  $x_2$ , not all angles are allowed. In the first drawing, a particle with a divergence greater than  $(x_{ES} - x_1)/L_{ES}$  will hit the septum. A similar situation exists for particles inside the septum, except that the electric field curves their orbits and modifies the forbidden angles. The forbidden shadow regions are:



## LOSSES AT THE ELECTROSTATIC SEPTUM IN NORMALISED PHASE SPACE



## REASONS FOR THE HARDT CONDITION

The Hardt Condition aligns the separatrices belonging to different momenta and amplitudes at the electrostatic septum to avoid particle losses due to the "shadow regions" shown above, while chromaticity and dispersion are finite. This then makes it possible to keep the bulk of the waiting beam stable and to control the spill.

If the chromaticity and dispersion were zero, then all triangles would have a common centre, but particles with different initial amplitudes would leave the machine along different separatrices and would arrive at the ES with different angles, leading to losses in the shadow regions. Due to the zero chromaticity the waiting beam could become unstable and the spill would be difficult to control.

In any other case, if the Hardt Condition is not fulfilled, particles with different momenta and different amplitudes arrive at the ES with different angles, causing losses in the shadow regions.

**Note:** With the Hardt Condition fulfilled, all separatrices are coincident and collinear and aperture requirements in the electrostatic septum are an absolute minimum.

## REVISION - EQUATION OF A SEPARATRIX

Re-express the separatrix equation with  $H$  in terms of  $Q'$  and  $\Delta p/p$

$$\left( X - D_n \frac{\Delta p}{p} \right) \cos(\alpha - \Delta\mu) + \left( X' - D'_n \frac{\Delta p}{p} \right) \sin(\alpha - \Delta\mu) = H$$

$$\left( X - D_n \frac{\Delta p}{p} \right) \cos(\alpha - \Delta\mu) + \left( X' - D'_n \frac{\Delta p}{p} \right) \sin(\alpha - \Delta\mu) = \frac{4\pi}{S} \delta Q$$

$$\left( X - D_n \frac{\Delta p}{p} \right) \cos(\alpha - \Delta\mu) + \left( X' - D'_n \frac{\Delta p}{p} \right) \sin(\alpha - \Delta\mu) = \frac{4\pi}{S} Q' \frac{\Delta p}{p}$$

The momentum dependence of the separatrix is now apparent in each of the three main terms. Adjusting the momentum dependent terms in a way that they sum to zero, establishes the Hardt Condition.

The above assumes that the beam is moved into the resonance without changing transverse beam parameters. The alternative of sweeping the resonance through the stack would require an additional time variation to be taken into account.

## HARDT CONDITION

To remove the momentum dependence from the separatrix, the equation below must be satisfied.

$$D_n \cos(\alpha - \Delta\mu) + D'_n \sin(\alpha - \Delta\mu) = -\frac{4\pi}{S} Q'$$

The above equation may appear very flexible, but there are some boundary conditions on the parameters.

- The choice of the angle  $(\alpha - \Delta\mu)$  is restrained by the geometry of the extraction. This will be discussed in Section A.
- $D_n$  and  $D'_n$  depend on the lattice design. This will be discussed in Section B.
- $Q'$  is the main variable, but for machines working below transition energy the stability of a coasting beam is improved by making  $Q'$  negative. This will be discussed in Section C.
- $S$  has been set, somewhat arbitrarily, to give an increase of 10 mm in the amplitude of the separatrix over 3 turns at the electrostatic septum. This is discussed in Section D.
- Finally, numerical values will be discussed in Section E.

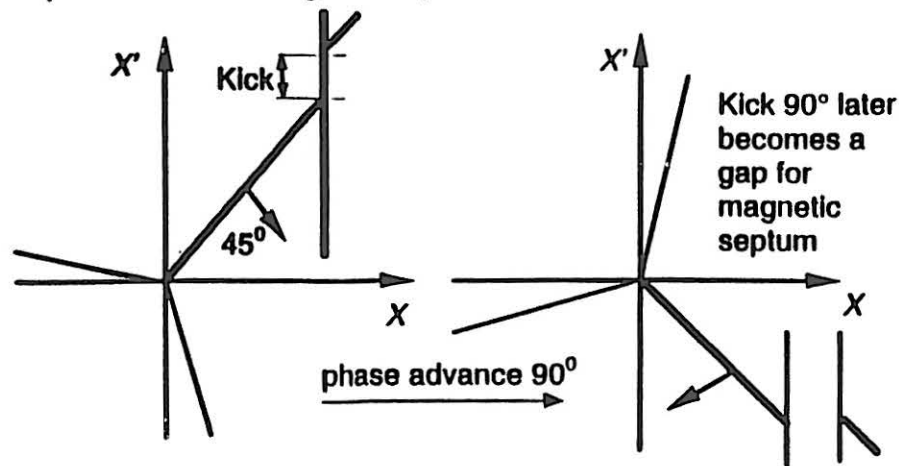
## SECTION A

## SEPARATRIX GEOMETRY FOR EXTRACTION (1)

Figures below show a logical layout in phase space for the septa and separatrices with the extraction separatrix at  $45^\circ$  and  $-45^\circ$ .

This foresees a  $90^\circ$  phase advance between the septa, which maximises the effect of the electrostatic septum's kick.

The other two separatrices are  $120^\circ$  apart in phase space. Thus, the extracting separatrix could be moved by a maximum of  $15^\circ$  anticlockwise before the preceding separatrix hits the electrostatic septum, or  $15^\circ$  clockwise before the following separatrix hits the magnetic septum.

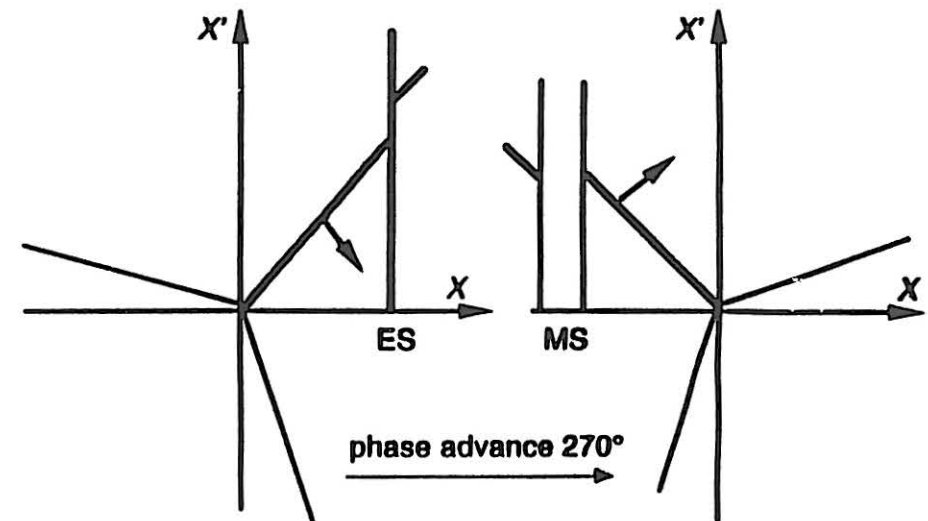


WHAT VARIATIONS EXIST ON THIS THEME ?

## SEPARATRIX GEOMETRY FOR EXTRACTION (2)

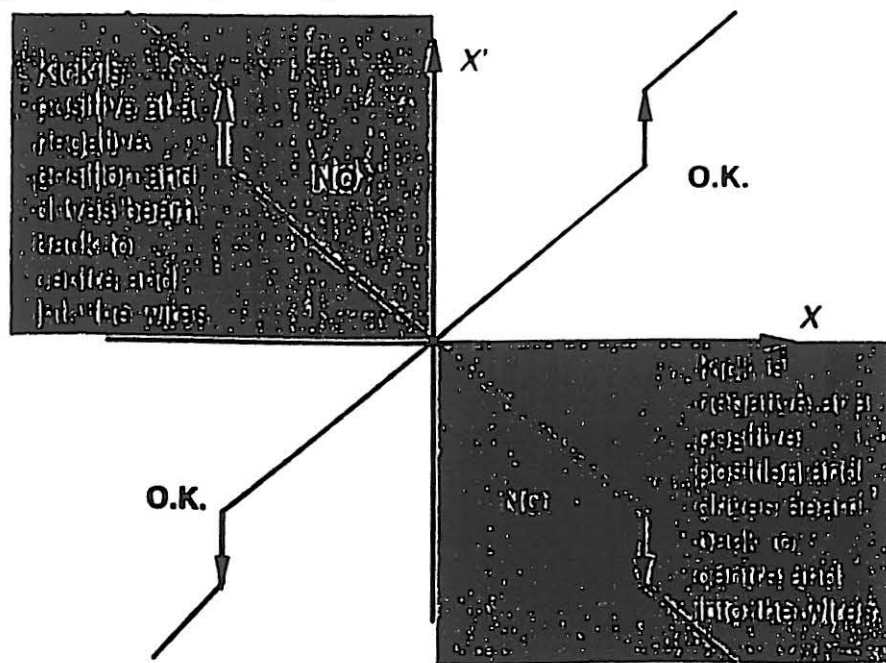
The alternatives to the layout on the previous page are limited. The first is to accept a much smaller phase advance of say  $40^\circ$  or less. This situation may be imposed by lack of space and requires much stronger electrostatic and magnetic septa. In the case of the electrostatic septum, this may have implications for the reliability.

The second alternative is to allow a  $270^\circ$  phase advance.



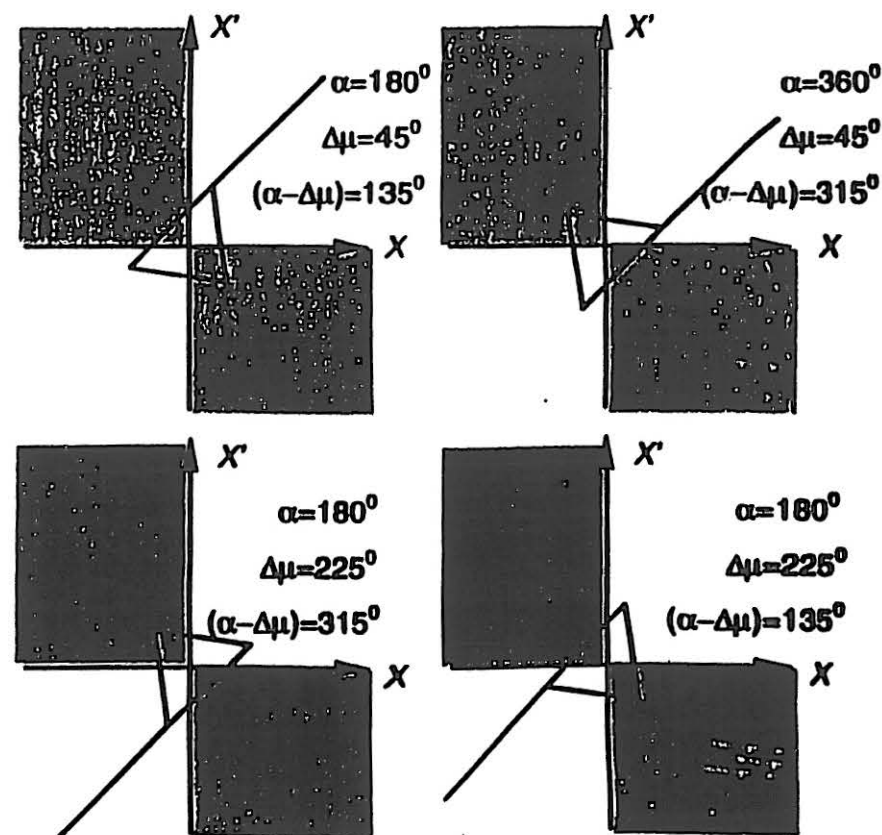
### SEPARATRIX GEOMETRY FOR EXTRACTION (3)

So far the kick of the electrostatic septum has been shown in the first quadrant only. In fact only the first and third quadrants are usable. In the second and fourth quadrants, the kick takes the beam back into the septum wires. The use of the third quadrant gives one extra possibility.



For ideal working conditions, the 1st or 3rd quadrants must be used, with  $90^\circ$  or  $270^\circ$  phase advance between the septa, and with a tolerance of  $\pm 15^\circ$  in the separatrix positions (for much less phase advance one must rely on very strong kicks).

### STABLE-TRIANGLE GEOMETRY FOR 1ST & 3RD QUADRANT OPERATION

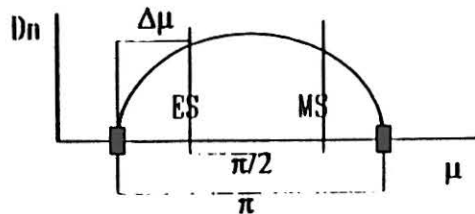


Thus, for the Hardt condition there are only two values for the phase term  $(\alpha - \Delta\mu)$  i.e.  $315 \pm 15^\circ$  and  $135 \pm 15^\circ$ .

## SECTION B

The normalised dispersion terms take a simple form in dispersion bumps,  $360^\circ$  achromatic arcs and regular FODO or doublet structures that are common in small machines.

### Dispersion bumps



$$\text{where, } D_n = D_{n,0} \sin \Delta\mu, \quad D'_n = D_{n,0} \cos \Delta\mu.$$

### Achromatic arcs

The variations of  $D_n$  and  $D'_n$  are very much the same as for the dispersion bump except that the curve is less smooth due to the distributed dipoles.

### Regular FODO and Doublet structures

In these structures the normalised dispersion function takes a form close to a sine wave with a dc offset.

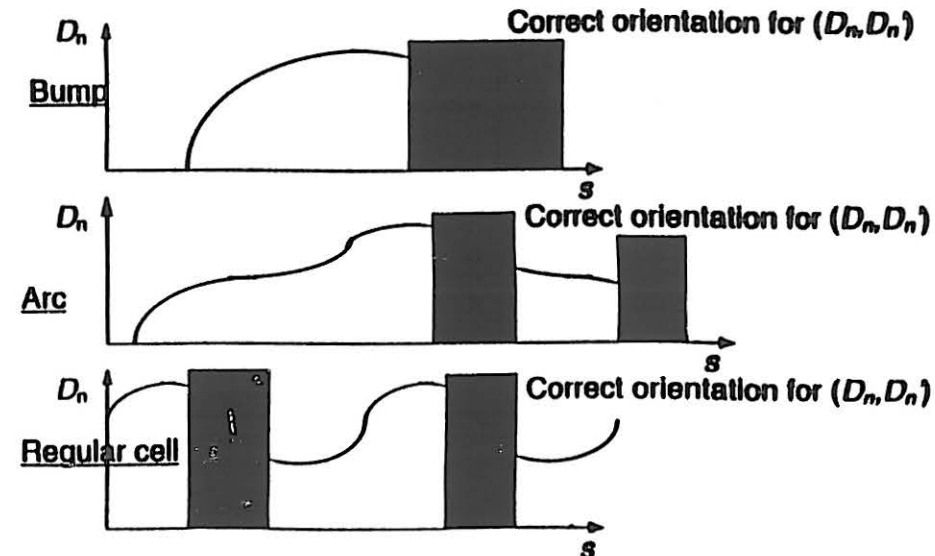
The relative usefulness of these structures can be demonstrated by numerical calculations.

## WHAT IS NEEDED OF THE $(D_n, D'_n)$ VECTOR

The  $(D_n, D'_n)$  vector moves the stable triangles for different momenta to superposition the separatrices.

The separatrices that can be used are at  $45^\circ \pm 15^\circ$  in the first quadrant and at  $225^\circ \pm 15^\circ$  in the third quadrant. Thus, the most efficient  $(D_n, D'_n)$  vectors for corrections will be at  $135^\circ \pm 15^\circ$  or  $315^\circ \pm 15^\circ$ , i.e. approximately at rightangles to the separatrices.

Thus, for bumps, arcs, regular lattices etc. the favoured position for an electrostatic septum is on the downward slope of  $(D, D')$ , but this is the least efficient for providing space for the magnetic septum without crossing dipoles between the septa.



## SECTION C

## STABILITY OF THE WAITING BEAM

Since any fluctuation in the waiting stack will appear, greatly magnified, in the spill, the stability of the waiting beam is of prime importance.

Below transition, beams are intrinsically stable longitudinally. The transverse stability is of more concern. The criterion for stability is,

$$|Z_T| \leq F_2 \frac{E_0}{e} \frac{4Q_0\gamma\beta}{IR} \frac{\Delta p_{fwhm}}{p_0} |(n-Q)\eta - Q|$$

where  $F_2$  is a form factor (close to unity),  $E_0$  is the proton rest energy,  $R$  is the average machine radius ( $R/Q_0$  can probably be replaced by the average betatron amplitude function),  $I$  is the current,  $n$  is the azimuthal mode number and  $\eta$  is the revolution frequency spread  $[(df/f)/(dp/p) = 1/\gamma^2 - 1/\eta^2]$ . The mode to be considered will probably be  $n$  close to  $Q$  with  $n > Q$ . This means that for maximum stability of the waiting stack  $Q'$  should be negative.

LEAR works very successfully with positive chromaticity, but LEAR has an active feed-back system and works with very small emittances achieved by cooling. Medical rings have larger emittances, especially with multi-turn injection. Octupoles may also provide some stability via an amplitude-frequency spread, but this distorts the resonance line.

## SECTION D

## SPIRAL STEP OR PITCH

## REVISION

The motion in phase space over time intervals of 3 turns was derived as,

$$\begin{aligned} \Delta X_3 &= \epsilon X'_0 + \frac{3}{2} S X_0 X'_0 \\ \Delta X'_3 &= -\epsilon X_0 + \frac{3}{4} S (X_0^2 - X_0'^2) \end{aligned}$$

If the motion is restricted to the vertical separatrix  $X = -(2/3)(\epsilon/S)$ , then

$$\begin{aligned} \Delta X_3 &= \epsilon X'_0 - \epsilon X'_0 = 0 \\ \Delta X'_3 &= \frac{2\epsilon^2}{3S} + \left( \frac{1\epsilon^2}{3S} - \frac{3}{4} S X_0'^2 \right) \end{aligned}$$

If this vector is allowed to rotate  $90^\circ$ , it changes from an angular step to a positional step given by,

Spiral step

$$\begin{aligned} \Delta X'_3 &= 0 \\ \Delta X &= \frac{\epsilon^2}{S} - \frac{3S}{4} X^2 \end{aligned}$$

## SECTION E

### NUMERICAL CALCULATIONS - STRATEGY

- To determine  $S$  on the basis of a 10 mm projection of the spiral step onto the  $x$  axis at the electrostatic septum.
- To use this value to determine the chromaticity via the Hardt Condition with whatever lattice functions are being proposed.
- To determine the  $\delta Q$  corresponding to the last stable orbit for the maximum emittance in the waiting stack.

First, assume that the spiral step along the separatrix is dominated by the second term, so as to eliminate the circular reference to  $\epsilon$ .

$$\Delta R \approx \frac{3S}{4} X^2$$

Set  $\Delta R = 0.01 / [\cos(\phi)\sqrt{\beta}]$  [ $m^{1/2}$ ] where  $\phi$  is the angle between the separatrix and the  $X$  axis and, initially,  $X = 0.03/\sqrt{\beta}$  [ $m^{1/2}$ ]. Then apply the Hardt Condition,

$$D_n \cos(\alpha - \Delta\mu) + D'_n \sin(\alpha - \Delta\mu) = \frac{4\pi}{S} Q'$$

with  $(\alpha - \Delta\mu) = 135^\circ$  or  $315^\circ$ .

Finally, find the tune shift for last stable triangle,

$$E_{\text{Beam}} = E_{\text{Last stable triangle}} = \frac{48\sqrt{3}\pi}{S^2} (\delta Q)^2 \pi$$

**ACHROMATIC TRANSFER  
BETWEEN  
ELECTROSTATIC SEPTUM  
AND MAGNETIC SEPTUM**

presented by  
M. Benedikt

February 13th and 14th 1996  
PS, CERN

**PARTICLE MOTION IN A LINEAR LATTICE**

Particle motion in a linear lattice (containing only dipoles and quadrupoles) can be described with transfer matrices.

**Transfer matrix for an on-momentum particle**

The motion of an on-momentum ( $\delta p=0$ ) particle between two lattice elements 1 and 2 with a betatron phase advance  $\mu$  is described by a 2x2 transfer matrix  $M$  (Twiss-matrix), where

$$M = \begin{pmatrix} \sqrt{\frac{\beta_2}{\beta_1}} (\cos\mu + \alpha_1 \sin\mu) & \sqrt{\beta_1 \beta_2} \sin\mu \\ \frac{-1}{\sqrt{\beta_1 \beta_2}} [(1 + \alpha_1 \alpha_2) \sin\mu + (\alpha_2 - \alpha_1) \cos\mu] & \sqrt{\frac{\beta_1}{\beta_2}} (\cos\mu - \alpha_2 \sin\mu) \end{pmatrix}$$

The horizontal position and angle of the particle at element 2 is then given by

$$\begin{aligned} x_2 &= m_{11} \cdot x_1 + m_{12} \cdot x'_1 \\ x'_2 &= m_{21} \cdot x_1 + m_{22} \cdot x'_1 \end{aligned}$$

### Transfer matrix for a particle with momentum deviation

The transfer matrix for a particle with a momentum error  $\delta p$  is a 3x3 matrix:

$$M = \begin{pmatrix} m_{11} & m_{12} & m_{13} \\ m_{21} & m_{22} & m_{23} \\ 0 & 0 & 1 \end{pmatrix}$$

with  $m_{11}$ ,  $m_{12}$ ,  $m_{21}$ ,  $m_{22}$  elements from the 2x2 matrix and  $m_{13}$ ,  $m_{23}$  depending on the dispersion function.

The horizontal position and angle of the particle at element 2 now depend on the momentum deviation  $\delta p$

$$x_2 = m_{11} \cdot x_1 + m_{12} \cdot x'_1 + m_{13} \frac{\delta p}{p}$$

$$x'_2 = m_{21} \cdot x_1 + m_{22} \cdot x'_1 + m_{23} \frac{\delta p}{p}$$

### Expression for $m_{13}$ and $m_{23}$

Consider a particle with a momentum error  $\delta p$  moving on the closed orbit belonging to  $\delta p$ . The horizontal position and angle of the particle at any position  $s$  in the machine is given by

$$x(s, \delta p) = D(s) \frac{\delta p}{p} \quad x'(s, \delta p) = D'(s) \frac{\delta p}{p}$$

and at elements 1 and 2

$$\begin{aligned} x_1(\delta p) &= D_1 \frac{\delta p}{p} & x'_1(\delta p) &= D'_1 \frac{\delta p}{p} \\ x_2(\delta p) &= D_2 \frac{\delta p}{p} & x'_2(\delta p) &= D'_2 \frac{\delta p}{p} \end{aligned}$$

By comparison with the transfer matrix  $M$  expressions for  $m_{13}$  and  $m_{23}$  are derived

$$D_2 = m_{11} \cdot D_1 + m_{12} \cdot D'_1 + m_{13}$$

$$D'_2 = m_{21} \cdot D_1 + m_{22} \cdot D'_1 + m_{23} \quad \text{and}$$

$$m_{13} = D_2 - D_1 \cdot \sqrt{\frac{\beta_2}{\beta_1}} \cdot (\cos\mu + \alpha_1 \sin\mu) - D'_1 \cdot \sqrt{\beta_1 \beta_2} \sin\mu$$

$$m_{23} = D'_2 + \frac{D_1}{\sqrt{\beta_1 \beta_2}} [(1 + \alpha_1 \alpha_2) \sin\mu + (\alpha_2 - \alpha_1) \cos\mu] - D'_1 \cdot \sqrt{\frac{\beta_1}{\beta_2}} (\cos\mu - \alpha_2 \sin\mu)$$

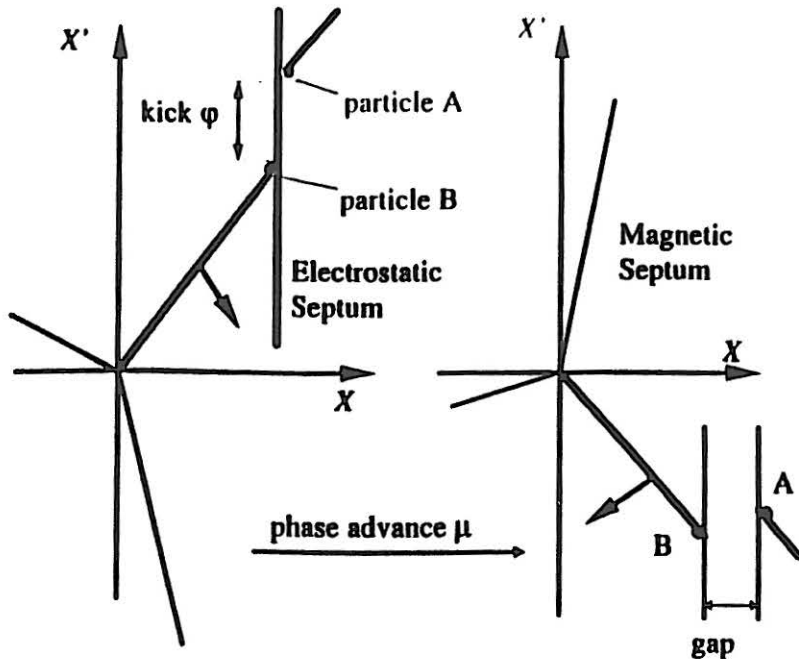
or when using  $D_n$  and  $D'_n$

$$m_{13} = \sqrt{\beta_2} (D_{n2} - D_{n1} \cos\mu - D'_{n1} \sin\mu)$$

$$m_{23} = \frac{1}{\sqrt{\beta_2}} (D'_{n2} - D_{n2} \alpha_2 + D_{n1} (\sin\mu + \alpha_2 \cos\mu) - D'_{n1} (\cos\mu - \alpha_2 \sin\mu))$$

### Effect of the Electrostatic Septum

The electrostatic septum cuts off particles from the separatrices. Particles inside the septum are kicked by the electrostatic field by a certain angle  $\varphi$ . This difference in angle between particles inside the septum and those remaining on the separatrix transforms into a gap further downstream, where the magnetic septum is positioned.



Compare the movement of two on-momentum particles from the electrostatic to the magnetic septum; particle A starts just inside the electrostatic septum, particle B just outside. As the thickness of the ES is about 0.1 mm consider both particles to start at the same position  $x_{ES}$ . Both particles start with the same angle but particle A gets an additional kick  $\varphi$  from the septum. With the 2x2 transfer matrix one finds the positions of the particles at the magnetic septum

$$\begin{aligned} \text{particle A} \quad x_{MS} &= m_{11} \cdot x_{ES} + m_{12} \cdot x'_{ES} + m_{12} \varphi \\ x'_{MS} &= m_{21} \cdot x_{ES} + m_{22} \cdot x'_{ES} + m_{22} \varphi \\ \text{particle B} \quad x_{MS} &= m_{11} \cdot x_{ES} + m_{12} \cdot x'_{ES} \\ x'_{MS} &= m_{21} \cdot x_{ES} + m_{22} \cdot x'_{ES} \end{aligned}$$

Thus, the effect of the kick of the electrostatic septum seen at the magnetic septum gives a difference in position and angle of the particles

$$\Delta x_{MS} = m_{12} \varphi \quad \Delta x'_{MS} = m_{22} \varphi$$

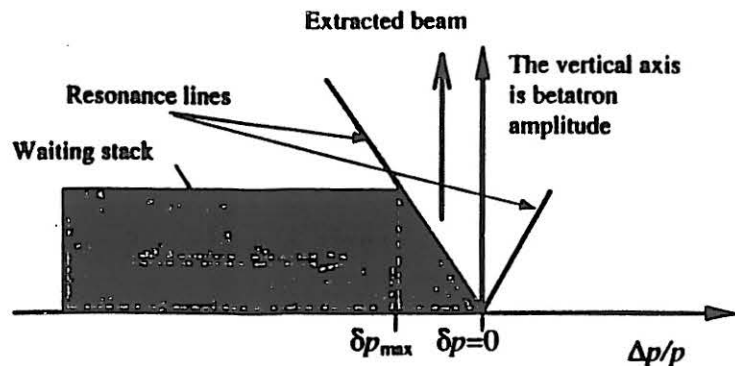
where  $\Delta x_{MS}$  is the gap for the thicker magnetic septum

$$\Delta x_{MS} = \varphi \sqrt{\beta_1 \beta_2} \sin \mu$$

**To make full use of the kick provided by the ES:**

- look for a phase advance of  $90^\circ + n \cdot 360^\circ$  (septa on same side of vacuum chamber) or
- $270^\circ + n \cdot 360^\circ$  (septa on opposite sides)
- look for reasonable values of  $\beta_{ES}$  and  $\beta_{MS}$

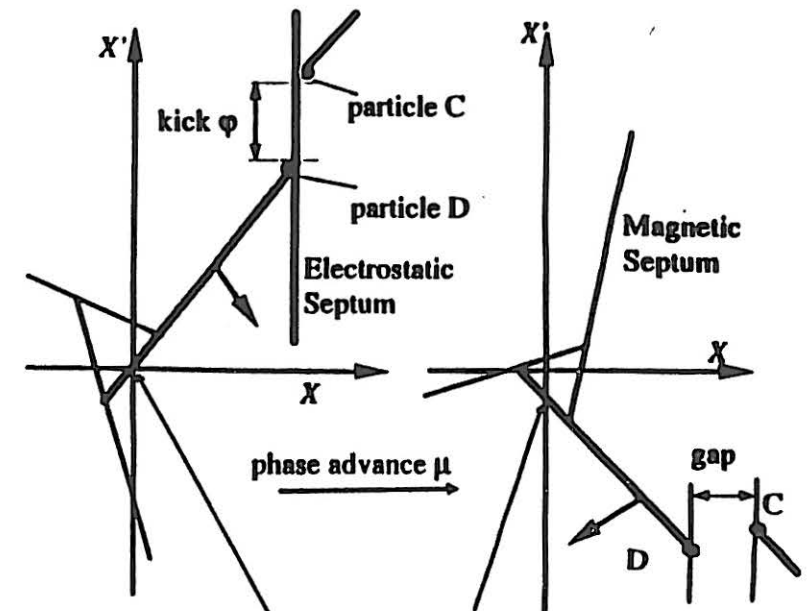
Generally, during the extraction process particles with different momenta are extracted at the same time. (This is not the case when using a transport mechanism that cuts slices of particles with equal momenta from the waiting stack and brings them into the resonance.)



If the Hardt Condition is fulfilled, separatrices for particles with different momenta and amplitudes are superimposed. Therefore, all extracted particles reach the electrostatic septum on the same separatrix. As the momentum spread is small (approximately 0.1%) all particles inside the electrostatic septum get almost the same kick.

**Transfer from ES to MS for particles with  $\delta p_{max}$**

Particle C starts just inside, particle D just outside the ES



Separatrix is aligned on origin by the Hardt Condition

Hardt Condition no longer applies at MS so separatrix moves away from origin

Using the 3x3 transfer matrix between the two septa, one finds:

particle C  $x_{MS} = m_{11} \cdot x_{ES} + m_{12} \cdot x'_{ES} + m_{13} \cdot \frac{\delta p}{p}$

$x'_{MS} = m_{21} \cdot x_{ES} + m_{22} \cdot x'_{ES} + m_{23} \cdot \frac{\delta p}{p}$

particle D  $x_{MS} = m_{11} \cdot x_{ES} + m_{12} \cdot x'_{ES} + m_{13} \cdot \frac{\delta p}{p}$  ← shift

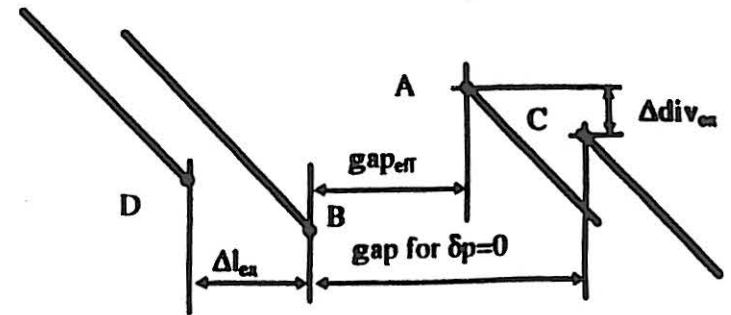
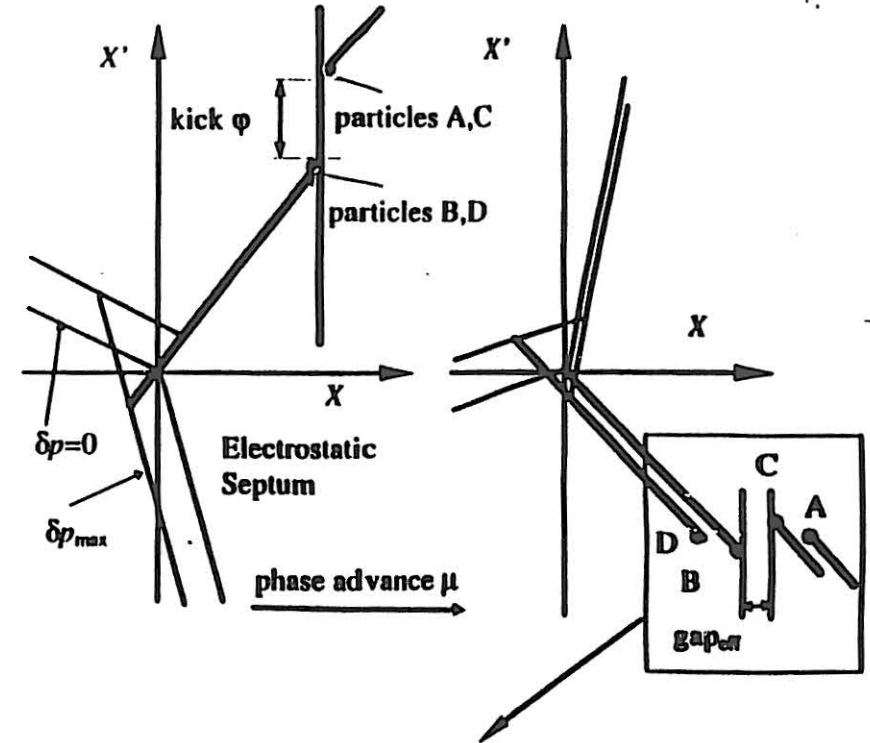
$x'_{MS} = m_{21} \cdot x_{ES} + m_{22} \cdot x'_{ES} + m_{23} \cdot \frac{\delta p}{p}$  ← shift

and

$$\Delta x_{MS} = m_{12} \varphi \quad \Delta x'_{MS} = m_{22} \varphi$$

The gap created by the ES is the same as for an on-momentum particle, but it appears at a different position and angle. The shift in position reduces the effective gap width for the magnetic septum.

### Geometric situation at the septa



## EFFECTS OF NON-ZERO $m_{13}$ AND $m_{23}$

A non-zero  $m_{13}$  causes a loss of space for the MS and has to be corrected with a stronger kick of the ES

$$\text{gap}_{eff} = m_{12} \cdot \psi - \left| m_{13} \cdot \frac{\delta p}{p} \right|$$

The extracted part of the beam becomes longer and requires a larger horizontal aperture in the MS

$$\Delta l_{ex} = \left| m_{13} \frac{\delta p}{p} \right|$$

A non-zero  $m_{23}$  is leading to a bigger divergence of the extracted beam at the MS and also requires a larger horizontal aperture in the MS

$$\Delta div_{ex} = \left| m_{23} \frac{\delta p}{p} \right|$$

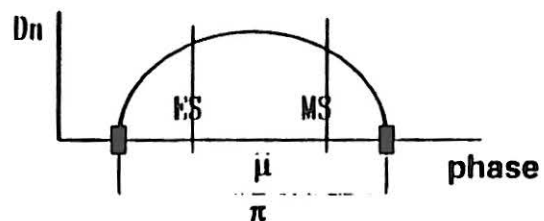
Note: At the ES any angle error will lead to losses, but at the MS there will be a small clearance of say 1 mm and angular spreads up to 1 mrad (approx.) will not lead to losses. For this reason, only the  $m_{13}$  will be considered further.

## MINIMISATION OF EFFECTS OF $m_{13}$

- To fulfill the Hardt Condition, the ES must be in a region with dispersion (to date, we have only considered positive dispersion at the ES). Fulfilling the Hardt Condition fixes the  $\delta p/p_{max}$  of the extracted beam and therefore it cannot be used to compensate the effects of a non-zero  $m_{13}$ .
- The loss of space for the magnetic septum due to  $m_{13}$  being non zero is proportional to  $\sqrt{\beta_{MS}}$ . Decreasing  $\beta_{MS}$  reduces the influence of  $m_{13}$ , but the gap created by the electrostatic septum is also proportional to  $\sqrt{\beta_{MS}}$  and becomes smaller. Overall the effective gap at the magnetic septum is reduced by decreasing  $\beta_{MS}$ .
- The only effective approach is to reduce  $m_{13}$  directly

### MINIMISATION OF $m_{13}$

#### 1 Both septa in a bending-free dispersion region



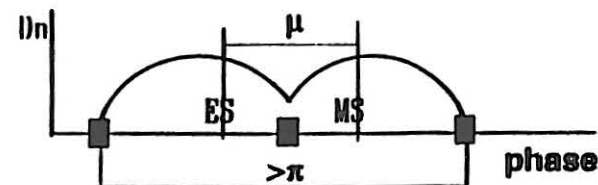
In a bending free-region, the dispersion behaves like a betatron oscillation and can therefore be described with a 2x2 transfer matrix

$$\begin{pmatrix} D \\ D' \end{pmatrix}_{MS} = \begin{pmatrix} m_{11} & m_{12} \\ m_{21} & m_{22} \end{pmatrix} \begin{pmatrix} D \\ D' \end{pmatrix}_{ES}$$

Using this transformation for  $D$  and  $D'$  it follows directly that  $m_{13}$  and  $m_{23}$  are zero and therefore:

The transfer via a dispersion region without crossing bending magnets is always achromatic with respect to position and angle.

#### 2 Both septa in regions with dispersion and bending



The transfer element  $m_{13}$  is given by:

$$m_{13} = \sqrt{\beta_{MS}} (D_{n,MS} - D_{n,ES} \cos \mu - D'_{n,ES} \sin \mu)$$

To make full use of the kick provided by the ES make the phase advance either  $\mu = 90^\circ + n \cdot 360^\circ$  or  $\mu = 270^\circ + n \cdot 360^\circ$ .

For  $\mu = 90^\circ + n \cdot 360^\circ$  it follows:

$$m_{13} = \sqrt{\beta_{MS}} (D_{n,MS} - D_{n,ES})$$

and therefore to make  $m_{13} = 0$

$$D_{n,MS} = D_{n,ES} \quad \text{Septa same side } 90^\circ$$

is required. But as shown in the presentation of the Hardt Condition, one needs to work with a negative  $D'_{n,ES}$  so  $m_{13}$  can only be made zero by having negative dispersion at the magnetic septum.

For  $\mu = 270^\circ + n \cdot 360^\circ$  it follows:

$$m_{13} = \sqrt{\beta_{MS}} (D_{n,MS} + D_{n,ES})$$

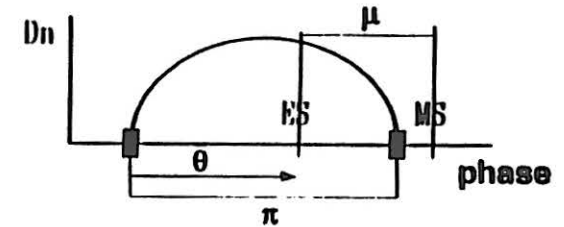
and therefore to make  $m_{13} = 0$

$$D_{n,MS} = -D_{n,ES} \quad \text{Septa opposite sides } 270^\circ$$

is required. In this case,  $m_{13}$  can be made zero by having a positive  $D_{n,MS}$  and a negative  $D'_{n,ES}$  just as required by the Hardt Condition. A disadvantage of this solution might be that the particles which are extracted have to be transported for a longer distance in the machine (e.g. crossing of sextupoles between the two septa would be more difficult to avoid)<sup>1</sup>

<sup>1</sup> If a sextupole is crossed (either resonance or chromaticity) between the ES and the MS, then there is a variable optical element in the extraction channel. Any change in the  $Q'$  or resonance strength alters the extraction geometry

### 3 Electrostatic septum in a dispersion region and magnetic septum in a zero-dispersion region



For  $D_{MS} = 0$ , the transfer element  $m_{13}$  is given by

$$m_{13} = -\sqrt{\beta_{MS}} (D_{n,ES} \cos \mu + D'_{n,ES} \sin \mu)$$

Position the ES in a  $180^\circ$  dispersion bump. If the bump was created by single kicks,  $D_n$  and  $D'_n$  can be described as follows:

$$D_n(\vartheta) = D_{n,0} \cdot \sin \vartheta \quad D'_n(\vartheta) = D_{n,0} \cdot \cos \vartheta$$

and a simple expression for  $m_{13}$  is derived

$$m_{13} = -\sqrt{\beta_{MS}} \cdot D_{n,0,ES} \sin(\vartheta + \mu) \quad \text{coming out of a}$$

$$m_{13} = 0 \quad \text{for } (\vartheta + \mu) = n \cdot 180^\circ \quad \text{dispersion bump}$$

It is difficult to use  $n=1$ , since this gives exactly the position of the dipole which is closing the bump. To keep  $m_{13}$  small, the MS has to be positioned as close to the dipole as possible. For larger  $n$ , there is again the problem of transporting the extracted part of the beam through a larger distance in the machine.

---

#### ***4 Transfer for un-fulfilled Hardt Condition***

Fulfilling the Hardt Condition fixes the chromaticity and the  $\delta p_{\max}$  of the extracted particles.

If one does not fulfill the Hardt Condition, the chromaticity can be used to adjust the  $\delta p_{\max}$  in a way that particles with different momenta arrive at the ES with different angles in order to compensate the effect of a non-zero  $m_{13}$ .

This method is used in the present PS slow extraction scheme.

#### ***5 Transfers from zero dispersion regions to zero dispersion regions are always achromatic***

---

**EMITTANCE OF THE  
SLOW-EXTRACTED  
BEAM**

Presented by  
M. Pullia

Meeting held  
February 13th and 14th 1996  
PS, CERN

**CONSERVATION OF PHASE SPACE**

In a linear machine, the  $(x, x')$ ,  $(z, z')$  and  $(\Delta p/p, t)$  phase spaces are uncoupled and independently conserved.

The presence of a sextupole introduces two couplings:

- (A) Firstly, between  $(x, x')$  and  $(\Delta p/p, t)$ .
- (B) Secondly, between  $(x, x')$  and  $(z, z')$ .

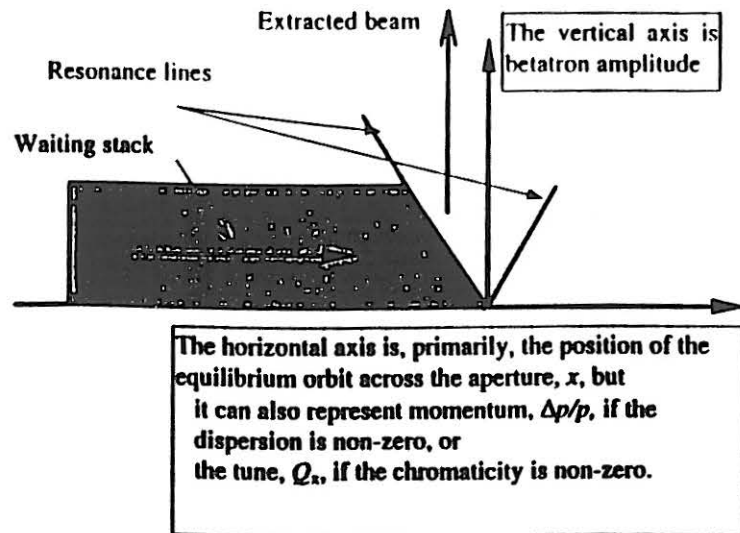
(A) is an essential part of the mechanism of extraction and arises from the time variation of the positions of the separatrices, which "cut" the phase space and "peel" off the particles from the waiting beam.

(B) is an effect that couples the emittances of the two transverse planes. It can be minimised by making the vertical excursions of the particles small compared to the horizontal ones ( $\beta_z \ll \beta_x$  at resonance sextupole). The effect is due to the high-order and cross terms in the magnetic fields; (see basic theory lecture);

$$B_x = 6A_3xz, \quad B_z = 3A_3(x^2 - z^2), \quad \text{where } A_3 = \frac{1}{6} \left( \frac{d^2 B_x}{dx^2} \right)_0.$$

## A GLOBAL VIEW OF THE EXTRACTED EMITTANCE (1)

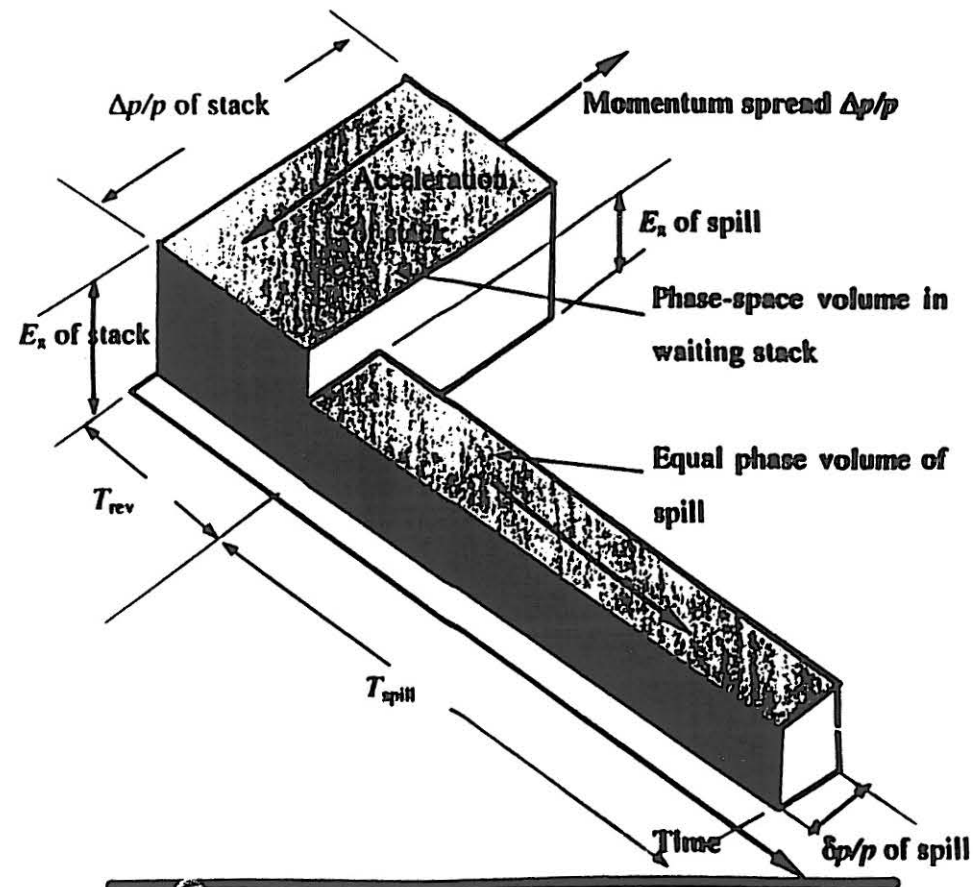
Consider a coasting beam with a relative momentum spread of say  $\Delta p/p = 0.005$  and let this beam be driven into the resonance over say 500 ms. This is represented by the diagrams below,



The Hardt condition is arranged so as to give typically a  $\delta p/p$  for the extracted beam of 0.001. This is determined by the slope of the resonance line. Over the time of the extraction the separatrix acts like a knife shaving off the beam and the phase space.

## A GLOBAL VIEW OF THE EXTRACTED EMITTANCE (2)

The transverse ( $x, x'$ ) and longitudinal ( $\Delta p/p, t$ ) phase spaces are jointly conserved as a phase-space volume. By virtue of this conservation, the effect of the extraction on the transverse phase space can be evaluated by considering the simple model below.



## A GLOBAL VIEW OF THE EXTRACTED EMITTANCE (3)

For the phase-space volumes,

$$E_{x,stack} \left( \frac{\Delta p}{p} \right)_{stack} T_{rev} = E_{x,spill} \left( \frac{\Delta p}{p} \right)_{spill} T_{spill}$$

Some order of magnitude numbers would be,  $E_{x,stack} = 10\pi \times 10^{-6}$  [m rad],  $(\Delta p/p)_{stack} = 0.005$ ,  $T_{rev} = 0.5 \times 10^{-6}$  s,  $(\delta p/p)_{spill} = 0.001$ ,  $T_{spill} = 500 \times 10^{-3}$  s, so that  $E_{x,spill} = 50 \times 10^{-12} \pi$  [m rad].

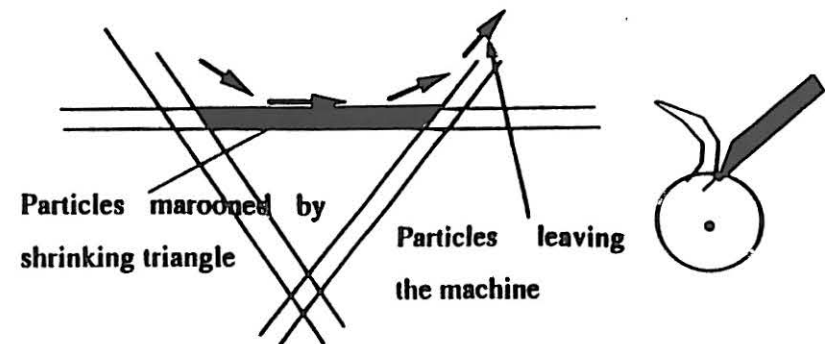
When dealing with small numbers of particles in irregularly shaped regions of phase space, the statistical expression for the emittance, given below, might be more meaningful, but the above can still be used as a guide to the extracted emittance.

$$E_x = \sqrt{\langle X^2 \rangle \langle X'^2 \rangle - \langle XX' \rangle^2}$$

Thus, the extracted emittance in the plane of the resonance will be extremely small. In fact, under ideal conditions (no noise), it will be quasi zero.

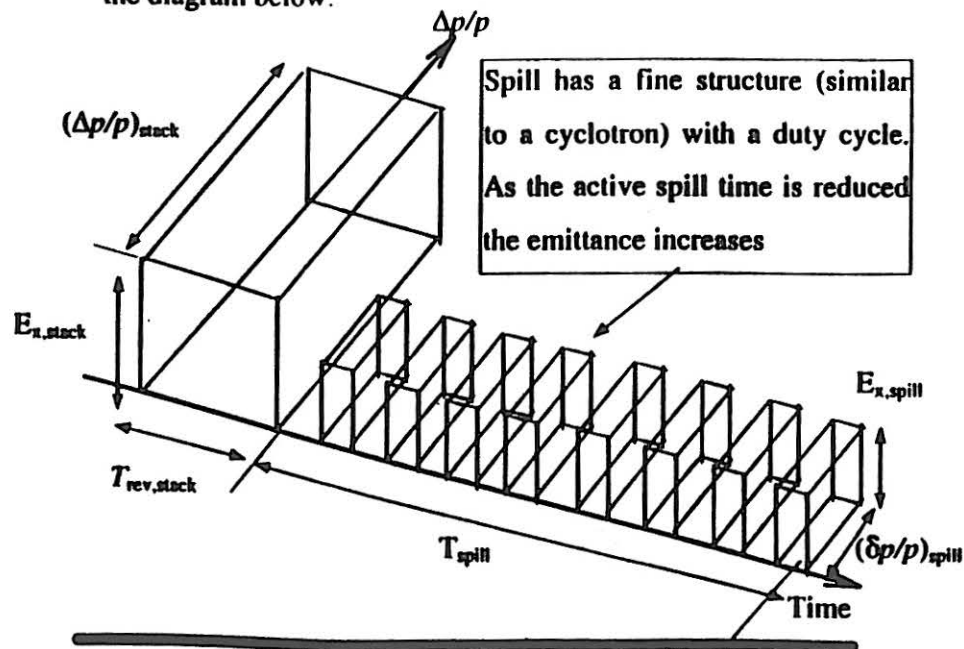
## DETAILED ACTION OF THE SEPARATRIX

Typically, a spill may last 500 ms and the revolution time will be of the order of 0.5  $\mu$ s, so that the full spill would take some  $10^6$  turns of the machine. If the stack has a  $\Delta p/p$  of 0.005 and the extracted beam a  $\delta p/p$  of 0.001, then the collapse of the stable triangle for one particular band of monoenergetic particles would take  $10^6/5 = 2 \times 10^5$  turns. It may take some particles as long as 100 turns to leave the machine, once they are unstable, but this is still very quick compared to the collapse time of the triangle. This means that the band of particles marooned outside the separatrix (unstable but not yet extracted) will never be wider than about  $10^{-3}$  of the full triangle height nor older than 100 turns. Thus, the emittance of the band that is being extracted is about  $10^{-6}$  of the original emittance, which agrees with the above.



## EMITTANCE WITH A TRANSPORT MECHANISM (1)

- Instead of slowly pushing the beam into the resonance, the waiting stack can be kept well away from the resonance and the particles delivered rapidly to the resonance in small "packets". This reduces the effects of power supply ripple.
- By crossing the resonance line faster, a larger emittance is "marooned" outside the separatrix and the extracted emittance increases.
- An alternative view of the increase in emittance is seen from the diagram below.



## EMITTANCE WITH A TRANSPORT MECHANISM (2)

The effect of the transport mechanism is to introduce a duty cycle into the spill. Since the active time of the spill is reduced, the extracted emittance increases.

$$E_{x,stack} \left( \frac{\Delta p}{p} \right)_{stack} T_{rev} = E_{x,spill} \left( \frac{\Delta p}{p} \right)_{spill} T_{spill} \left( \frac{1}{\text{Spill duty factor}} \right)$$

where

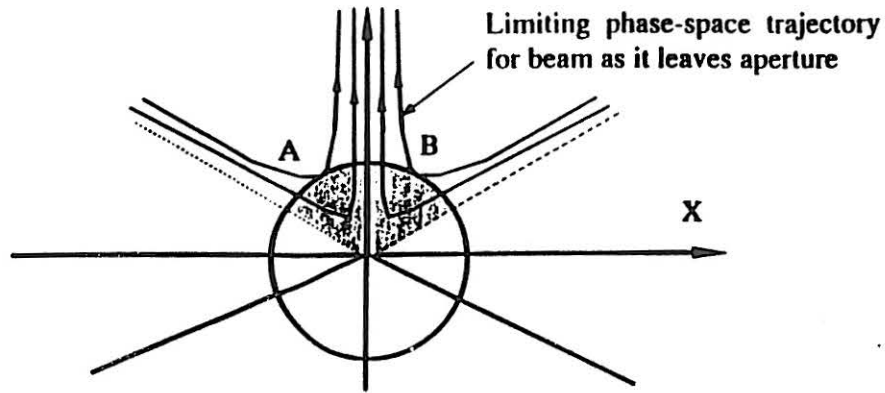
Spill duty factor = Time to cross resonance region (i.e. region covered by the sloping resonance line) over the period between beam packets.

## EMITTANCE WITH RESONANCE WOBBLE

Wobbling the resonance has the same effect as above, as it increases the rate at which the beam crosses the resonance. As the resonance line advances it takes beam and when it retreats there is a pause in the spill.

## WHAT IS THE MAXIMUM EMITTANCE THAT CAN BE EXTRACTED?

This can be calculated by considering the rather impractical case of a monoenergetic beam that is exactly on the resonance tune and is suddenly subjected to a sextupole field. The beam then finds itself instantaneously sitting on phase-space trajectories that leave the aperture as shown below. The stable triangle referred to earlier has collapsed infinitely quickly and left all the particles "marooned" and unstable.



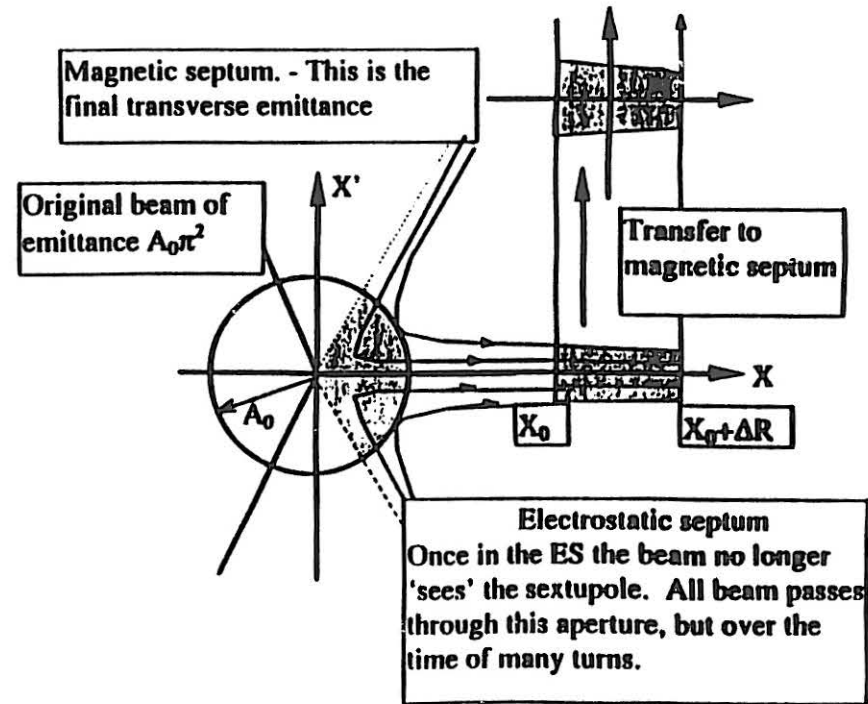
$$H = \frac{\epsilon}{2}(X^2 + X'^2) + \frac{S}{4}(3XX'^2 - X^3) \quad (1)$$

Put  $\epsilon = 0$ , (i.e. infinitely fast application of the resonance) and evaluate  $H$  at the point A or B on the limiting phase trajectories for the beam as it leaves the aperture.

$$H_0 = \frac{S}{4} \left( 3A_0 \cos \frac{\pi}{3} A^2_0 \sin^2 \frac{\pi}{3} - A^3_0 \cos^3 \frac{\pi}{3} \right) \quad (2)$$

$$H_0 = \pm \frac{S}{4} A_0^3 \quad (3)$$

For convenience the diagram is now rotated by  $90^\circ$  and  $X$  becomes  $X'$  and  $X'$  becomes  $X$ . One third of the beam leaves along each separatrix (see below).



Substitute (3) in (1) and rotate by  $90^\circ$ ,

$$A_0^3 = \mp (3X'X^2 - X'^3) \quad (4)$$

The transverse emittance is found by integrating between  $X_0$  and  $X_0 + \Delta R$  (the aperture of the electrostatic septum). Once the beam is as far out as the electrostatic septum  $X' \ll X$  and the  $X'^3$  term can be neglected. Thus,

$$\text{Area} = 2 \int_{X_0}^{X_0 + \Delta R} \left( \frac{A_0^3}{3X^2} \right) dX = \frac{2}{3} A_0^3 \left[ \frac{1}{X_0} - \frac{1}{X_0 + \Delta R} \right] \quad (5)$$

Now express the area as a fraction of the initial emittance, ( $\pi A_0^2$ ) and make the approximation  $(1 + \Delta R/X_0)^{-1} \approx (1 - \Delta R/X_0)$ ,

$$\text{Max. fraction of } E_x \text{ that can be extracted} \approx \frac{2A_0 \Delta R}{3\pi X_0^2} \quad (6)$$

The spiral step  $\Delta R$  has been set already to  $0.01/\sqrt{\beta}$  [ $\text{m}^{1/2}$ ] and  $X_0$  will be  $0.03/\sqrt{\beta}$  [ $\text{m}^{1/2}$ ] or very close to this value. If  $A_0$  is chosen as  $0.01/\sqrt{\beta}$  [ $\text{m}^{1/2}$ ] then the absolute maximum emittance that can be extracted under these conditions is just 2.4% of the original beam.

## EMITTANCE CONTROL

The emittance is important for the spot size at the patient and the optics of the gantry. The preference is for equal transverse emittances, but it seems to be impossible to extract anywhere near equal emittances.

So what methods do exist for controlling the emittance at the moment of extraction, or can the "equal emittance criterion" be relaxed, or what else can be done?

### *At the moment of extraction*

In fact there is little point in varying the emittance between zero and say 1%, but for the completeness of the discussion it can be added that:

- (i) The spill time does enter into the emittance, but the spill time must be fixed according to the operating plan for the machine and will not be an effective means of controlling emittance.
- (ii) The steeper the resonance line, the smaller the extracted momentum spread and therefore the larger the extracted transverse emittance. But again, the slope of the resonance line will not be a free parameter. This is set by the Hardt Condition.
- (iii) The use of a transport mechanism does introduce some flexibility, but it is not sure that a suitable mechanism exists.

### Relaxing the 'equal emittance' requirement

[The following scheme is believed to have been suggested by L. Teng, FNAL, and was reproduced by C. Carli.]

The normal modes in the transfer line preceding the gantry are rotated to match the gantry angle.

If this is done in a bending-free region, the dispersion vector, which behaves like a betatron oscillation, is also rotated.

This scheme has two advantages:

(i) Unequal emittances can be used, just as if the system had normal optics

(ii) It is no longer necessary to start and finish with zero dispersion, which is difficult in the limited space of the gantry with the large bending angles. The dispersion can now be launched from earlier in the transfer line (likewise, the focusing can be partially moved to the transfer line). This may reduce the number of quadrupoles and the length of the gantry.

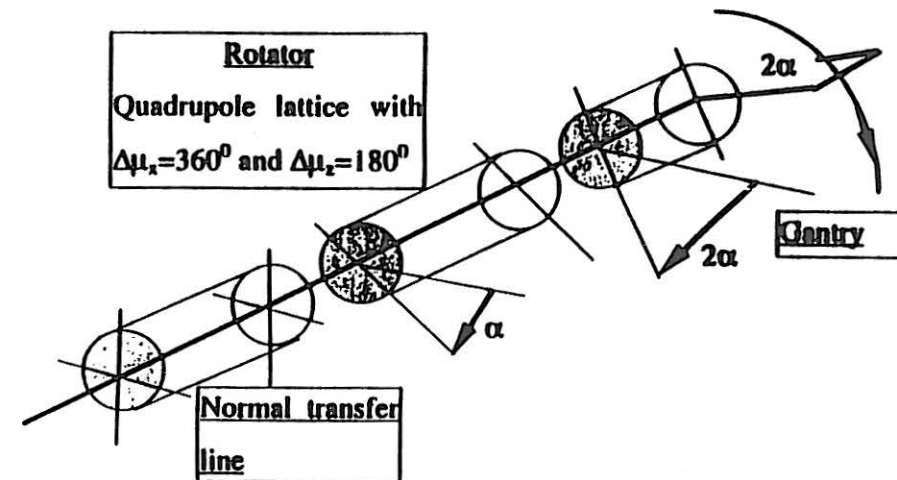
On the negative side, a straight section of transfer line must have its quadrupoles mounted in roller-cradles, but it is relatively easy to rotate a quadrupole compared to a gantry. Moreover, additional space may be required for the rotator.

### NORMAL MODE ROTATION

- Consider a section of bending-free transfer line with a betatron phase advance of  $360^\circ$  in the  $x$ -plane and  $180^\circ$  in the  $z$ -plane. The transfer matrix for the normal modes of this line will be;

$$M_{\text{rotator}} = \begin{pmatrix} 1 & 0 & 0 & 0 \\ 0 & 1 & 0 & 0 \\ 0 & 0 & -1 & 0 \\ 0 & 0 & 0 & -1 \end{pmatrix} \quad (1)$$

- This line is rotated by  $\alpha$ , which is set to be half the angle of the gantry,  $2\alpha$ .



- Due to the rotation, the angles and positions of each particle in the beam will be resolved into the normal modes of the rotated section according to;

$$\begin{pmatrix} u \\ u' \\ v \\ v' \end{pmatrix}_{\text{Rot}} = \begin{pmatrix} \cos\alpha & 0 & \sin\alpha & 0 \\ 0 & \cos\alpha & 0 & \sin\alpha \\ -\sin\alpha & 0 & \cos\alpha & 0 \\ 0 & -\sin\alpha & 0 & \cos\alpha \end{pmatrix} \begin{pmatrix} x \\ x' \\ z \\ z' \end{pmatrix}_{\text{In}} \quad (2)$$

- If now the gantry follows at an angle  $2\alpha$  (i.e. the rotator is at half the gantry angle) the normal modes are again resolved to give the overall transfer matrix

$$\begin{pmatrix} \cos\alpha & 0 & \sin\alpha & 0 \\ 0 & \cos\alpha & 0 & \sin\alpha \\ -\sin\alpha & 0 & \cos\alpha & 0 \\ 0 & -\sin\alpha & 0 & \cos\alpha \end{pmatrix} \begin{pmatrix} 1 & 0 & 0 & 0 \\ 0 & 1 & 0 & 0 \\ 0 & 0 & -1 & 0 \\ 0 & 0 & 0 & -1 \end{pmatrix} \begin{pmatrix} \cos\alpha & 0 & \sin\alpha & 0 \\ 0 & \cos\alpha & 0 & \sin\alpha \\ -\sin\alpha & 0 & \cos\alpha & 0 \\ 0 & -\sin\alpha & 0 & \cos\alpha \end{pmatrix}$$

$$\begin{pmatrix} \cos\alpha & 0 & \sin\alpha & 0 \\ 0 & \cos\alpha & 0 & \sin\alpha \\ -\sin\alpha & 0 & \cos\alpha & 0 \\ 0 & -\sin\alpha & 0 & \cos\alpha \end{pmatrix} \begin{pmatrix} \cos\alpha & 0 & \sin\alpha & 0 \\ 0 & \cos\alpha & 0 & \sin\alpha \\ \sin\alpha & 0 & -\cos\alpha & 0 \\ 0 & \sin\alpha & 0 & -\cos\alpha \end{pmatrix}$$

$$\begin{pmatrix} \cos^2\alpha + \sin^2\alpha & 0 & \sin\alpha\cos\alpha - \cos\alpha\sin\alpha & 0 \\ 0 & \cos^2\alpha + \sin^2\alpha & 0 & \sin\alpha\cos\alpha - \cos\alpha\sin\alpha \\ -\sin\alpha\cos\alpha + \cos\alpha\sin\alpha & 0 & -\cos^2\alpha - \sin^2\alpha & 0 \\ 0 & -\sin\alpha\cos\alpha + \cos\alpha\sin\alpha & 0 & -\cos^2\alpha - \sin^2\alpha \end{pmatrix}$$

$$\begin{pmatrix} u \\ u' \\ v \\ v' \end{pmatrix}_{\text{Gantry}} = \begin{pmatrix} 1 & 0 & 0 & 0 \\ 0 & 1 & 0 & 0 \\ 0 & 0 & -1 & 0 \\ 0 & 0 & 0 & -1 \end{pmatrix} \begin{pmatrix} x \\ x' \\ z \\ z' \end{pmatrix}_{\text{Input}} \quad (3)$$

Thus, the normal modes  $(x, x')$  and  $(z, z')$  map directly into the gantry modes  $(u, u')$  and  $(-v, -v')$  independent of the gantry angle.

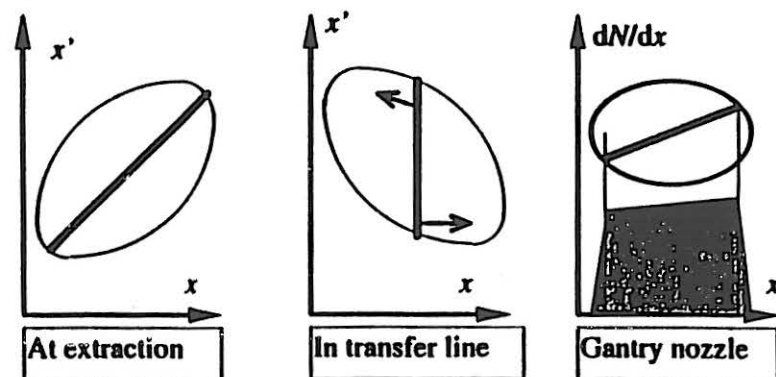
The rotator is optically very simple and could be 4 FODO cells with  $90^\circ$  phase advance in one plane and  $45^\circ$  in the other.

## OTHER CONSIDERATIONS

If a rotator is used to match the normal modes to the gantry angle, then the dispersion vector  $(D, D')$  would also be rotated and matched to the normal modes.

## CONTROLLING THE SPOT SIZE

- At extraction, the beam has its original vertical emittance. Horizontally, it has quasi-zero emittance and is a line distribution about 12 mm long when projected on the  $x$ -axis.
- A 'rotator' makes it possible for this large emittance ratio to be accepted by the gantry, independent of the gantry angle.
- Despite the small horizontal emittance, the spot size can still be controlled with zero dispersion at the patient.
- The horizontal emittance has the form of a very thin "bar" that can be matched to the axis of an ellipse at the input to the transfer line. This ellipse is transferred to the gantry "nozzle". Providing the optical design is 'smooth', the "bar" will remain straight. By adjusting the ellipse size and the phase advance (i.e. the angle of the "bar") any spot size from very small to at least the original 12 mm can be obtained.



## MONTE CARLO SIMULATION OF THE SLOW EXTRACTION

A Monte Carlo simulation of the extraction process has been written with the following approximations:

- 1) the accelerator is not considered in detail, it only appears in the one-revolution matrix in the normalised phase space:

$$\begin{pmatrix} \cos(2\pi Q) & \sin(2\pi Q) \\ -\sin(2\pi Q) & \cos(2\pi Q) \end{pmatrix}$$

- 2) only one sextupole (eventually the corresponding virtual one) is considered. Moreover, it is considered to be a thin lens, that is its only effect is a kick  $\Delta X' = S \cdot (X^2 - \beta_x Z^2 / \beta_x)$  and  $\Delta Z' = -2 S \beta_x X Z / \beta_x$ , where  $S$  is the normalised sextupole strength and  $\beta_x$  and  $\beta_z$  are the betatron amplitudes at the sextupole.
- 3) the beam is generated according to a gaussian density probability in the  $(x, x')$  and  $(z, z')$  phase spaces and with a uniform distribution in momentum of a given width.
- 4) the beam can be accelerated into the resonance by adding a constant  $\Delta p$  to each particle at each turn. All the particles get the same  $\Delta p$ .
- 5) no ripples are considered at the moment.
- 6) the electrostatic septum (ES) is considered infinitely thin and no losses are taken into account. A particle is considered to be extracted when its  $X$  position at (the beginning of) the ES exceeds the  $X$  coordinate of the ES.

## FIRST SIMULATION

## Input parameters:

Alphatx	0.0	
Betatx	7.0	
Epsx	1.38e-6 $\pi$ m rad	(1 $\sigma$ emittance = 40 %)
Alphaty	0.0	
Betaty	2.0	
Epsy	1.38e-6 $\pi$ m rad	(1 $\sigma$ emittance = 40 %)
BetaES	7.0	
Dn	7.405	(to satisfy the Hardt condition)
Dpn	-7.405	(to satisfy the Hardt condition)
MuES	0.78539	
MuESy	0.78539	
PSpread	0.00	(monoenergetic beam)
Qx	2.3333333	(beam on resonance)
Qy	1.58	
Qpx	-5.0	
Qpy	-5.0	
S	-6.0	
dppt	0.0	(no acceleration)
xES	0.03	(m, real space)
Seed	3	(random number seed)

4000 particles have been used, allowing for a maximum number of 500 000 turns  
The first particle is extracted in 129 turns, while the last needs 112 994 turns.  
If the emittance is evaluated using the statistical definition

$$\epsilon = \sqrt{\left( \langle (x - \langle x \rangle)^2 \rangle \langle (x' - \langle x' \rangle)^2 \rangle - \left( \langle (x - \langle x \rangle)(x' - \langle x' \rangle) \rangle \right)^2 \right)}$$

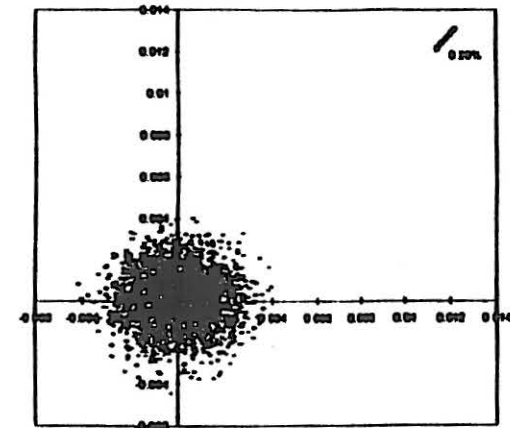
considering all the extracted particles, we get:

$$\epsilon_0 = \text{initial emittance calculated on the generated distribution} = 1.39 \cdot 10^{-6} \pi \text{ m rad}$$

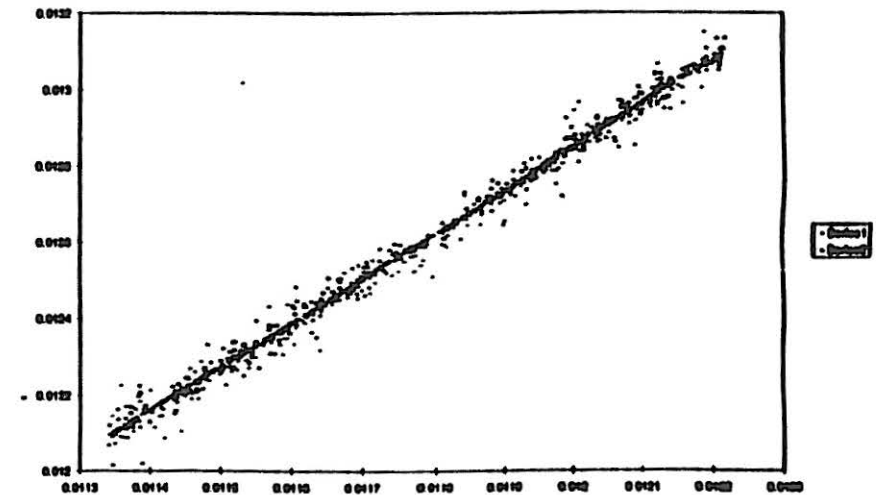
$$\epsilon_E = \text{extracted emittance} = 3.57 \cdot 10^{-9} = 0.0026 \epsilon_0$$

A detailed analysis shows that the extracted emittance varies during the spill from about  $9.4 \cdot 10^{-9}$  at the beginning of the spill to  $1.2 \cdot 10^{-9}$  at the end.

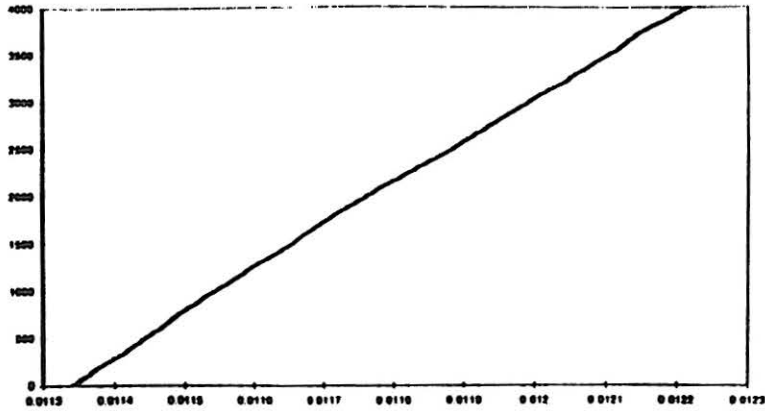
Monoenergetic beam on resonance (extracted in 112 000 turns)



Original beam at the origin and extracted beam in the corner



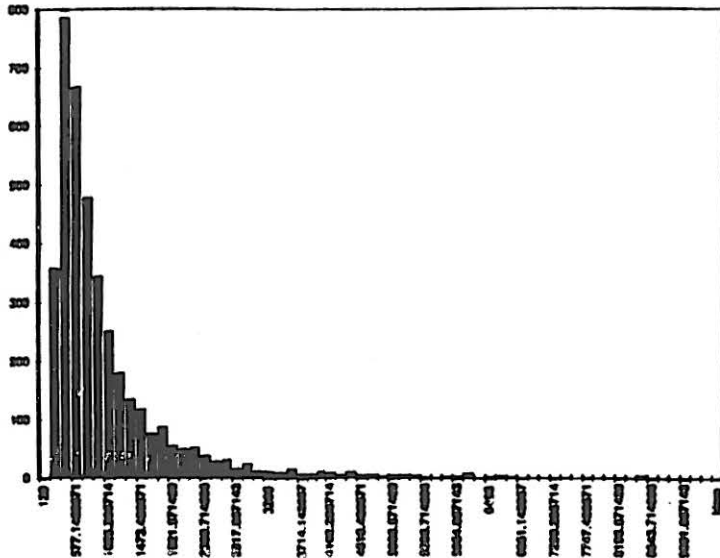
Detailed image of the extracted beam: magenta points represent the first 500 extracted particles; the blue points represent the last 500 extracted particles.



$\int_{XES}^X \rho(a) da$  vs  $X$ . Where  $\rho(X)$  is the density of the extracted beam. This picture shows that the extracted beam is uniform.

shows that the extracted beam is uniform.

Number of extracted particles vs time

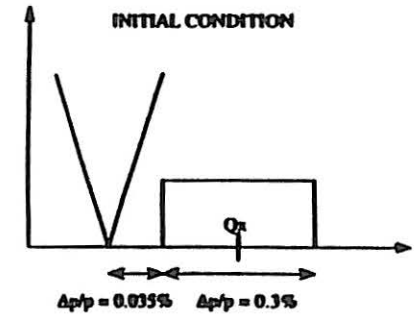


Extracted current vs time

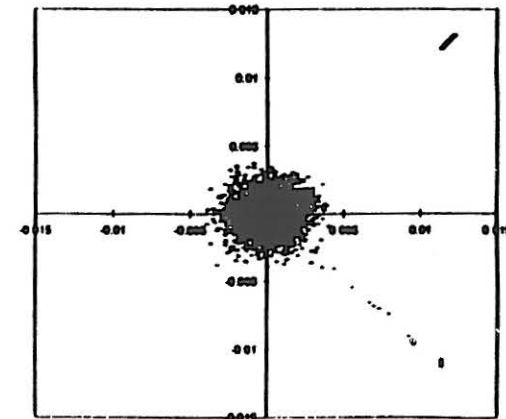
SECOND SIMULATION

Alphatx	0.0
Betatx	7.0
Epsx	5.5e-6
Alphaty	0.0
Betaty	2.0
Epsy	5.5e-6
BetaES	7.0
Dn	7.405
Dpn	-7.405
MuES	0.78539
MuESy	0.78539
PSpread	0.0015
Qx	2.3425833
Qy	1.58
Qpx	-5.0
Qpy	-5.0
S	-6.0
xES	0.03

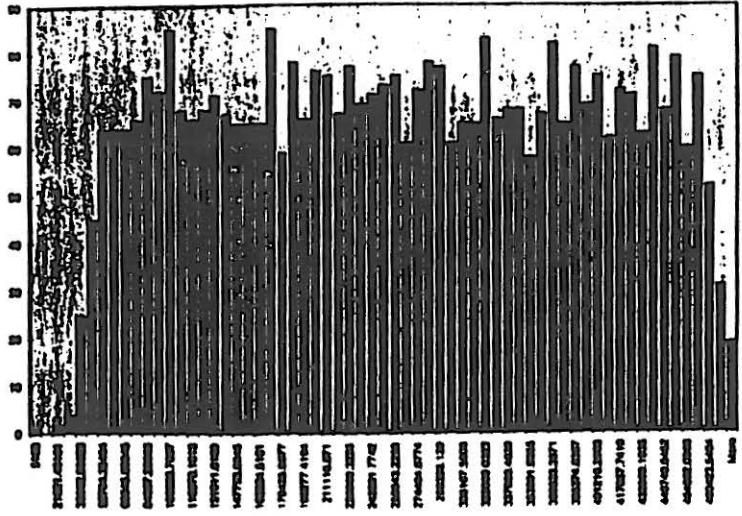
dppt	6.7e-9
Seed	4



The acceleration is such to bring all the beam to the resonance in 500 000 turns. Neglecting the 37 particles out of the 4000 generated that showed a strange behaviour ending their run in the 4th quadrant (see fig.), the emittance of the extracted beam is 1.3 % of the original one.



Time structure of the extracted beam



---

**STRATEGY**  
**FOR THE TRANSVERSE**  
**PHASE SPACE**

presented by  
P.J. Bryant

February 13th and 14th 1996

PS, CERN

---

---

**GENERAL**

•The present aim is to design to a second-generation medical synchrotron that has customised lattice functions to perform specific tasks in different sections of the machine and to implement active energy variation and positional scanning. First-generation machines are characterised by regular lattices with passive scattering systems for changing beam momentum and shape.

•The natural starting point is the resonance extraction and the conditions it imposes upon the machine design.

•Transverse and longitudinal problems will, in many cases, be treated separately, for convenience.

**The initial questions are:**

- How do we manipulate the resonance and the waiting stack?
  - How do we layout the components for the resonant extraction?
  - How do we adapt the lattice to achieve the desired result?
-

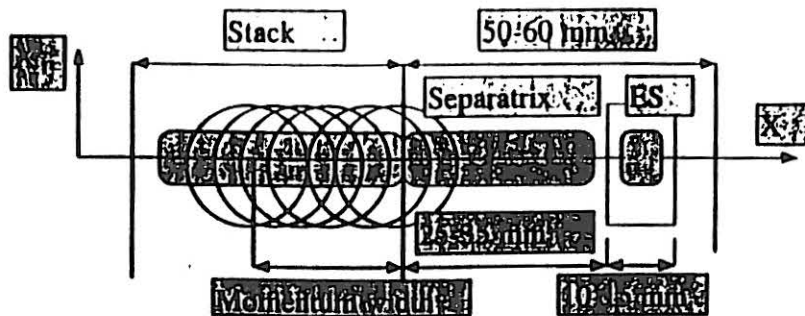
### LAYOUT OF APERTURE

•The resonance needs to be in (or near) the centre of the chamber to give a balanced aperture for the growth of the separatrices.

•For negative chromaticity ( $Q' < 0$ ) the waiting stack must be

In outer half of chamber, if below resonance	In inner half of chamber, if above resonance
---	---

•Approximate dimensions should be:



•Extra aperture and a single passage through the “poor field” region might be needed between the electrostatic and magnetic septa.

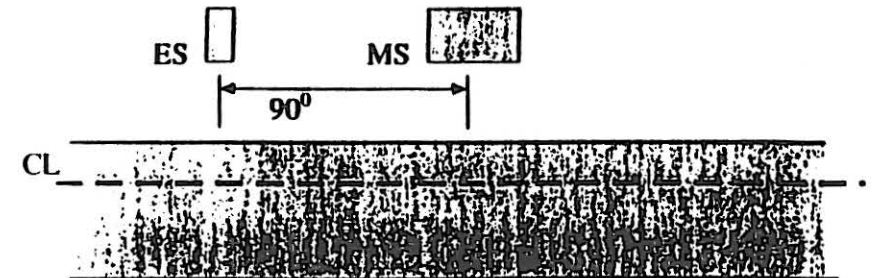
•It is likely that the separatrices (during their final 3 turns) define the maximum aperture requirement.

•The closer the ES is to the resonance, the shorter the separatrices, but the stronger the sextupole, which has a number of disadvantages.

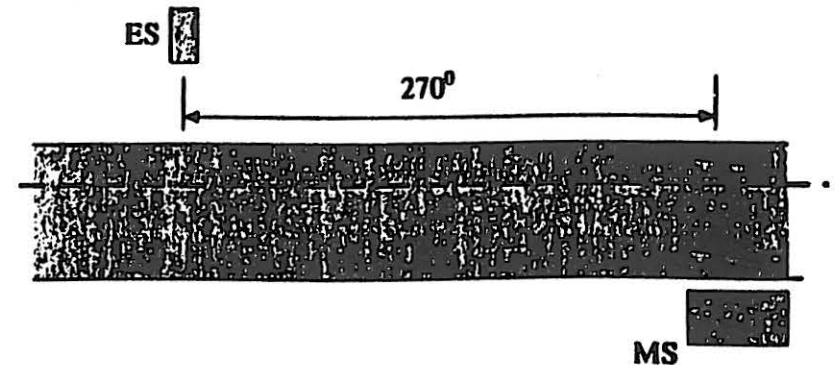
### LAYOUT OF EXTRACTION ELEMENTS

Two principal possibilities exist:

• Septa on the same side of the chamber (inner or outer)



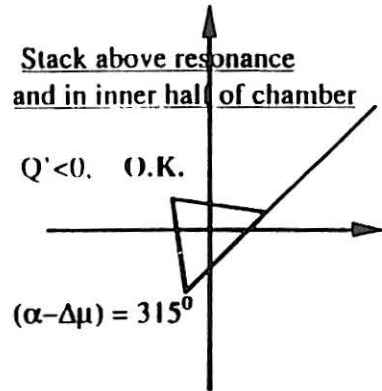
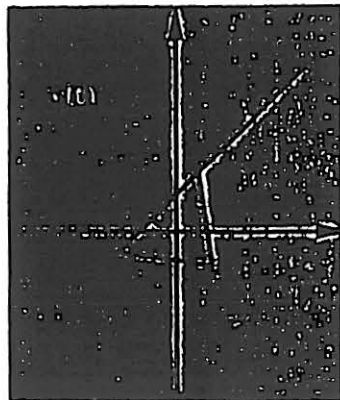
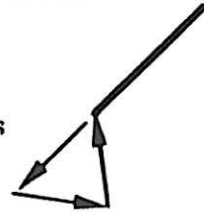
• Septa on opposite sides of chamber



• The electrostatic and magnetic septa will be at approximately equal distances from the centre line, since the electrostatic septum is best positioned at the 45° point on a “rising” separatrix and the magnetic septum at 45° on a “falling” separatrix.

**1ST & 3RD QUADRANT OPERATION**

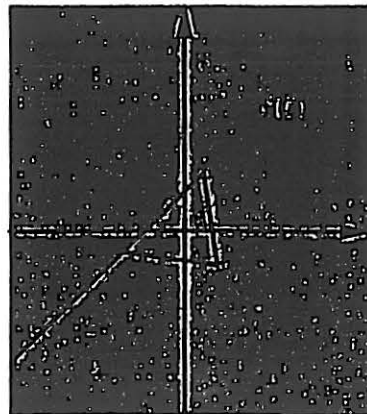
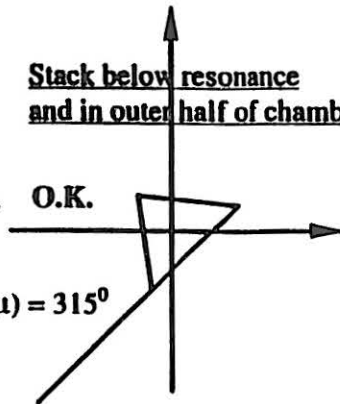
- Note: Anti-clockwise rotation = below resonance
- Negative chromaticity rules out the two possibilities for  $(\alpha - \Delta\mu) = 135^\circ$  in 1st & 3rd quadrants (see earlier)



Stack below resonance and in outer half of chamber

$Q' < 0$ , O.K.

$(\alpha - \Delta\mu) = 315^\circ$



**Second Conclusion**

Of the above two possibilities, the stack positioned above resonance in the inner half of the chamber with  $90^\circ$  phase advance between the septa is preferred. This determines the term  $(\alpha - \Delta\mu)$  for the Hardt Condition to be  $315^\circ$ .

The second choice is the stack below resonance in the outer half of the chamber, but with  $270^\circ$  phase advance to bring the magnetic septum to the outside for easy extraction. This again determines the term  $(\alpha - \Delta\mu)$  for the Hardt Condition to be  $315^\circ$ .

• Operation of the ES in the 2nd and 4th quadrants was ruled out by losses on the septum wires (see Hardt Condition).

• The  $270^\circ$  phase advance is not ruled out, but has two unfavoured aspects: Firstly, it is more likely that it will be necessary to accept a sextupole between the electrostatic and magnetic septa, which puts a variable element into the extraction geometry if the resonance excitation and/or chromatic conditions are changed.

Secondly, it feels, intuitively, that aperture will be lost for the stack by "encasing" it between the two septa. However, that depends on the local lattice functions and may not be a valid objection.

## BUILDING THE LATTICE

*Two things are now required of the lattice for extraction:*

- To satisfy the Hardt Condition with negative chromaticity.
- To provide a  $90^\circ$ , or  $270^\circ$ , achromatic transfer between the electrostatic and magnetic septa.

*A number of candidate lattice types exist:*

- "Square" lattice, using the "corner" dipoles to create dispersion bumps on two opposite sides and dispersion-free straight sections on the remaining two sides.
- The "extended-dispersion-bump" that increases the free space within the dispersion bump by adding a central dipole.
- Lattices that use two arcs separated by dispersion-free straight sections.
- It appears to be very difficult to satisfy all of the "ideal optics conditions" completely, but workable compromises can be found.
- Some discussion of the various lattice types can be found in the chapter Lattice Considerations.

## THE FINAL STRATEGY

- Start from a lattice with two  $360^\circ$ -betatron-phase-advance, achromatic arcs, joined on each side by two dispersion-free straight sections.
- Place the electrostatic septum in the second half of the arc where the Hardt Condition can be adequately fulfilled.
- It is then necessary to relax the requirement of the achromatic transfer between the septa.
- Analytic solutions do exist for crossing dipoles achromatically, but in general these require more phase advance (at least  $270^\circ$ ) than is conveniently available. Large phase advances also increase the possibility of having to include a sextupole between the septa.
- The first compromise is to search for a small  $m_{13}$  term and to leave the  $m_{23}$  term free.
- For the phase advance between septa, look for a compromise that fulfills the Hardt Condition and creates a reasonable gap for the MS while not creating a large  $m_{13}$ .

---

## LATTICE CONSIDERATIONS

M. Benedikt

February 13th and 14th 1996

PS, CERN

---

---

## THE RING

- The underlying construction.
- General features
- The resonance extraction.

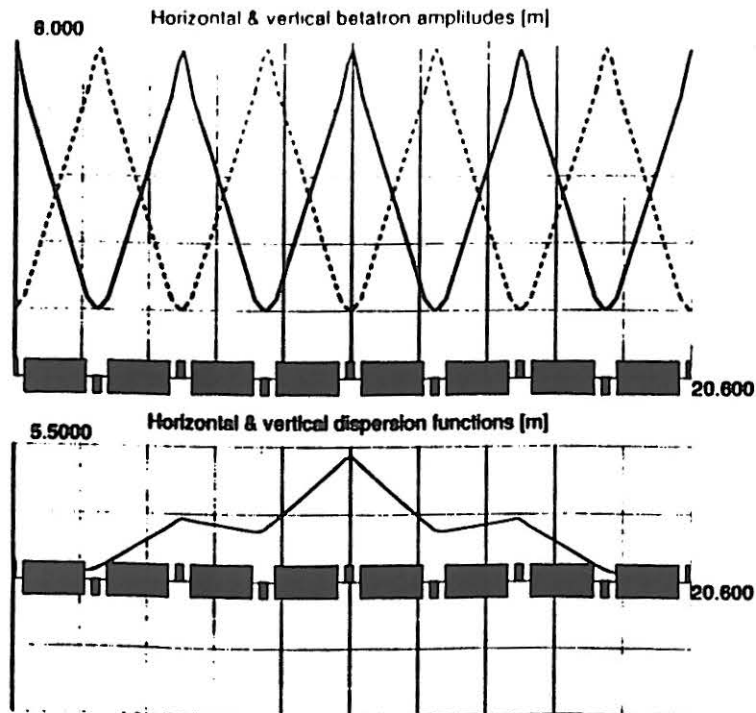
### The underlying construction

- The design is based on two achromatic arcs ( $\mu_x$  and  $\mu_z = 360^\circ$ ,  $180^\circ$  bending) that have been detuned and joined by two dispersion-free straight sections.
    - This type of arc is extremely useful at the start of matching in a symmetric structure, as it will accept any Twiss input values and return them at the exit, always with the same phase advance.
    - A symmetric structure is preferred, since in general it requires fewer quadrupole families.
    - The arc was based on a FODO cell, in which the F was later split to form a FODOF with longer drift spaces after each pair of dipoles. One advantage is that the  $\beta_x$  and  $\beta_z$  are quasi-constant in these drifts. In the normal FODO, they vary rapidly across drift spaces and tune changes can alter values at monitors etc. more easily.
-

• Alternatively, the arc can be described as a series of triplets, in which the  $\beta_x$  is kept small and the vertical focussing of the rectangular dipoles is used to limit the peaks of  $\beta_z$ . The smaller  $\beta_x$  is important for the aperture as the  $D_x$  maximum is large.

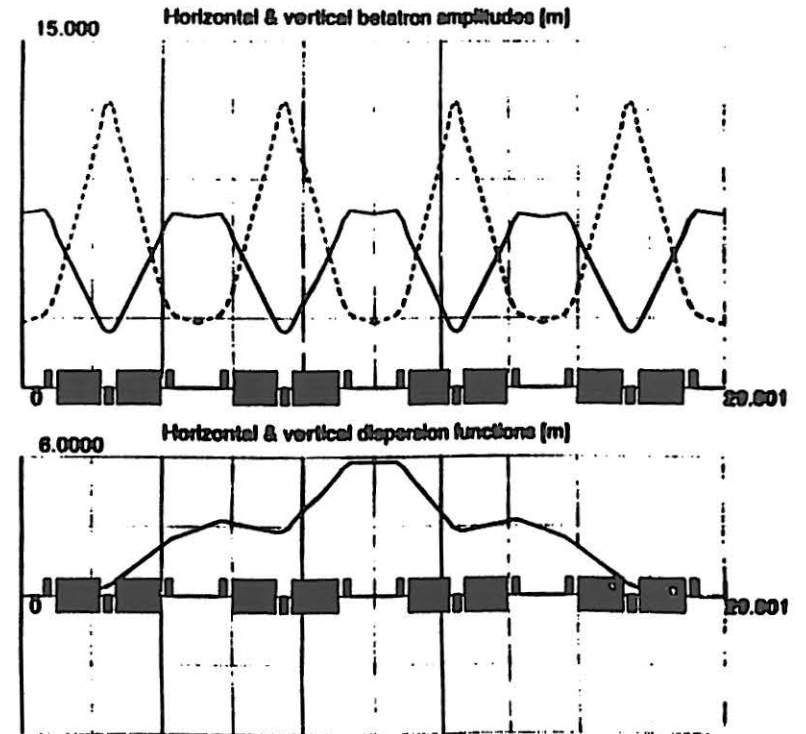
### INITIAL FODO ARC

$$\mu_x = \mu_z = 360^\circ, \quad \beta_{x,in} = \beta_{x,out} = 7.84 \text{ m}, \quad \beta_{z,in} = \beta_{z,out} = 1.616 \text{ m}$$



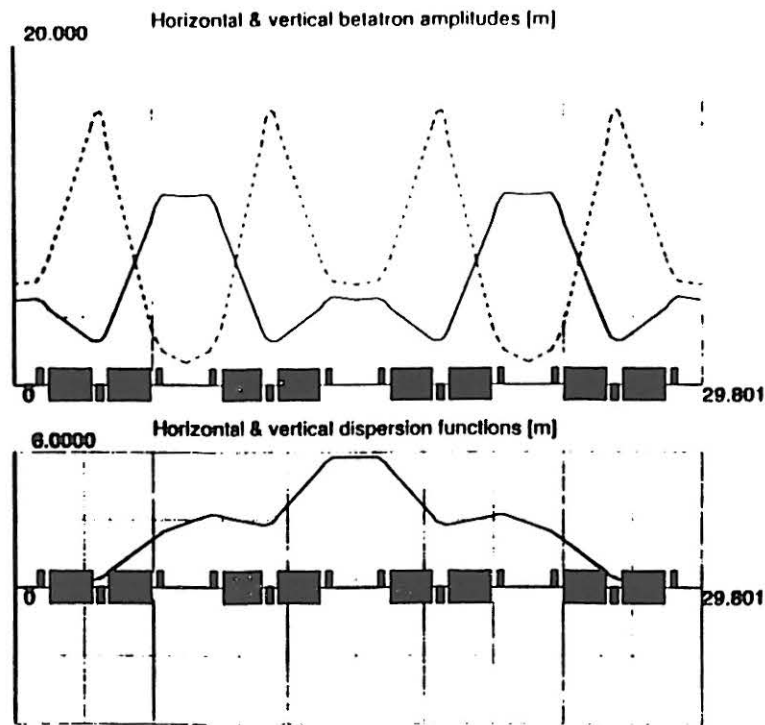
### SPLIT-FODOF-ARC

$$\mu_x = \mu_z = 360^\circ, \quad \beta_{x,in} = \beta_{x,out} = 7.53 \text{ m}, \quad \beta_{z,in} = \beta_{z,out} = 2.81 \text{ m}$$



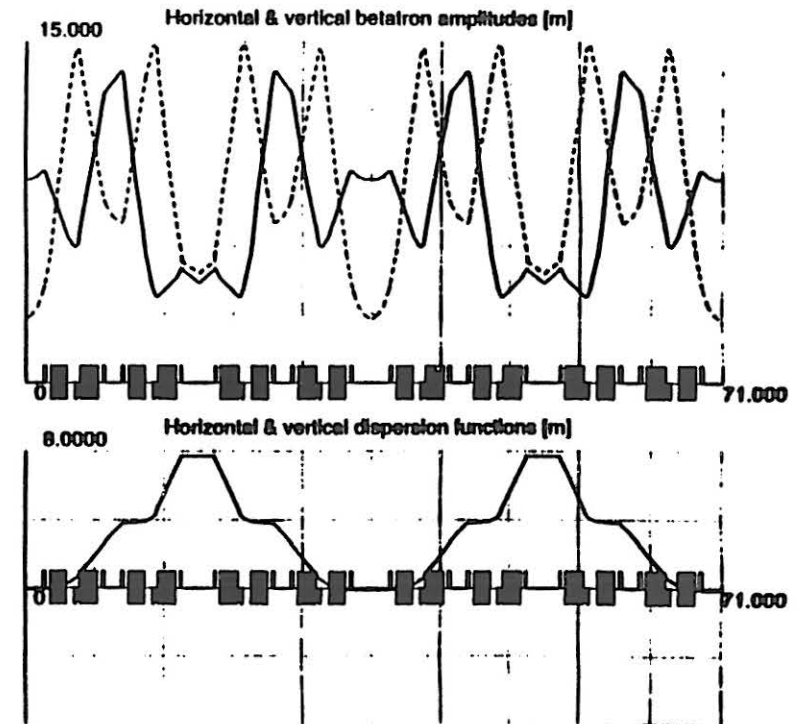
## FLEXIBILITY OF THE SPLIT-FODOF- ARC

$$\mu_x = \mu_z = 360^\circ, \quad \beta_{x,\text{in}} = \beta_{x,\text{out}} = 5 \text{ m}, \quad \beta_{z,\text{in}} = \beta_{z,\text{out}} = 6 \text{ m}$$



The above graph illustrates the ability of the 1:1 mapping arc to return any input values at the exit.

## LATTICE FUNCTIONS

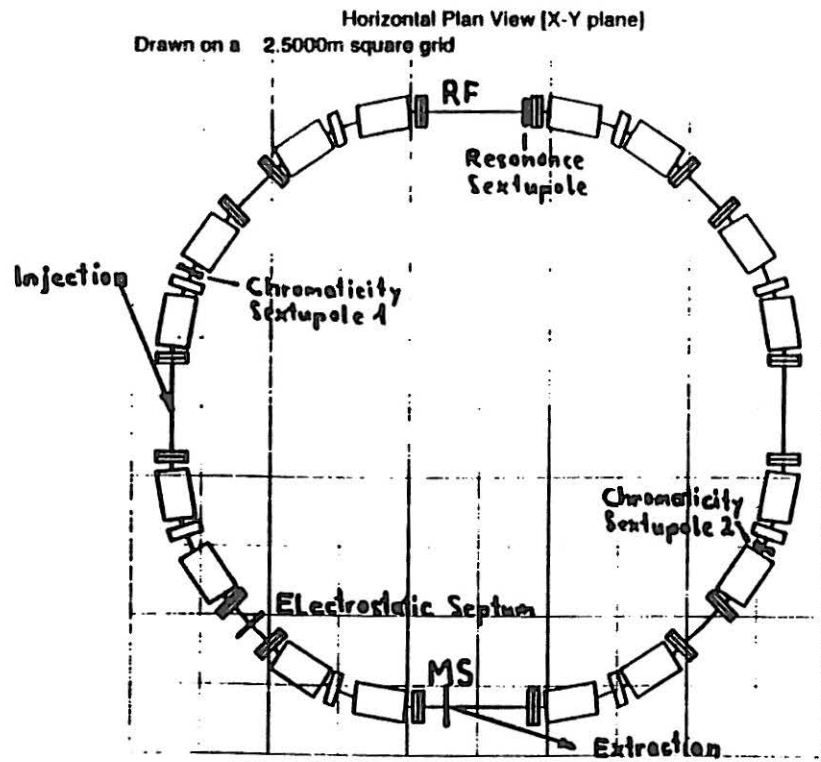


The lattice as shown has 2 quadrupole families. A third family may be introduced later to ensure adequate tuning for space-charge effects at injection.

$$Q_x = 1.66, \quad Q_z = 1.58$$

$$Q'_x = -1.47, \quad Q'_z = 0.44$$

## GEOMETRY



2 superperiods, with mirror symmetry within a superperiod.

Circumference is 71 m

$\gamma_1 = 2.01$

## GENERAL DESIGN FEATURES

• The two dispersion-free regions are reserved for the RF-system(s), resonance sextupole(s) and the magnetic septum. The  $\beta_z$  value has been reduced in these spaces to make the ratio with  $\beta_x$  small ( $\beta_z/\beta_x = 0.33$ ). This minimises the coupling between the two transverse planes ( $\Delta X' = S \cdot (X^2 - Z^2) \beta_z / \beta_x$ ). The low value of  $\beta_z$  is maintained throughout the extraction septum to reduce the vertical aperture. In fact,  $\beta_z$  has its overall minimum for the ring at this position (a 2.8 m waist in the centre of the drift space). Elsewhere, the  $\beta_z$  is limited between 15 m and 4.8 m and  $\beta_x$  between 13.7 m and 3.8 m.

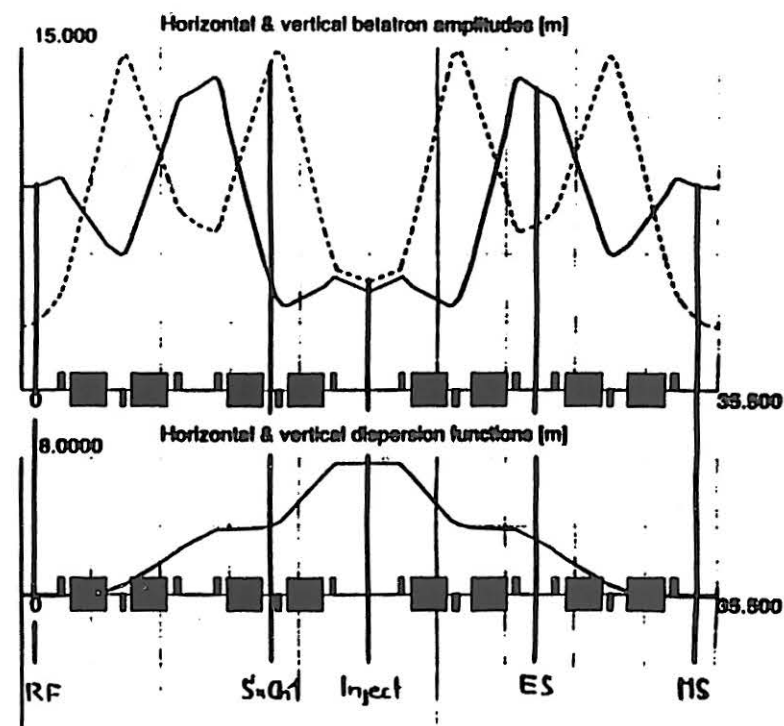
• At the centre of the arc, there is a 9.2 m drift space for multi-turn injection with a combination of betatron and momentum stacking. For this reason  $\beta_x$  is small (4.4 m) and  $D_x$  is large (7.75 m).

• The electrostatic septum has a drift space of 1.7 m

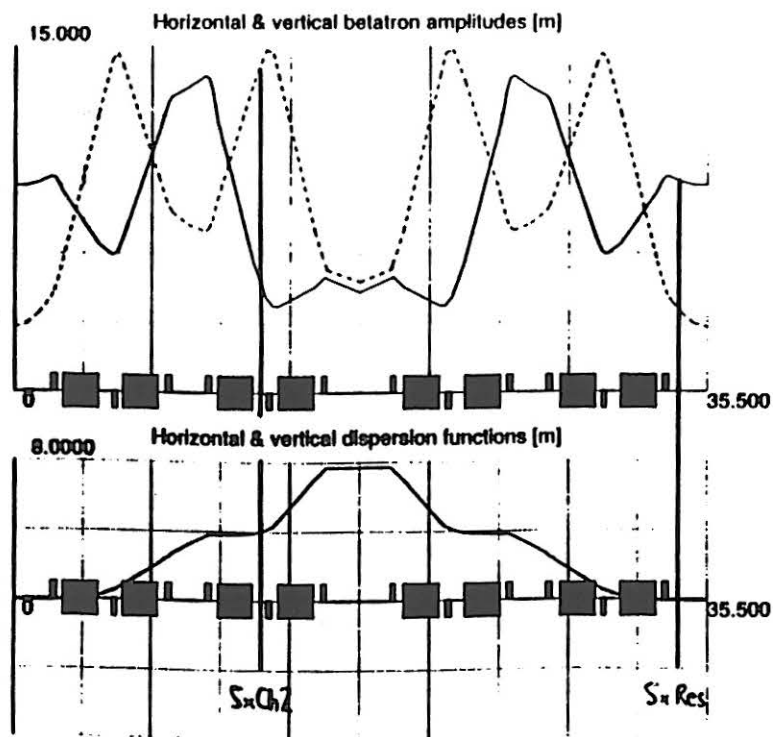
• The magnetic septum has a drift space of 3.8 m, which will mean that only relatively weak septa will be needed.

- The RF has a drift space of 3.8 m.
- The chromaticity sextupoles fit naturally into the arc.
- There are 2 quadrupole families. The quadrupoles are low-field, straight-pole units.
- The very smooth Twiss functions avoid high quadrupole strengths.
- The dipoles are 1.4 T, rectangular magnets 1.85 m long. The sagitta is  $\pm 4.5$  cm, which could be accepted by widening the pole or by slipping the laminations radially to give some curvature.
- Each quadrupole triplet with its two dipoles has a central drift space for diagnostic, vacuum equipment and chromaticity sextupoles.
- The lattice is very flexible and can be tuned over a wide range. This is important for the space charge at injection.

## LAYOUT OF EQUIPMENT IN FIRST HALF OF RING



## LAYOUT OF EQUIPMENT IN SECOND HALF OF RING



## THE RESONANCE

- Both septa are on the same side of the vacuum chamber.
- The electrostatic septum is in the second half of the arc in order to have  $D_n$  positive and  $D'_n$  negative. This allows the Hardt Condition to be satisfied in the most efficient way.

- The magnetic septum is placed in the following dispersion-free drift space. The phase separation of the septa is  $50^\circ$ , which gives 80% of the maximum theoretical gap opened by the kick of the electrostatic septum. The phase shift of  $50^\circ$  has been chosen as a compromise with the  $45^\circ$  that reduces the  $m_{13}$  term to zero. The terms in the transfer matrix quantify this balance:

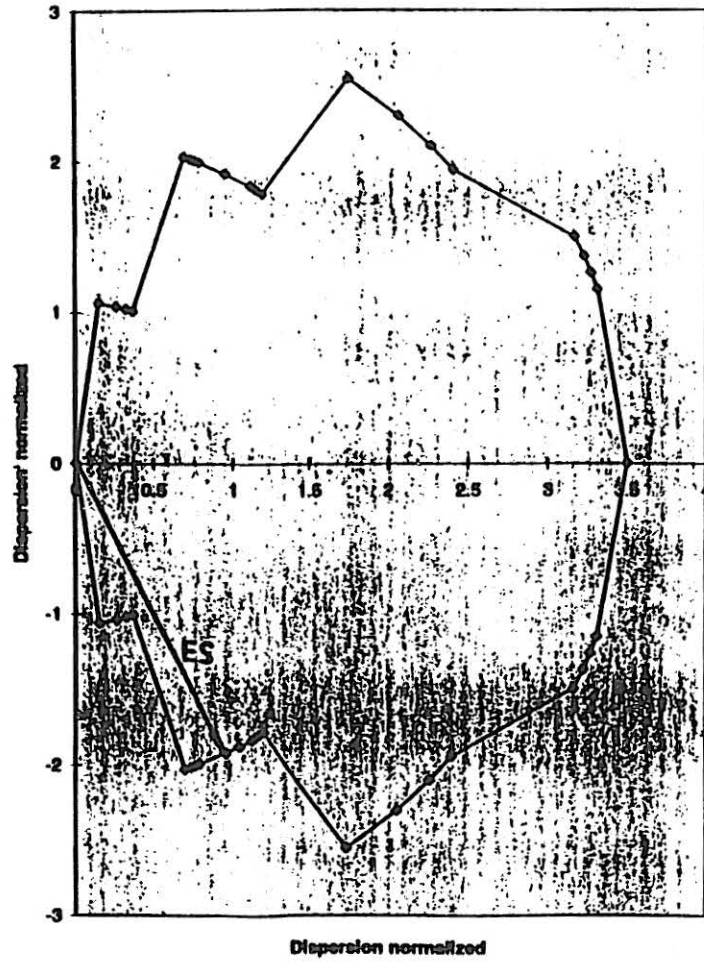
$m_{12} = 8.6$ , which with a 2 mrad kick gives 17.2 mm

$m_{13} = 2.9$ , which with  $\Delta p/p = 0.001$  cuts the gap by 2.9 mm.

- Since phase advance between the septa is less than  $90^\circ$ , the separatrix has been advanced in phase to make it more perpendicular to the  $D_n, D'_n$  vector.

- The  $Q'_x$  is negative (Hardt Condition), which ensures the stability of the coasting beam.  $Q'_z$  must be set negative.

### $D'_N$ VERSUS $D_N$ FOR ONE SUPERPERIOD



### EXTRACTION PLOTS AT ES AND MS

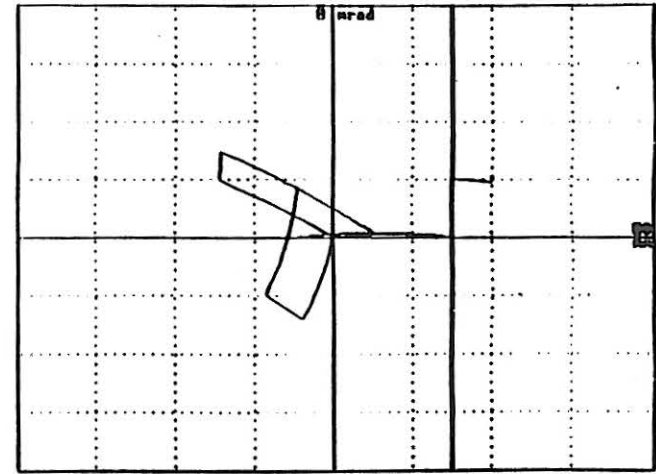


Fig. 1 : PHASE PLANE AT ES

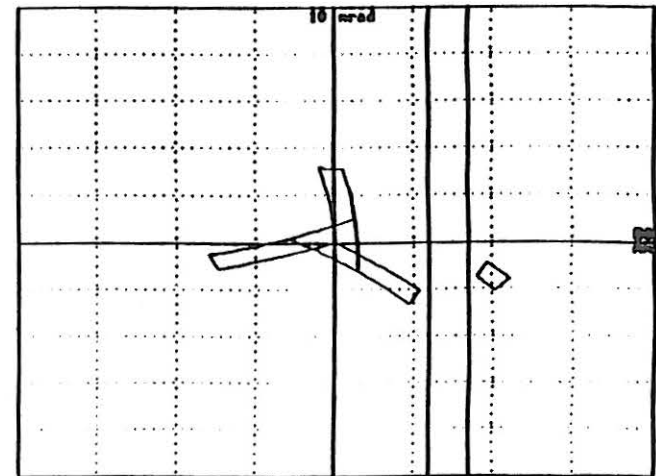


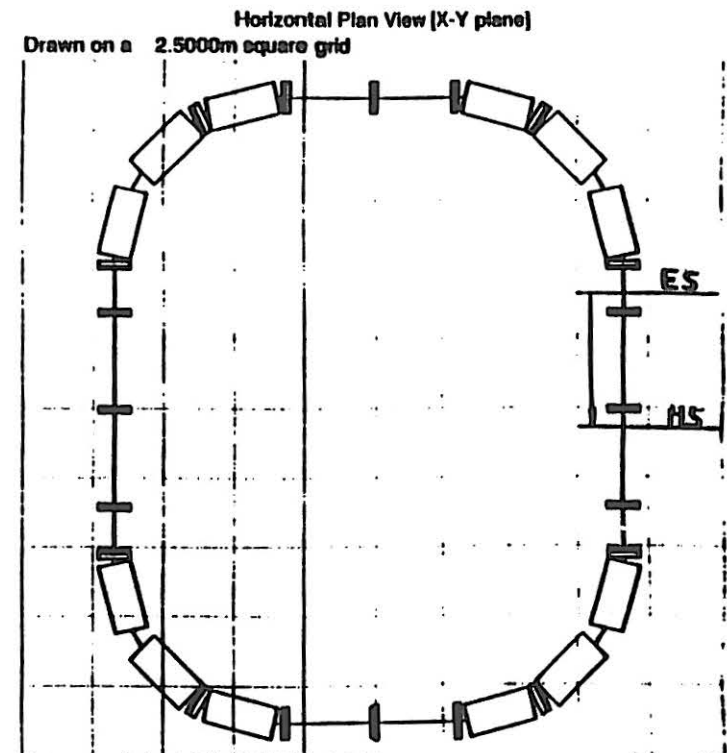
Fig. 2 : PHASE PLANE AT SEPTUM

## GENERAL CONSIDERATIONS FOR OTHER LATTICE TYPES

### Square lattice with two 180° dispersion bumps

- The septa are positioned in the straight section in one dispersion bump on the same side of the vacuum chamber.
- As there are no dipoles in between the septa the transfer is achromatic
- The phase advance between the septa is small and therefore a much stronger kick of the electrostatic septum is required.
- The Hardt Condition can be fulfilled but with positive chromaticity, which is unfortunate for stability.

## "SQUARE" LATTICE



$$Q_x = 1.66; Q_z = 1.57$$

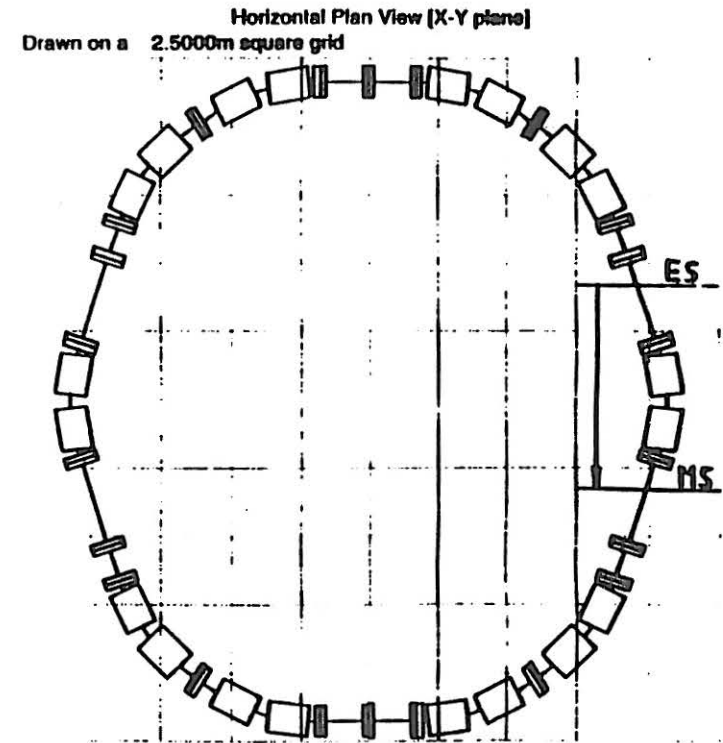
$$\text{Circumference} = 71.8 \text{ m}$$

$$\text{Phase advance ES to MS} = 32^\circ$$

### Lattice with an extended dispersion bump

- To increase the phase advance between the septa a dipole(s) is added to make a double bump.
- The septa are positioned on either side of the central dipole(s) on the same side of the vacuum chamber.
- As there is now a dipole(s) in between the septa the transfer is no longer achromatic
- The phase advance between the septa is increased with respect to the "square" lattice and the electrostatic septum kick is reduced.
- It is difficult to fulfill the Hardt Condition with negative chromaticity.

### Extended dispersion bump lattice



$$Q_x = 2.33; Q_z = 1.58$$

Circumference = 72 m

Phase advance ES to MS =  $77^\circ$

## LONGITUDINAL ASPECTS OF SLOW EXTRACTION

Combined notes on :

Stochastic and other means of rf acceleration to  
'feed' the resonance, 'Empty bucket'  
stabilisation of the spill and General  
longitudinal strategy

presented by  
R. Capi

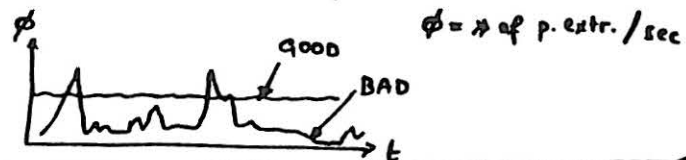
February 13th and 14th 1996

PS, CERN

### INTRODUCTION

what is the problem?

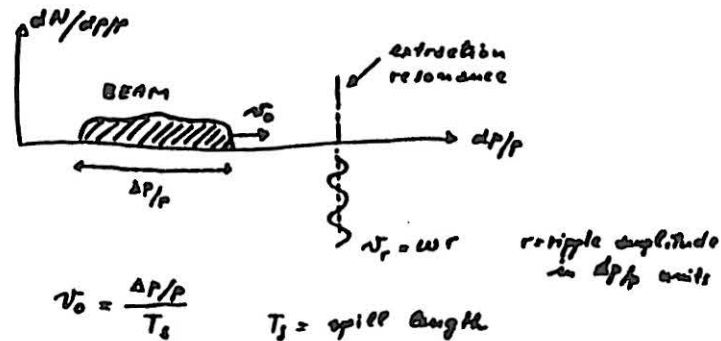
The non uniform structure of  
the extracted particle flux



- 1) low frequency : 50 ± 1000 Hz due to power supply ripple
- 2) medium frequency: 10 ± 1000 kHz " revolution freq. structure
- 3) high frequency : 1 ± 100 MHz " RF freq. structure

Generally the "low frequency" is considered  
the most annoying one.

in a standard "extraction"



$$v_0 = \frac{\Delta p/p}{T_s} \quad T_s = \text{spill length}$$

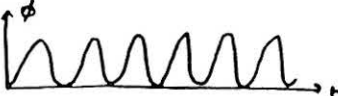
- if
- $v_0 \ll \nu_r \Rightarrow \text{HIGH ripple} \Rightarrow \text{BAD}$
  - $v_0 \gg \nu_r \Rightarrow \text{LOW ripple but } T_s \text{ SMALL}$

example:  $\omega = 2\pi \cdot 50 \text{ Hz}$ ,  $r = 10^{-4}$ ,  $\frac{\Delta p}{p} = 3 \cdot 10^{-3}$   
 then for  $v_0 = \omega r$ :  $T_S = 100 \text{ ms}$

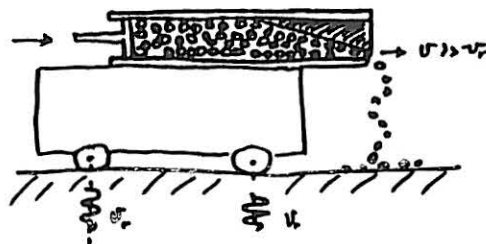
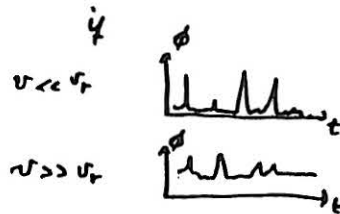
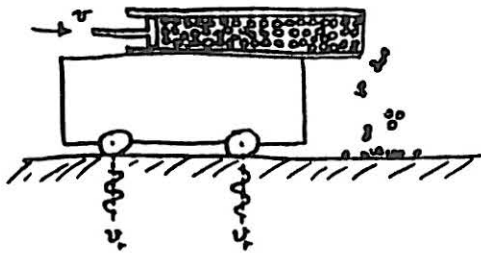
DUTY FACTOR F

$$F = \frac{\langle \phi \rangle^2}{\langle \phi^2 \rangle} = \frac{1}{1 + \frac{1}{2} \left( \frac{\omega r}{v_0} \right)^2} \quad 0 < F < 1$$

if  $\omega r = v_0 \Rightarrow F = 2/3$



a mechanical analogy:



$T_S$  is large

DIFFUSION ... A REMINDER

1<sup>st</sup> Analogy: MOLECULAR DIFFUSION

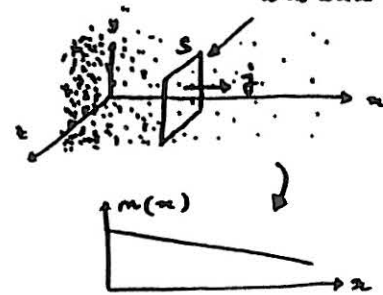
Remarks:

- 1) one has a molecular diffusion when the spatial distribution of  $p$  is not uniform.
- 2) diffusion is always toward low concentration

$n = \# \text{ of } p. / m^3 = \text{concentration} = \text{density}$

$j = \text{current density}$

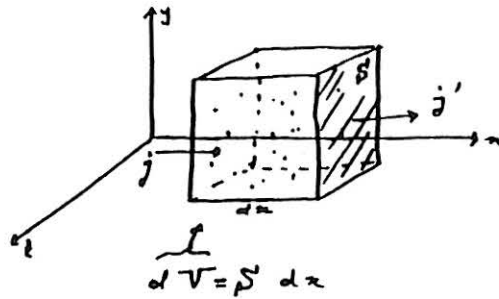
=  $\# \text{ of } p. \text{ traversing } S \text{ in one second}$   
 ↓  
 unit area [ $m^2$ ]



NB: if  $n = \text{constant} \Rightarrow j = 0$

$$j = -D \frac{\partial n}{\partial x} \quad (*)$$

where  $D = \text{diffusion coefficient}$



\* of  $p$  in  $dV = dN = n dV$

input flux  $\phi_{in} = j \rho'$

output  $\phi_{out} = j' \rho'$

accumulation rate =  $\phi_{in} - \phi_{out} = (j - j') \rho' = -\frac{\partial j}{\partial x} \rho' dx$  (\*\*)

↓  
but also

↓  
accumulation rate =  $\frac{\partial n}{\partial t} dV = \frac{\partial n}{\partial t} \rho' dx$  (\*\*\*)

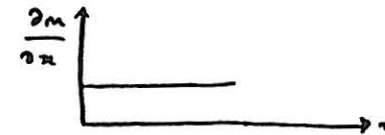
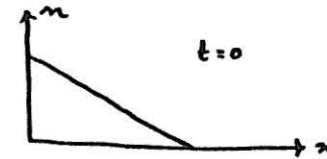
Combining (\*\*) & (\*\*\*)  $\frac{\partial n}{\partial t} = -\frac{\partial j}{\partial x}$

and (\*)

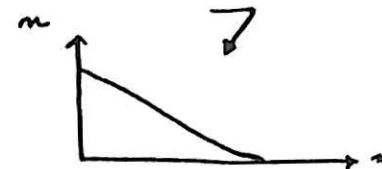
$$\frac{\partial n}{\partial t} = \frac{\partial}{\partial x} D \frac{\partial n}{\partial x}$$

DIFFUSION  
EQUATION

EXAMPLE #1



$t = \infty$

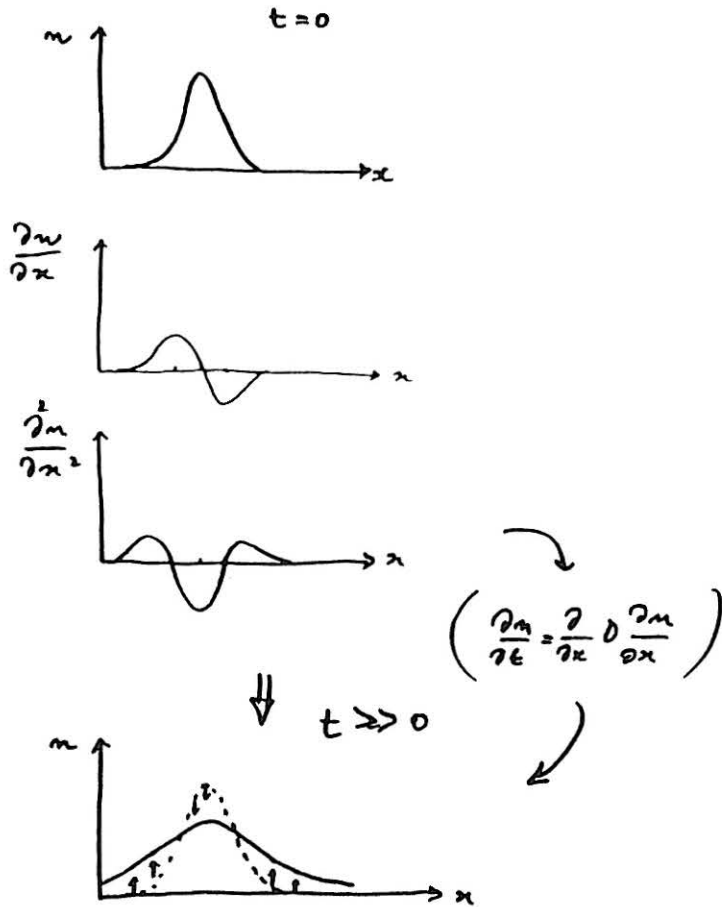


i.e. no change



STEADY STATE

EXAMPLE # 2



... BACK TO STEADY STATE ...

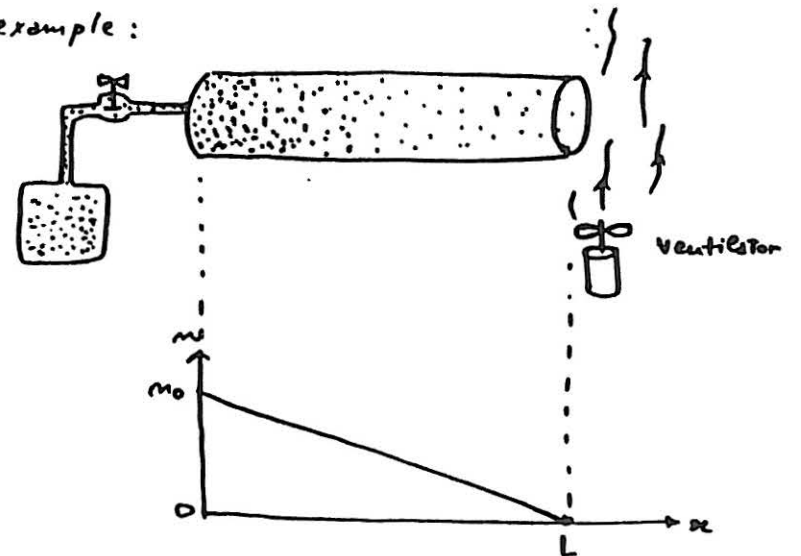
$$m = m(x, \cancel{t})$$

i.e. the concentration is stationary

$$\frac{\partial m}{\partial t} = 0 \Rightarrow \frac{\partial}{\partial x} D \frac{\partial m}{\partial x} = 0$$

i.e.  $-D \frac{\partial m}{\partial x} = \text{constant} = j = \text{constant flux} = \text{no accumulation}$

example:

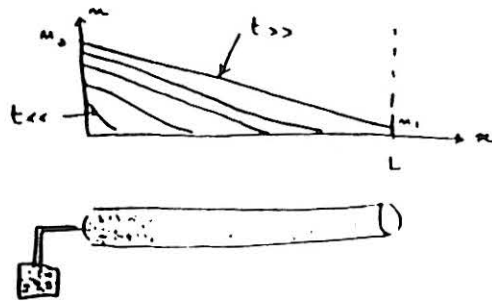


$$j = -D \frac{\partial m}{\partial x} = D \frac{m_0}{L}$$

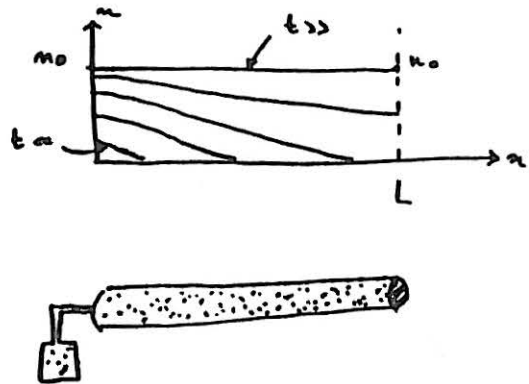
Remarks:

How the steady state is reached?

CASE #1: OPEN PIPE



CASE #2: CLOSED PIPE



2<sup>nd</sup> Analogy: THERMAL DIFFUSION

that is a transfer of energy (or heat)

Remarks:

- 1) one has thermal diffusion when there is a temperature (T) difference
- 2) the direction is from HOT to COLD  
(T >>) (T <<)

as in molecular diffusion exchanging  $n \rightarrow T$  as per

$$\text{the energy density current } j_E = -D \frac{\partial T}{\partial x}$$

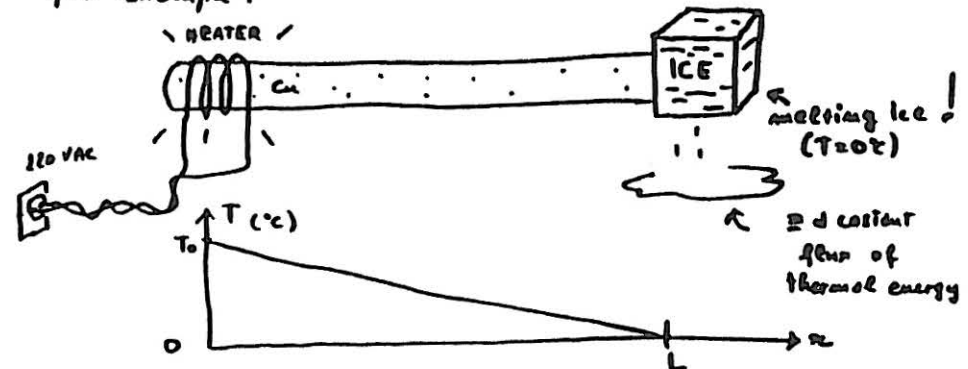
and the DIFFUSION EQ.

$$\frac{\partial T}{\partial t} = \frac{\partial}{\partial x} D \frac{\partial T}{\partial x}$$

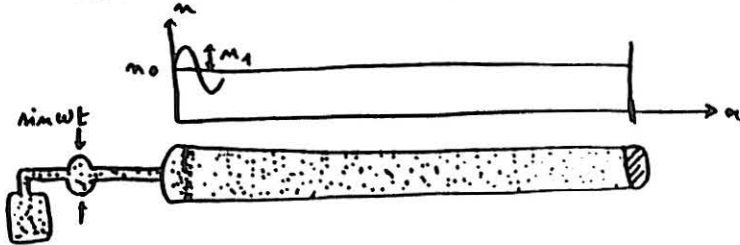
THE STEADY STATE, that is  $T_{\text{stationary}} = T(x, X)$

$$\text{means } D \frac{\partial T}{\partial x} = -j_E = \text{constant}$$

for example:



PERTURBATION PROPAGATION



Given a perturbation like:

$$n = n_1 \sin \omega t$$

will this perturbation propagate like a travelling wave like

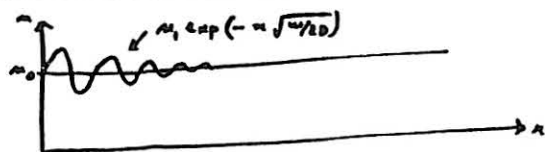
$$n(x, t) = n_0 + n_1 \sin(\omega t - kx) \quad ?$$

$$\left. \begin{aligned} \frac{\partial n}{\partial t} &= n_1 \omega \cos(\omega t - kx) \\ \frac{\partial^2 n}{\partial x^2} &= -k^2 n_1 \sin(\omega t - kx) \end{aligned} \right\} \text{ they do not satisfy: } \frac{\partial n}{\partial t} = \frac{\partial}{\partial x} D \frac{\partial n}{\partial x}$$

the answer is: no. BUT

$$n = n_0 + n_1 \exp\left[-x \sqrt{\frac{\omega}{2D}}\right] \cdot \sin\left[\omega t - x \sqrt{\frac{\omega}{2D}}\right]$$

will!



NB:  $k = \frac{2\pi}{\lambda} = \sqrt{\frac{\omega}{2D}}$        $v = \lambda f = \frac{\omega}{k} = \sqrt{2D\omega}$

② if  $D \gg \Rightarrow$  the damping is small

③ the group velocity:  $v_g = \frac{d\omega}{dk} = \sqrt{2D\omega} > v$

BACK TO OUR ACCELERATOR

$$n \text{ [p/m}^3] \rightarrow \Psi \text{ [p/\Delta p]} = \text{proton density in } \frac{\Delta p}{p} \text{ space}$$

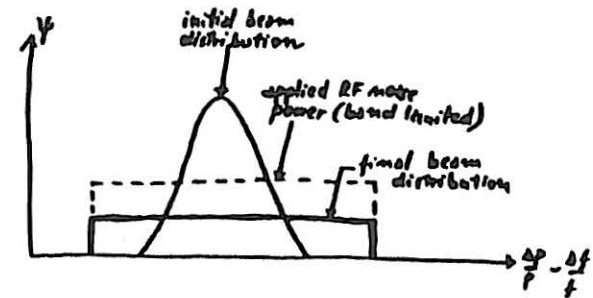
$$j \text{ [p/mec]} \rightarrow \phi \text{ [p entr./s]}$$

$$j = -D \frac{\partial n}{\partial x} \rightarrow \phi = -D \frac{\partial \Psi}{\partial p}$$

$$\frac{\partial n}{\partial t} = \frac{\partial}{\partial x} D \frac{\partial n}{\partial x} \rightarrow \frac{\partial \Psi}{\partial t} = \frac{\partial}{\partial p} D \frac{\partial \Psi}{\partial p}$$

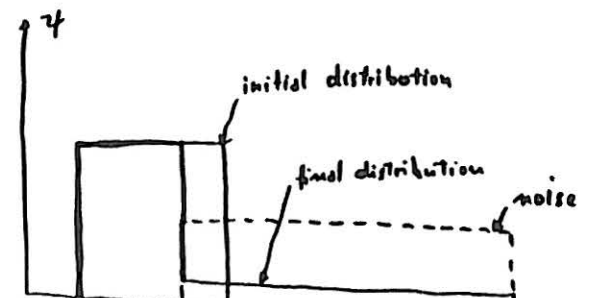
APPLICATIONS:

1) Beam shaping



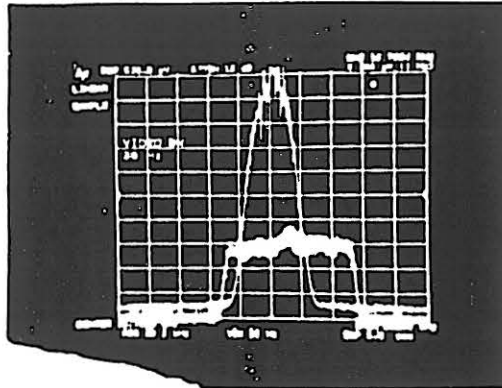
see also Fig. 1

2)



Test stochastic extr:  
Shaping:  $f = 16.76$  MHz  
 $T = 49$  MeV

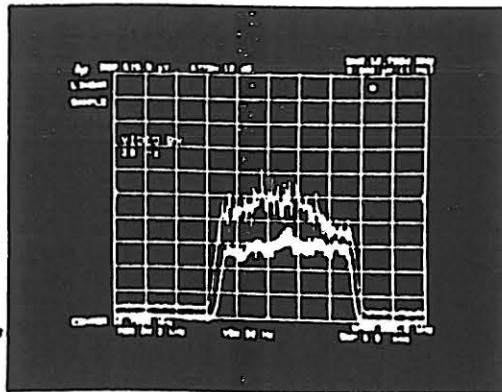
Fig 1. Beam shaping in LEAR



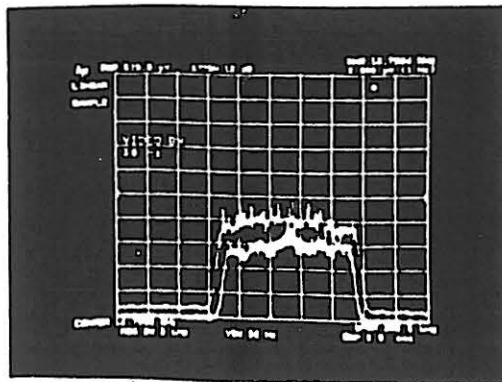
- 1) Beam distribution
- 2) Noise spectrum

$$P_A = 0.6W$$

Initial conditions

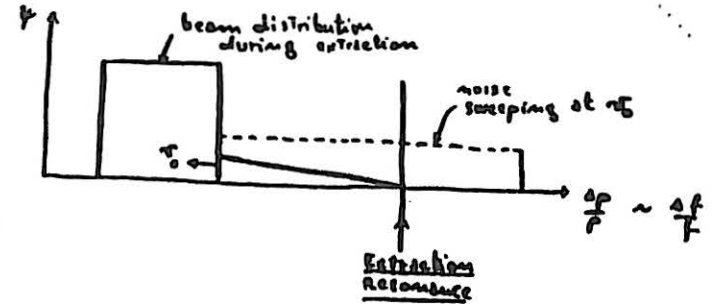


10 sec later



20 sec. later

3) STOCHASTIC EXTRACTION



See also Fig 2.

REMARKS:

- For a p. in Brownian motion, the rms distance from the origin after a time  $t$  (where  $r=0$  at  $t=0$ ) is:  
 $\langle r^2 \rangle = 2 n D t$        $n = \#$  of space dimensions

- The rms energy gain given by a noise with bandwidth  $W$  (overlapping only one harmonic of the revolution frequency) and rms voltage  $V_n$  is

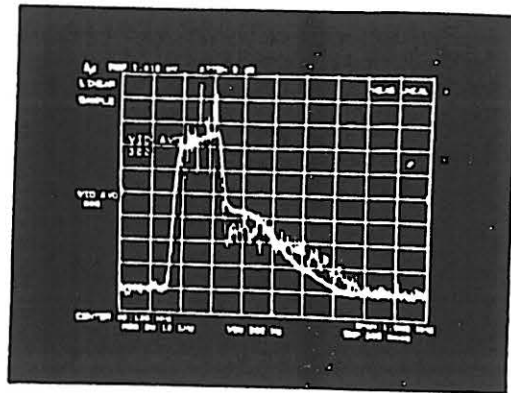
$$\frac{dE^2}{dt} = \frac{f_0}{W} \frac{(eV_n)^2}{T_0} = \frac{1}{W} \left( \frac{eV_n}{T_0} \right)^2$$

from  $D = \frac{1}{2} \frac{d(\Delta p/p)^2}{dt}$

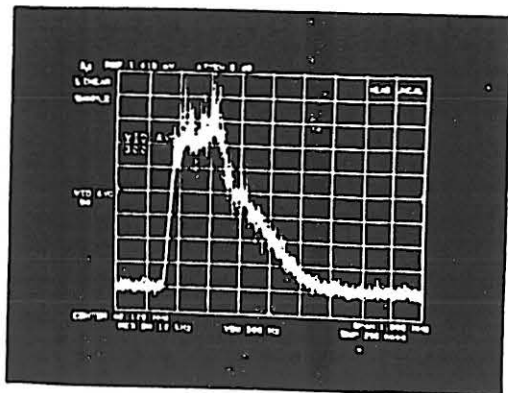
and knowing that  $\Delta p = \frac{1}{\rho c} \Delta E$ ,  $\rho = eB/g$ ,  $f_0 = \frac{c}{2\pi R}$   
we obtain

$$D = \frac{1}{2W} \left( \frac{V_n}{2\pi R g B} \right)^2$$

-  $F = \frac{1}{1 \pm \frac{1}{2} \frac{WR^2}{D}} \Rightarrow$  if  $\boxed{D > WR^2} \Rightarrow$  OK (Figs)



Sweep 10s  
 $P_A = 0.6W$



Sweep 100s  
 $P_A = 0.16W$

Fig. 2 . Stochastic extraction in LEAR  
 Beam distribution during extraction

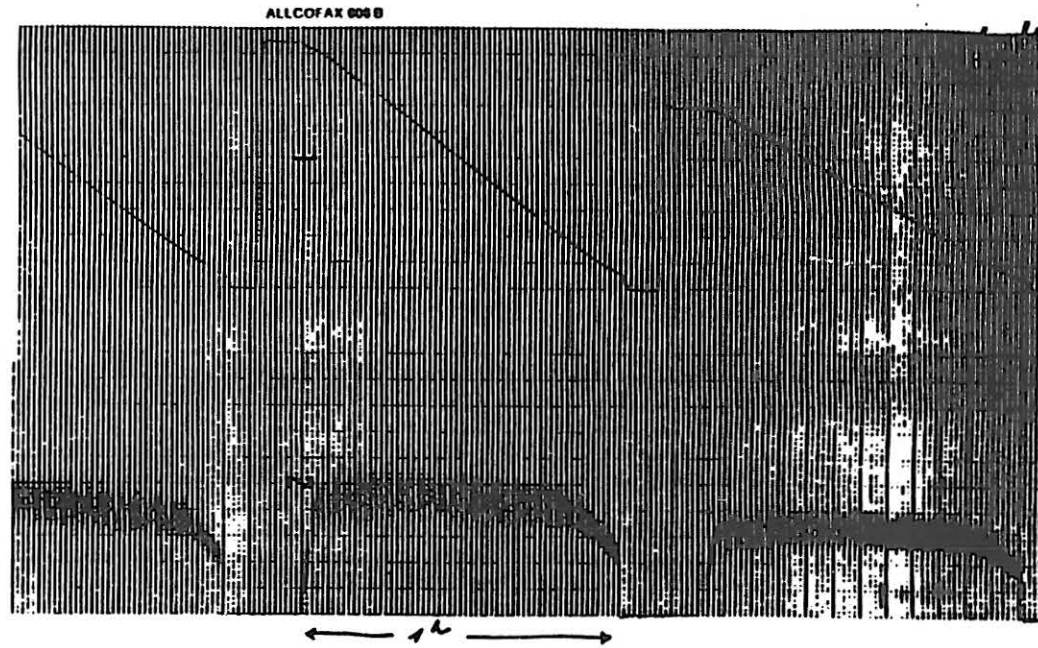
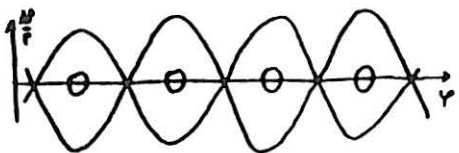


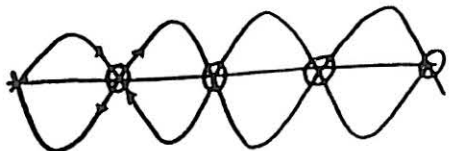
Fig. 3 First 1<sup>h</sup> stochastic extraction in LEAR  
 Top trace : circulating beam current  
 bottom - : extracted flux

PRESENT PS SLOW EXTRACTION

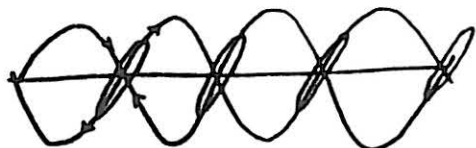
a) Phase jump debunching (24 GeV/c)



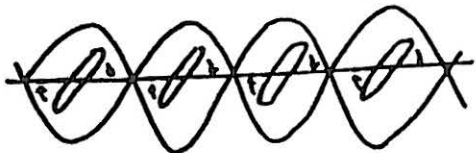
initial conditions  
( $v = v_{max}$ )



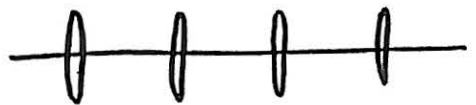
180° jump on  
unstable phase



drive the beam to  
to stretch



back on  
stable phase



switch OFF  
the RF when  
 $\frac{\Delta P}{P}$  max



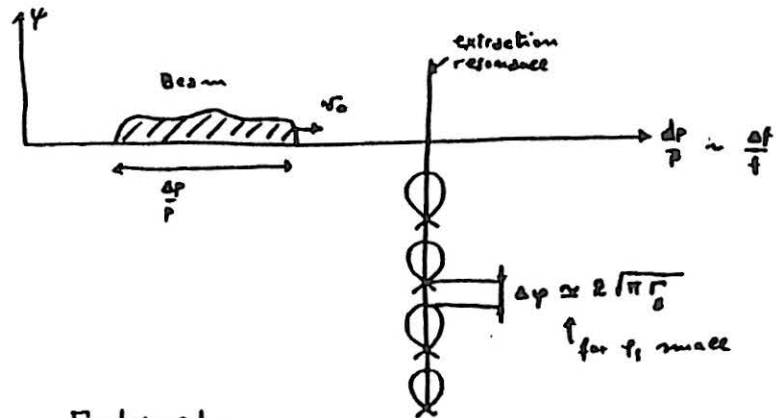
wait for  
debunching  
to take place

$$T_d = \frac{2\pi}{2\pi f \eta \frac{\Delta P}{P}}$$

b) The beam is 'pushed' to the resonance by decreasing the B field

c)  $\omega R \approx 2\pi \cdot 50 \cdot 10^{-4} = .03$ ,  $v_0 = \frac{3 \cdot 10^{-3}}{100} = .01 \Rightarrow F \approx 0.2$

EMPTY BUCKET CHANNELING



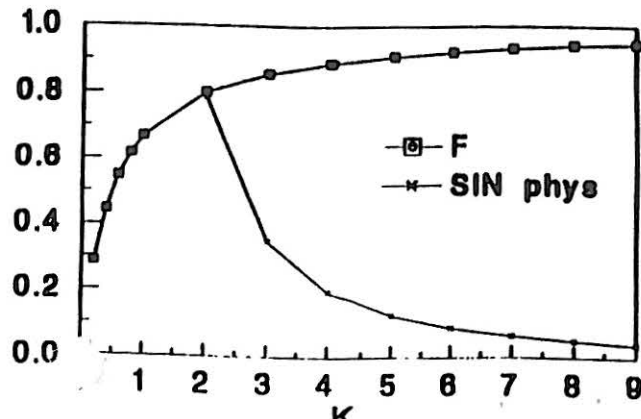
$$\Gamma_s = |\sin \phi_0| =$$

$$\approx 2\pi R \rho \frac{\dot{B}}{V_{RF}} \left( \frac{\partial^2}{\partial \delta^2 - \delta_0^2} \right) \rightarrow \text{if } \delta B \neq 0 \text{ a } f = \text{const.}$$

$$\sigma = \frac{\delta P/P}{T_s} \times \kappa \quad \text{where } \kappa = \frac{2\pi}{\Delta \phi} \approx \sqrt{\frac{\pi}{\Gamma_s}}$$

for example: if  $\Gamma_s \approx \sin 1.7^\circ \approx .025 \Rightarrow \kappa \approx 10$

$$F = \frac{1}{1 + \frac{1}{2} \left( \frac{\omega R}{\kappa v_0} \right)^2}$$



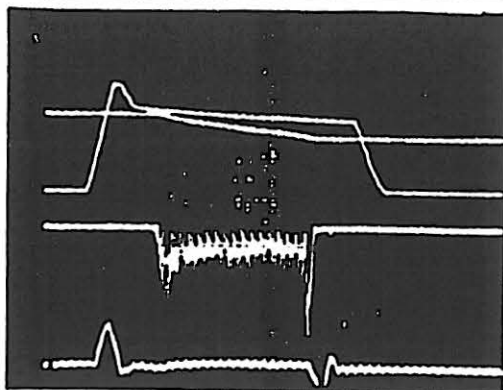
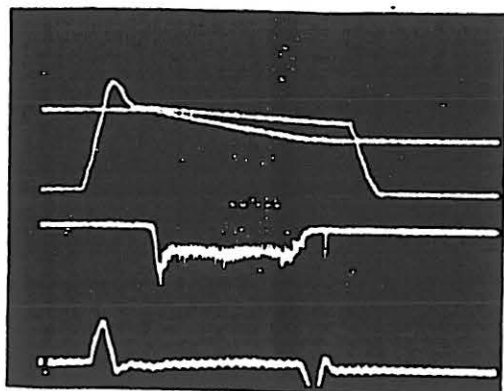
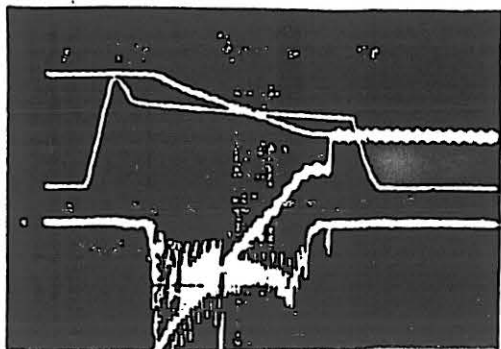


Fig. 4: Empty-bucket channelling

I  
P  
DQ  
SE 62 spill  
① No RF  
Servo loop current  
Hor. = 100 ns/div.

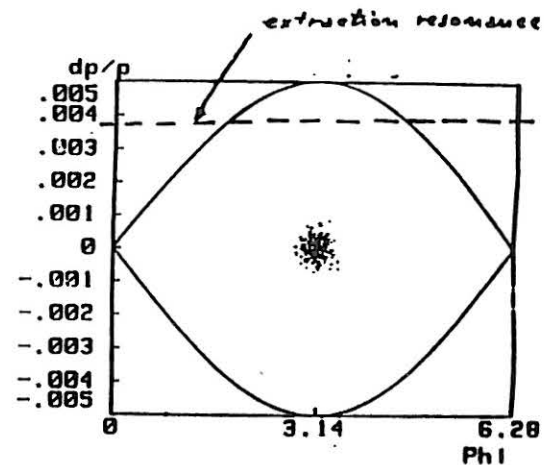


② RF on



③ RF on only during the 2nd half of extraction  
(4th trace: losses in s.o. 61)

NOISY BUCKETS



- 1) Moving, with a perturbation on the radial loop, the beam close to the extr. resonance
- 2) shaking, with noise in the phase loop, the bunch to increase  $E_c$

⇓  
Should provide a fair control of the spill

- NB:
- tails during  $E_c$  blow-up are welcome!
  - the strong RF structure should not be a problem for medical applications
  - no debunching
  - no gap relays
  - facilitate beam diagnostic (intensity, position, ...)

---

 SUMMARY

## ○ STOCHASTIC EXTRACTION

- + good F for long spills ( $\gg 1 \mu\text{s}$ )
- + hardware simplicity
- + operational "
- moderate spill control
- problems for short spill ( $< 1 \mu\text{s}$ )

## ○ PHASE JUMP DEBUNCHING

- + operationally simple & fast
- distribution not very rectangular
- hardware complicated

 ○ RESONANCE FEEDING WITH  $\beta$  SLOPE

- + hardware simplicity (?)
- poor F
- poor spill control

## ○ EMPTY BUCKET CHANNELLING

- + good for short spills ( $< 1 \mu\text{s}$ )
- hardware complicated
- poor spill control

## ○ NOISY BUCKETS

- + hardware simplicity
- + good spill control
- + no debunching
- + facilitate instrumentation
- strong RF structure (may be acceptable?)

## ○ UNSTACKING

- + facilitate instrumentation
- RF structure (may be acceptable?)
- hardware complicated
- operationally "
- poor F

## References

- 1) S. van der Meer, Stochastic extraction, a low ripple version of resonant extraction, CERN/PS/AA 78-6
  - 2) W. Hardt, Ch. Steinbach, R. Cappi, Ultraslow extraction with good duty factor, Proc. of the XI th. Int. Conf. on High En. Accel., CERN, July 7-11, 1980, p.335-340 or CERN/PS/OP/DL 80-16
  - 3) D. Boussard, M. Gyr, K.H. Kissler, T. Linnecar, Slow extraction at 400 GeV/c with stochastic RF noise, SPS Improvement report No. 179, 24th July, 1980
  - 3a) R. Giannini, W. Hardt, R. Cappi, Ultraslow extraction, Proc. of LEAR workshop, Erice, May 9-16, 1982 or CERN/PS/LEA 82-3
  - 4) see for ex. The Feynman Lectures on Physics
  - 5) Ch. Steinbach, R. Cappi, Improvement of the low frequency duty factor of slow extraction by RF phase displacement, CERN/PS/OP 80-10
  - 6) S. Hensen, A. Hofmann, E. Peschardt, F. Sacherer, W. Schnell, Longitudinal bunch dilution due to RF noise, Proc. 1977 PAC, Chicago, March 16-18 1977 or CERN-ISR-RF-TH/77-25
-

## PHASE DISPLACEMENT

### ACCELERATION

presented by  
E. Ciapala, SL

February 13th and 14th 1996

PS, CERN

### Longitudinal Phase Space

- Particle motion described by :

$$\dot{\phi} = \frac{\omega_m h \eta}{\beta^3 E} \quad \eta = \frac{\delta T}{T} / \rho$$

$$\dot{E} = \frac{\omega_m e V_{RF}}{2\pi} (\sin \phi - \sin \phi_s)$$

- For small amplitudes w.r.t. synchronous particle :

$$\text{For } \Omega_s^2 = \frac{e V_{RF} \omega_m^2 h \eta \cos \phi_s}{2\pi E \beta^3} \text{ positive - stable motion}$$

$$\delta \dot{\phi} = a \delta E \quad \delta \dot{E} = -b \delta \phi$$

$$\Omega_s^2 = ab = \frac{e V_{RF} \omega_m^2 h \eta \cos \phi_s}{2\pi E \beta^3}$$

- For large amplitudes :

$$\Delta \ddot{\theta} = \frac{\Omega_s^2}{\cos \phi_s} (\sin \phi - \sin \phi_s) = 0$$

- See phase plane trajectories :

=> Stationary bucket

=> Moving bucket

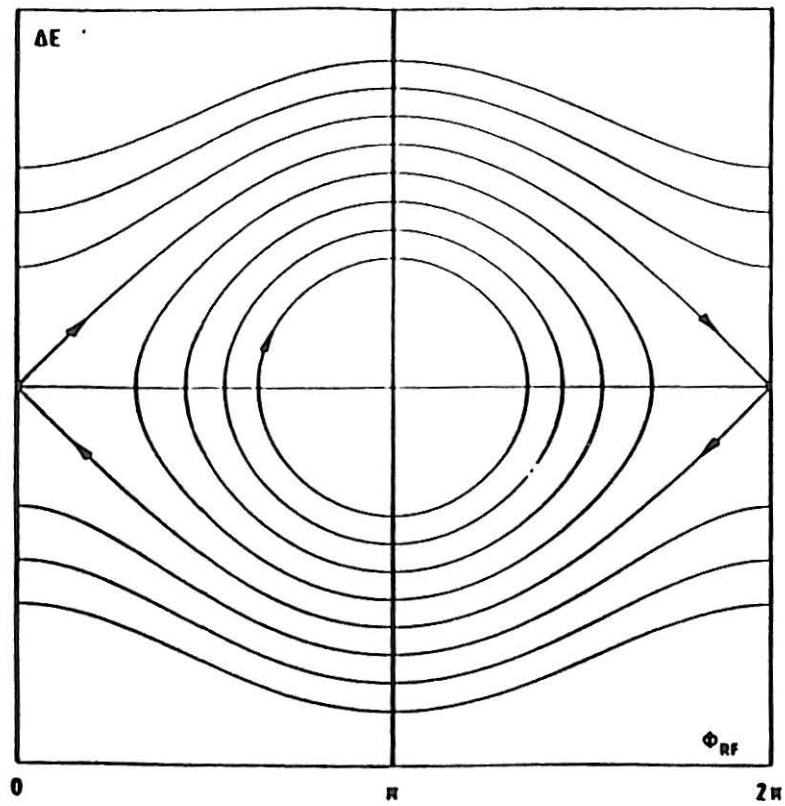


Fig. 2.3 Stationary RF bucket above transition

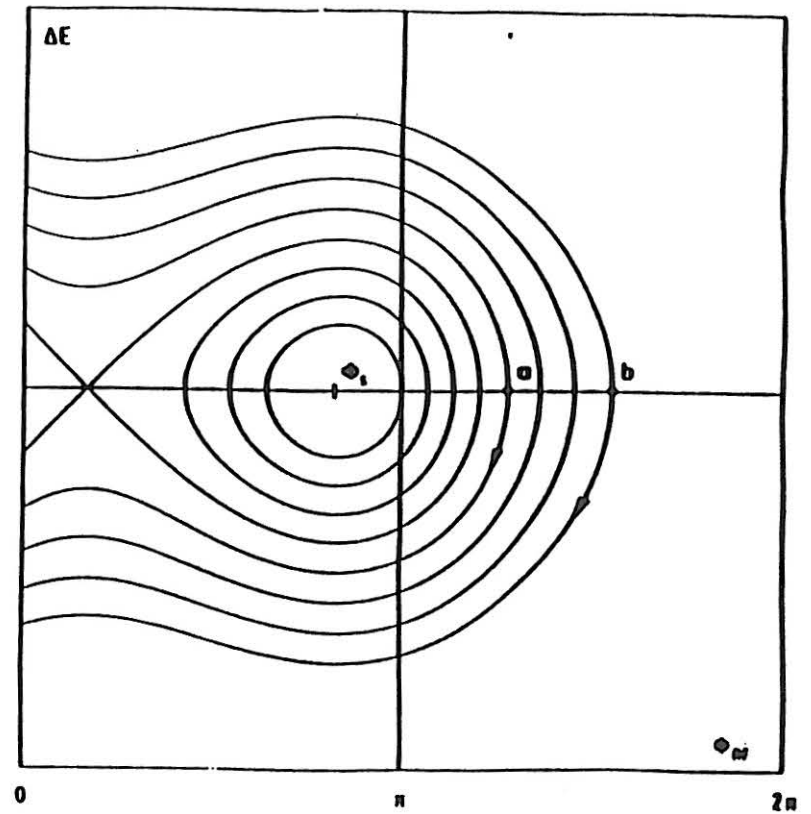


Fig. 2.4 Accelerating RF bucket  $\Gamma = 0.5$

### Phase Displacement

- RF bucket moving through a coasting beam (stack) results in an overall displacement in the opposite direction:

- Particles cannot enter bucket and move round to new energies.  
(Phase space density inside coasting beam cannot increase)

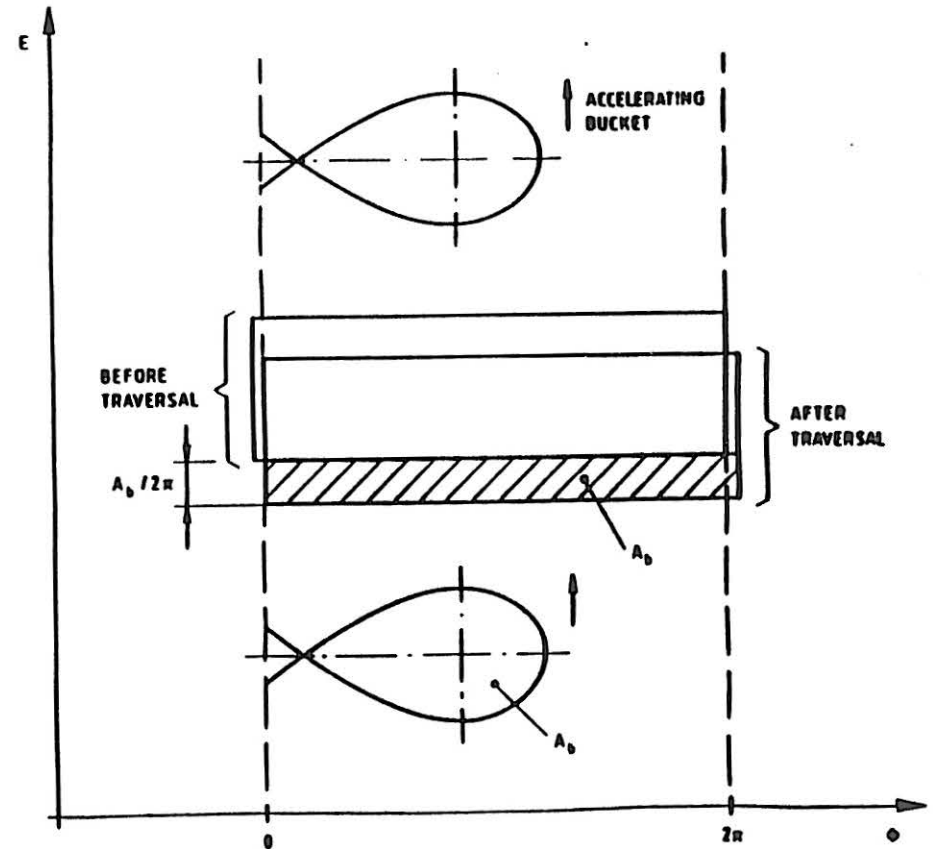
- For bucket height  $\ll$  stack 'width' the net displacement is the bucket area.

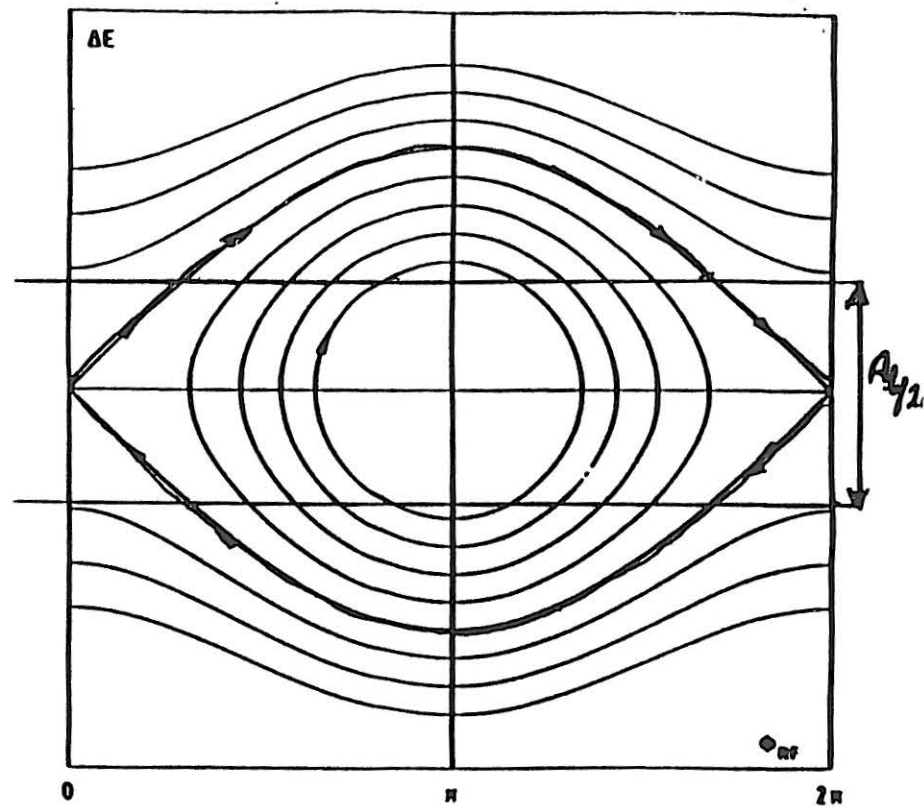
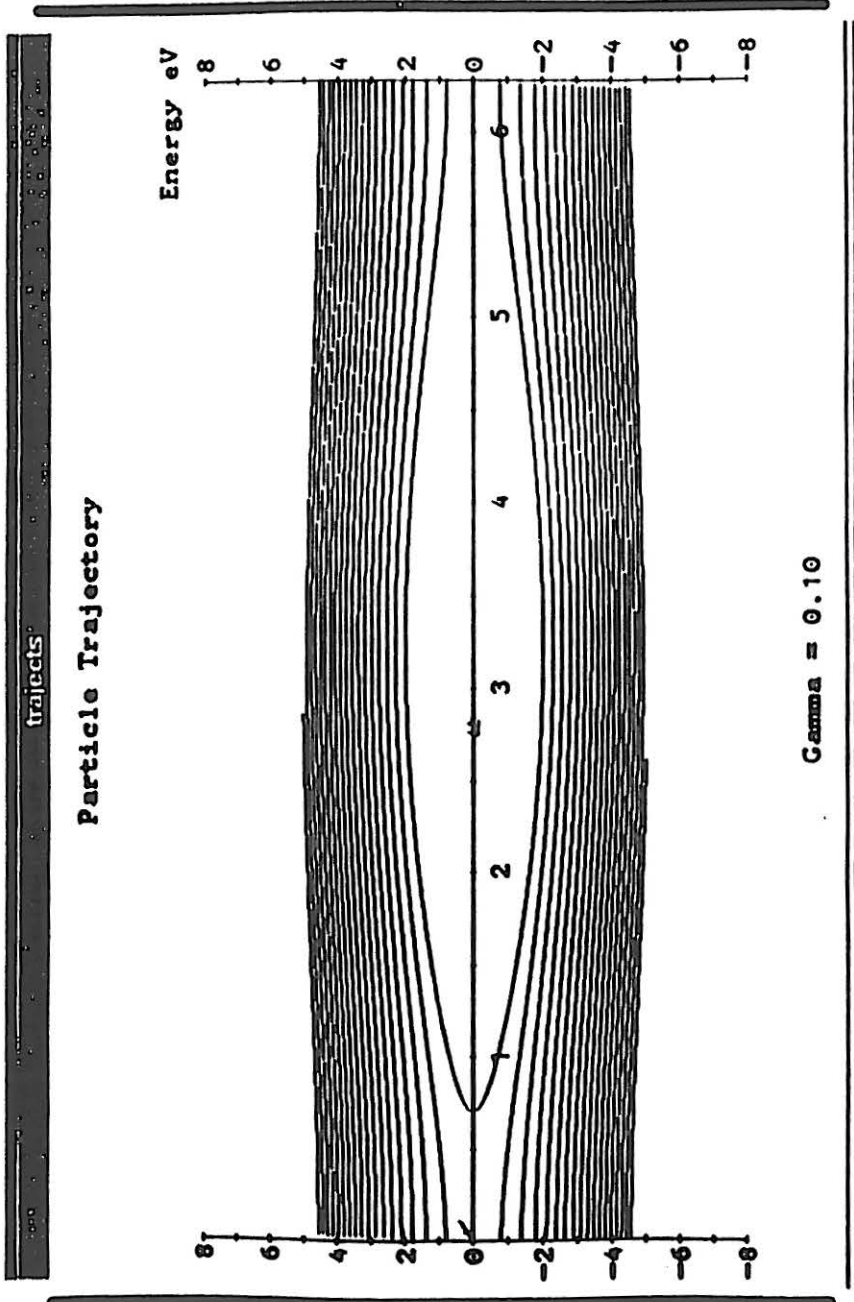
- Illustrated in Figure and Simulation.

- Scattering effect - Dependent on  $\Gamma$

- Motion complex, Solutions need computation.

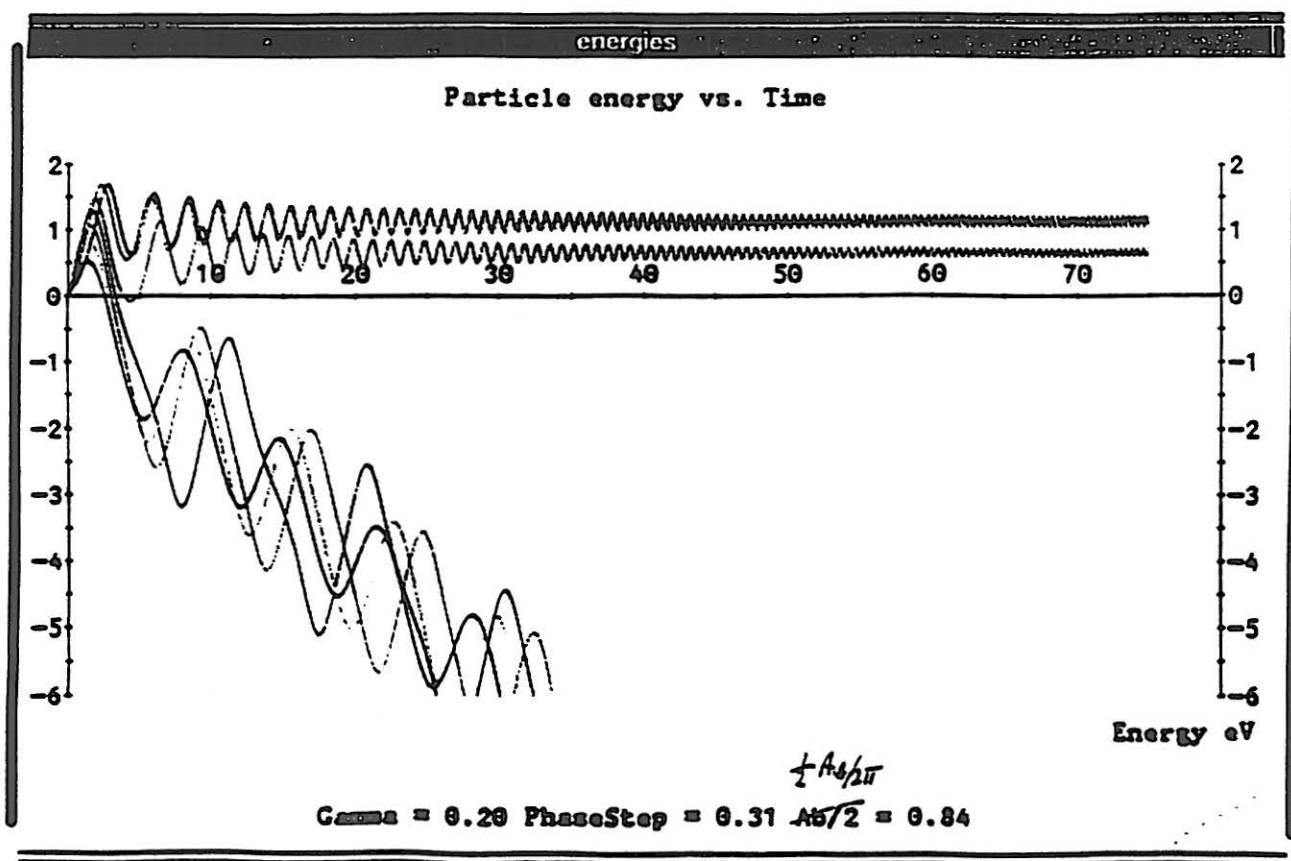
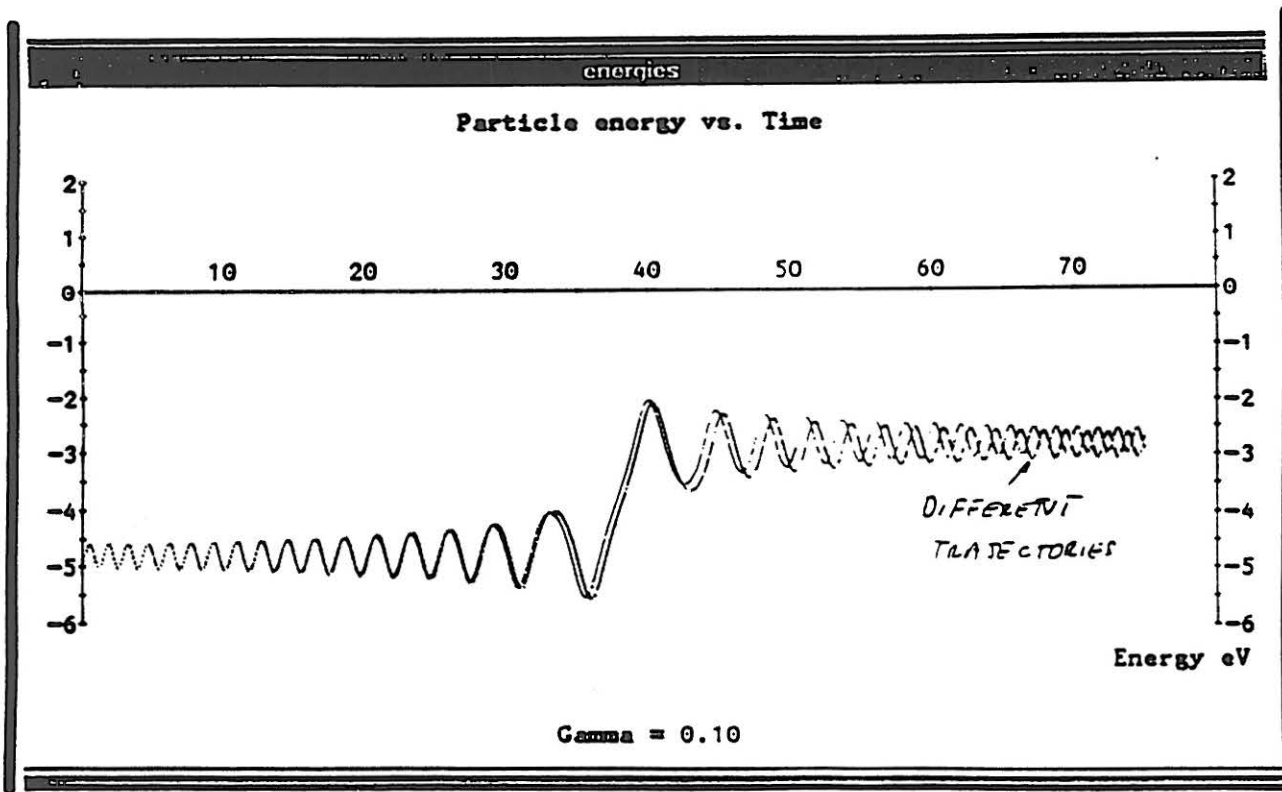
Usually analysed by computer simulations of particle motion.

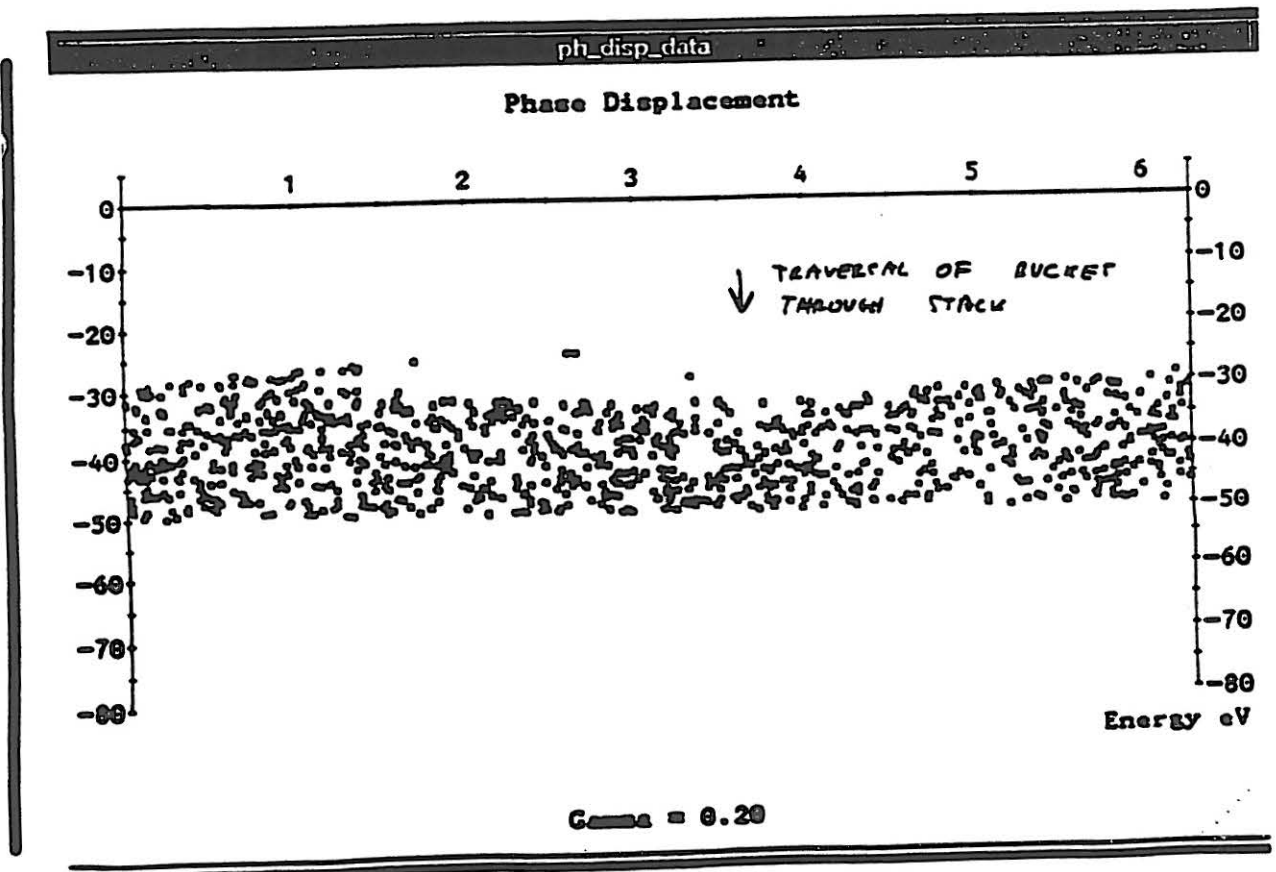
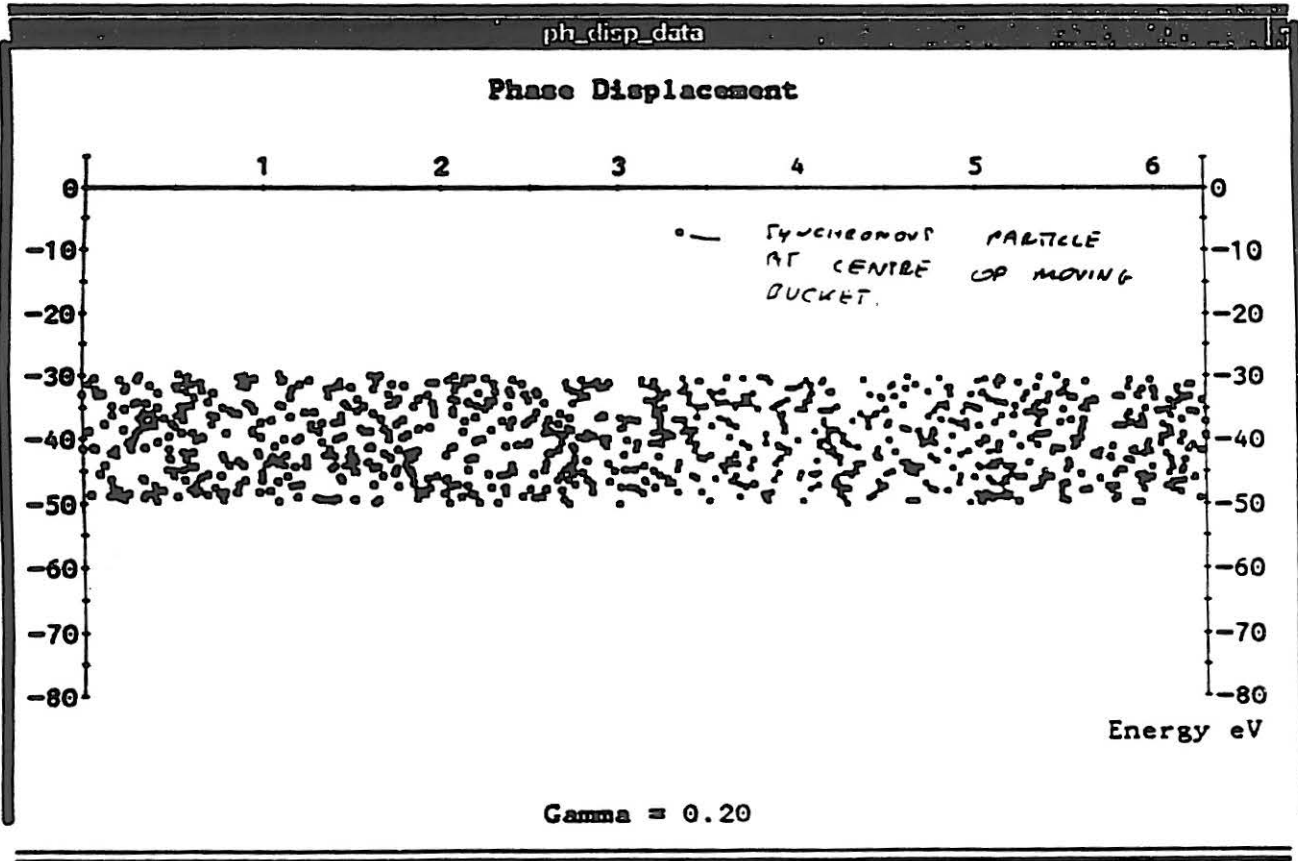




NEAR  
 Fig. 2.3. Stationary RF bucket above transition

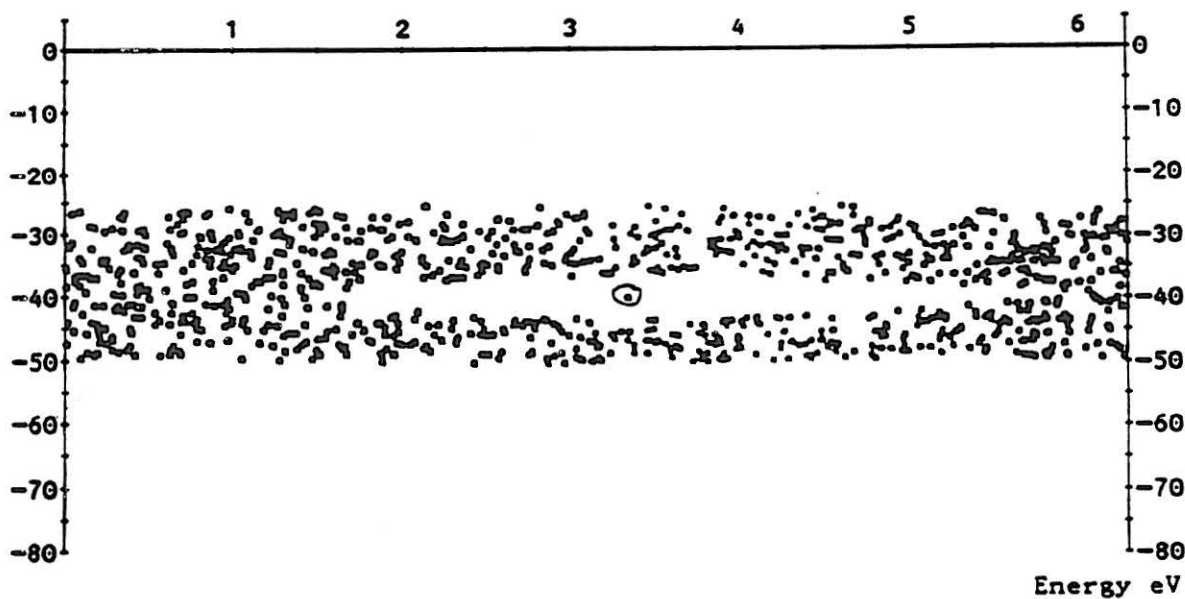
$$\Delta E = \frac{A\beta}{2\pi}$$





ph\_disp\_data

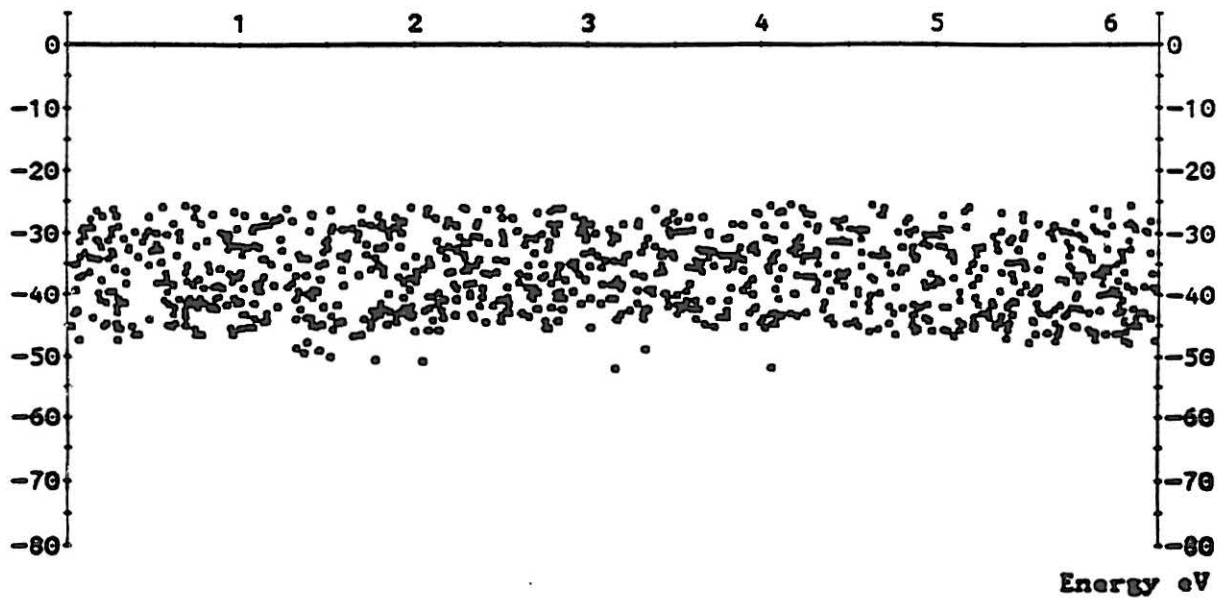
Phase Displacement



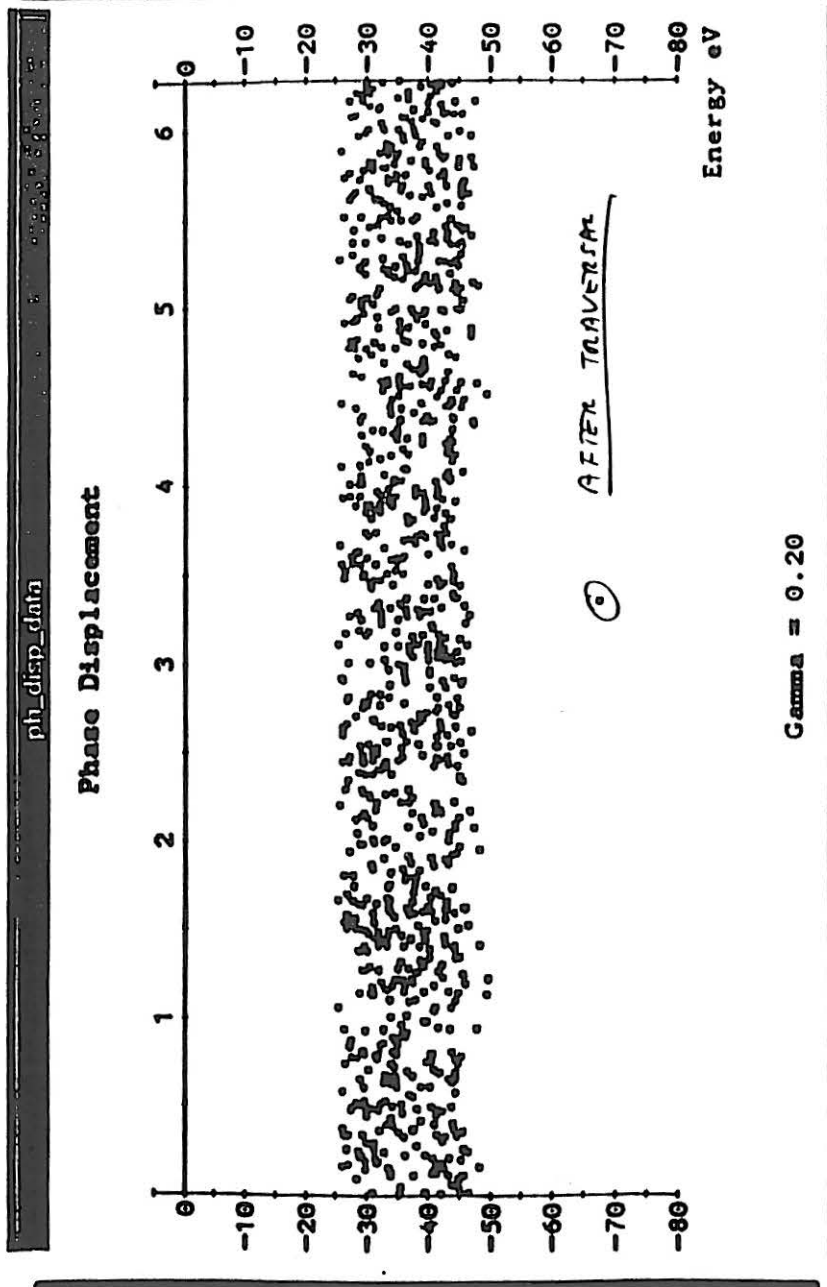
Gamma = 0.20

ph\_disp\_data

Phase Displacement



Gamma = 0.20



## Factors Affecting Efficiency of Phase Displacement

### • Particle Scattering

For each sweep

$$\Delta E_{\text{rms}} = \Gamma A_{\text{in}} / 2\pi \quad \Delta E_{\text{rms}} = \Gamma$$

Result obtained from simulations, confirmed by experiment (ISR)

### • RF Noise

- Allows particles to enter bucket during sweep

e.g. modulation near synchrotron frequency causes particles to spiral in and out of bucket

- Results in :

- Increased energy spread
- Reduced energy displacement
- Larger rms width increase per sweep

- Cures :

- Phaselock
- Careful design of low level RF (reduce phase noise)

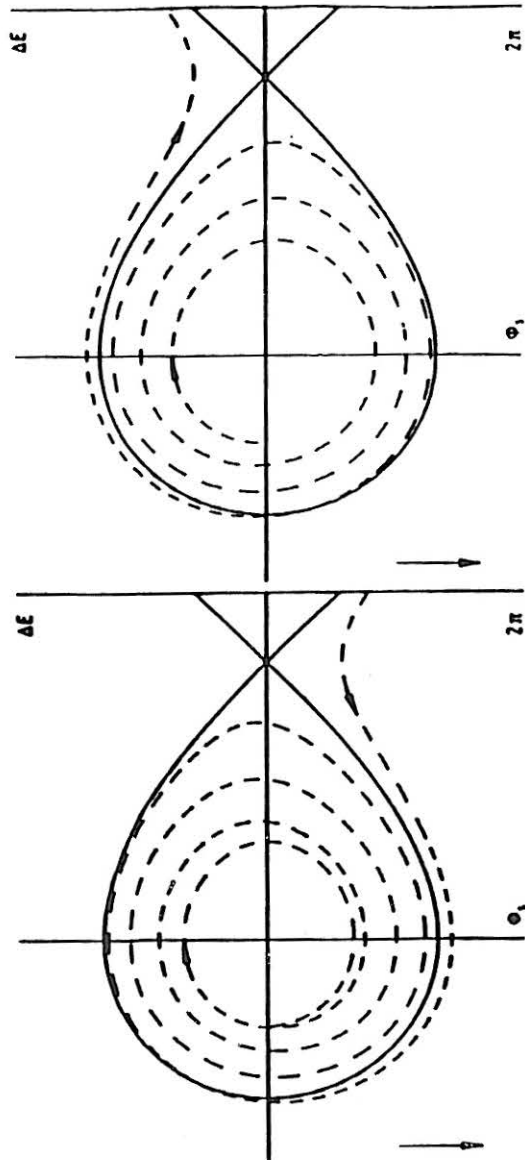


Fig. 4.3 Trajectories of a particle brought in and then out of a decelerating bucket above transition by RF phase modulation.

• Variation in Bucket Parameters

Assumption of constant bucket area during sweep not completely valid.

Change of real bucket area during the sweep will produce the same effects as RF noise.

Special case : CERN ISR,  $\gamma \gg \gamma_r$  and  $|\eta| \ll 1$

For the variation in area of a stationary bucket :

$$\frac{\Delta A_b}{A_b} \approx -\frac{\Delta E}{2E}$$

i.e. the area increases with decreasing bucket energy

For fixed rate frequency sweep the real value of  $\Gamma = \sin \phi$ , changes :

$$\frac{\Delta \Gamma}{\Gamma} = -\frac{\Delta E}{E}$$

i.e. The real value of  $\Gamma$  increases, resulting in a decreasing bucket area.

The two effects are opposite and can be made to cancel out.

If  $\alpha(\Gamma)$  is the ratio of the area of a moving bucket to a stationary bucket, then for approximately constant bucket area through the sweep :

$$\frac{\Delta A_b}{A_b} = \frac{\Delta A_{b0}}{A_{b0}} + \frac{\Delta \alpha(\Gamma)}{\alpha(\Gamma)} = 0$$

This satisfied for  $\Gamma = 0.25$

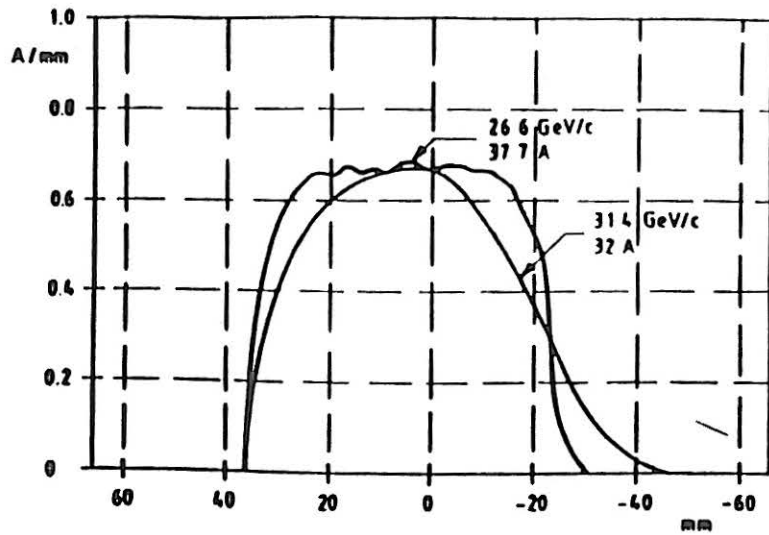


Fig. 4.2 ISR stack density profiles before and after phase displacement acceleration (R933P, Ring 1, 1978)

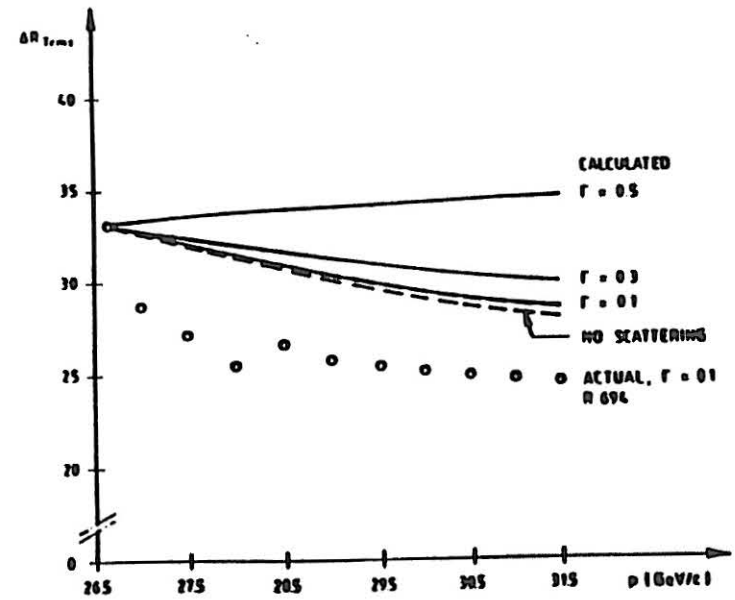
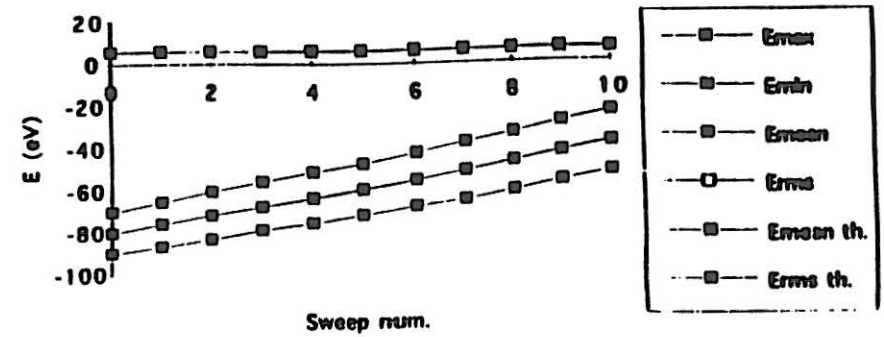


Fig. 4.1 rms radial beam width  $v_r$  momentum (ISR)

Ph. Disp Accn 1000p Gamma 0.1



---

## Conclusions

- Simple means of acceleration or displacement of coasting beam
  - Some overall loss in phase space density inevitable (occurs mostly at start of process)
  - Losses, blow up per sweep become stable after a number of sweeps
  - Care needed in RF system design (Noise, program linearity ..)
  - Simulations play main role in analysis (Straightforward nowadays ..)
-

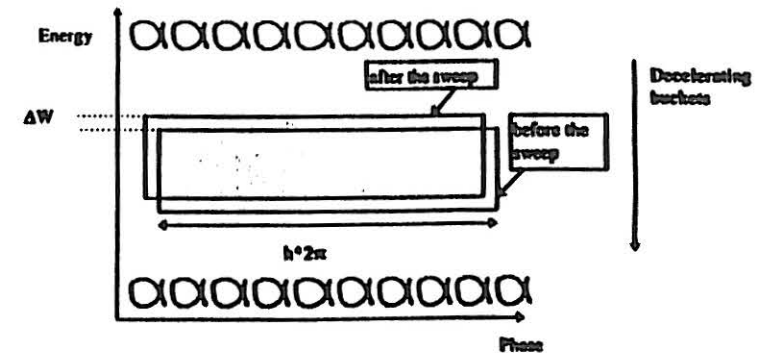
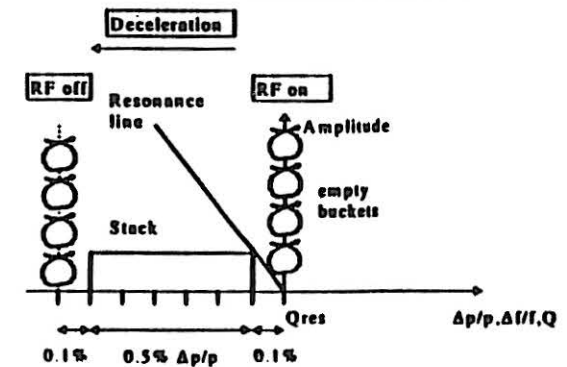
**FEASIBILITY OF A PHASE-DISPLACEMENT  
ACCELERATION SYSTEM AND A  
MICRO-BUCKET TRANSFER SYSTEM  
FOR 'FEEDING' THE RESONANCE**

presented by  
M. Crescenti

February 13th and 14th 1996

PS, CERN

**PHASE DISPLACEMENT ACCELERATION**



Small empty buckets are created at the resonance energy.

The buckets are decelerated through the stack, that is swept to higher energy ( $\Delta W = A_{bucket} / 2\pi$ ). During the sweep, a  $\Delta P/P$  increase occurs (stack dilution).

The particles are extracted in small micropulses (not continuous process) with a  $\Delta P/P = 0.1\%$ .

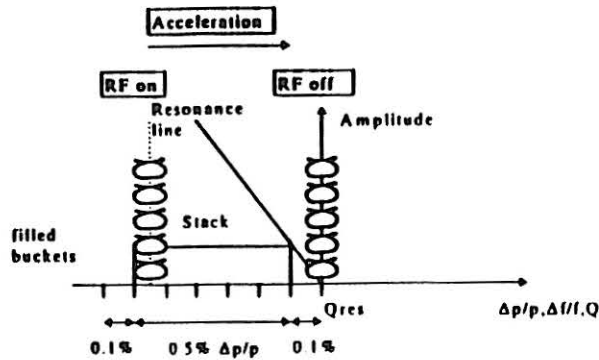
The speed of the sweep (i.e. of the acceleration) is limited by the synchrotron frequency.

The bucket dimensions are kept small in comparison with the stack to limit disturbances to a small portion of the stack.

The extraction stops if the RF power is switched off.

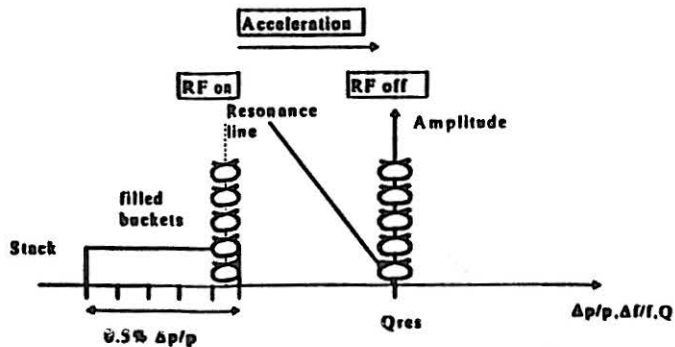
**FEEDING THE RESONANCE BY UNSTACKING**

**ACCELERATION STARTING FROM THE BOTTOM OF THE STACK.**



The beam is trapped in small buckets created at the bottom of the stack.  
 The buckets are accelerated through the stack until the particles are extracted.  
 The number of particles extracted at each sweep is proportional to the bucket area.  
 The stack is swept down by  $\Delta W = A_{\text{bucket}}/2\pi$ , stack dilution is not avoided.  
 The frequency swing is constant.

**ACCELERATION STARTING FROM THE TOP OF THE STACK.**



The beam is trapped in small buckets created at the top of the stack.  
 The buckets do not traverse the stack, thus avoiding stack dilution.  
 The frequency swing is variable.

**BUCKET CALCULATIONS**

stationary bucket area [eV x s]:

$$A_{bs} = A_b(0) = 16 \times \frac{\beta}{2 \times \pi \times f_{rf} \times h} \times \sqrt{\frac{h \times e \times V_{rf} \times W}{2 \times \pi \times |\eta|}}$$

stationary bucket height [eV]:

$$H_{bs} = \frac{(2 \times \sqrt{2} \times \beta)}{h} \times \sqrt{\frac{h \times e \times V_{rf} \times W}{\pi \times |\eta|}}$$

stable phase and related parameters:

$$\phi_s, \Gamma = \sin \phi_s, \alpha(\Gamma) = \frac{A_b(\Gamma)}{A_b(0)}, Y(\Gamma)$$

bucket area [eV x s]:

$$A_b = \alpha(\Gamma) \times A_{bs}$$

bucket height [eV]:

$$H_b = Y(\Gamma) \times \frac{H_{bs}}{\sqrt{2}}$$

synchrotron frequency [Hz]:

$$\Omega_s = \sqrt{\frac{e \times V_{rf} \times 2 \times \pi \times f_{rev}^2 \times h \times \eta \times \cos(\phi_s)}{W \times \beta^2}} \times \frac{1}{2 \times \pi}$$

## ACCELERATION

frequency sweep [Hz]:

$$\Delta f_{sweep} = \frac{\Delta P}{P} \times \eta \times f_{rev} \times h$$

kinetic energy increase per sweep [eV]:

$$\Delta W_{sweep} = \frac{A_b}{2 \times \pi}$$

number of sweeps (theoretically):

$$N = \frac{\Delta W_{tot}}{\Delta W_{sweep}}$$

maximum speed of the sweep [Hz/s]:

$$\dot{f}_{rf} = \frac{\eta \times f_{rf}^2}{\beta^2 \times W \times h} \times e \times V_{rf} \times \Gamma$$

## TENTATIVE PARAMETERS

- $\Delta P/P_{beam} = 0.5 \%$

limited by the dimensions of the vacuum chamber.

- $h = 10/100$

tentative to provide an as much as possible uniform "feeding" of the resonance.

- $\phi_r = 15 \text{ deg}$

usually chosen between 10/20 to keep constant bucket area during the frequency swing.

- $V_{rf}$  less than 3 kV

need to keep it as small as possible to reduce the RF system requests.

- number of sweeps < 100

need to limit stack dilution to a max  $\Delta P/P_{tot} = 0.7 \%$ .

- spill time = 250 ms

need to limit the treatment time.

- nr of particles per micropulse ~ 1E9 protons, ~ 1E7 ions.

- nr of particles per pulse ~ 1E11 protons, ~ 1E9 ions.

tentative to cope with voxel scanning specifications.

TENTATIVE CHOICES FOR A PHASE DISPLACEMENT ACCELERATION INTO THE RESONANCE (h=10)

kinetic energy per nucleon	60MeV p*	300MeV p*	120MeV/u <sup>12</sup> C <sup>3+</sup>	400MeV/u <sup>12</sup> C <sup>3+</sup>
$\gamma$	1.064	1.32	1.120	1.426
$\beta$	0.342	0.653	0.463	0.713
$\eta$ ( $\eta=3$ )	0.772	0.463	0.575	0.38
$f_{rev}$ [MHz]	1.348	2.576	1.826	2.815
$\Delta p/p$ total ( $\Delta p/p$ beam=0.5%) [%]	0.7	0.7	0.7	0.7
$\Delta t_{sweep} = \Delta p/p \times f_{rev} \times \eta \times h$ [KHz]	73	89.5	85.3	74.9
h	10	10	10	10
<b>BUCKETS</b>				
$\phi_s$ [deg]	15	15	15	15
$\Gamma = \sin \phi_s$	0.259	0.259	0.259	0.259
$V_{rf}$ [V]	25	170	700	2700
$F_{rf}$ [Hz]	1.35E+07	2.68E+07	1.83E+07	2.82E+07
Abucket [eV*rad]	1.24E+04	1.78E+05	4.65E+05	3.42E+06
Hbucket [eV]	4.66E+03	7.14E+04	1.86E+05	1.37E+06
Synchrotron Frequency [Hz]	7.80E+03	6.32E+03	2.48E+04	1.88E+04
$\Delta p/p$ increase per sweep [%]	3.67E-06	2.23E-05	8.60E-06	3.02E-05
<b>PHASE DISPLACEMENT</b>				
mean current [nA]	3.2	3.2	3.86	3.86
total particles	1.00E+11	1.00E+11	1.00E+09	1.00E+09
$\Delta W_{total}$ [eV]	7.30E+04	7.80E+05	2.47E+06	1.41E+07
$\Delta W_{sweep}$ [eV]	1971	2.84E+04	7.40E+04	6.45E+05
nsweps	38	28	34	26
<b>PULSED FASHION</b>				
Tsweep [ $\mu$ s]	8816	7891	3260	6586
Tmicropulse [ $\mu$ s]	702	886	407	103
nparticlesperasweep	>1e9	>1e9	>1e7	>1e7
Tspill [s]	0.21	0.217	0.243	0.224
maxspeedofsweep [Hz/sec]	1.30E+08	1.05E+08	2.65E+08	8.63E+06
$\Delta p/p$ of extracted beam [%]	0.1	0.1	0.1	0.1

TENTATIVE CHOICES FOR A PHASE DISPLACEMENT ACCELERATION INTO THE RESONANCE (h=100)

kinetic energy per nucleon	60MeV p*	300MeV p*	120MeV/u <sup>12</sup> C <sup>3+</sup>	400MeV/u <sup>12</sup> C <sup>3+</sup>
$\gamma$	1.064	1.32	1.120	1.426
$\beta$	0.342	0.653	0.463	0.713
$\eta$ ( $\eta=3$ )	0.772	0.463	0.575	0.38
$f_{rev}$ [MHz]	1.348	2.576	1.826	2.815
$\Delta p/p$ total ( $\Delta p/p$ beam=0.5%) [%]	0.7	0.7	0.7	0.7
$\Delta t_{sweep} = \Delta p/p \times f_{rev} \times \eta \times h$ [KHz]	730	835	893	749
h	100	100	100	100
<b>BUCKETS</b>				
$\phi_s$ [deg]	15	15	15	15
$\Gamma = \sin \phi_s$	0.259	0.259	0.259	0.259
$V_{rf}$ [V]	50	350	1400	5500
$F_{rf}$ [Hz]	1.35E+08	2.58E+08	1.83E+08	2.82E+08
Abucket [eV*rad]	5.54E+03	8.09E+04	2.08E+05	1.55E+06
Hbucket [eV]	2.22E+03	3.24E+04	8.24E+04	6.18E+05
Synchrotron Frequency [Hz]	3.13E+04	2.87E+04	1.18E+05	8.93E+04
$\Delta p/p$ increase per sweep [%]	4.34E-06	1.00E-05	3.69E-06	1.36E-05
<b>PHASE DISPLACEMENT</b>				
mean current [nA]	3.2	3.2	3.86	3.86
total particles	1.00E+11	1.00E+11	1.00E+09	1.00E+09
$\Delta W_{total}$ [eV]	7.30E+04	7.80E+05	2.47E+06	1.41E+07
$\Delta W_{sweep}$ [eV]	881	1.28E+04	3.31E+04	2.46E+05
nsweps	84	61	76	57
<b>PULSED FASHION</b>				
Tsweep [ $\mu$ s]	2800	2832	3280	4264
Tmicropulse [ $\mu$ s]	350	480	407	633
nparticlesperasweep	>1e9	>1e9	>1e7	>1e7
Tspill [s]	0.236	0.232	0.243	0.244
maxspeedofsweep [Hz/sec]	2.60E+08	2.18E+08	2.85E+08	1.76E+08
$\Delta p/p$ of extracted beam [%]	0.1	0.1	0.1	0.1

**TENTATIVE CHOICES FOR A MICROBUCKETS ACCELERATION TO FEED THE RESONANCE (h=10, proton case considered)**

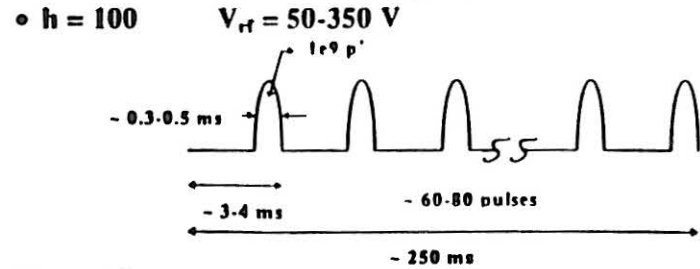
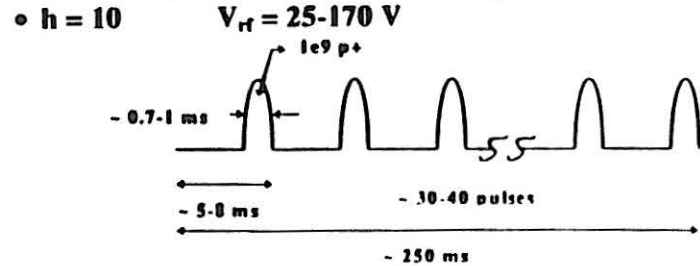
ACCELERATION FROM THE BOTTOM OF THE STACK			ACCELERATION FROM THE TOP OF THE STACK			
kinetic energy	60MeV p <sup>+</sup>	300MeV p <sup>+</sup>	60MeV p <sup>+</sup>		300MeV p <sup>+</sup>	
totalparticles	1.00E+11	1.00E+11	1.00E+11		1.00E+11	
nparticlespersweep	>1e9	>1e9	>1e9		>1e9	
h	10	10	10		10	
φ <sub>s</sub> [deg]	15	15	15		15	
V <sub>n</sub> [V]	20	140	20		140	
F <sub>n</sub> [Hz]	1.35E+07	2.69E+07	1.35E+07		2.69E+07	
Δp/p incr. due to trav. bucket[%]	1.47E-06	9.05E-06	/		/	
Synchrotron Frequency [Hz]	6.26E+03	5.74E+03	6.26E+03		5.74E+03	
maxspeedofsweep[Hz/s]	1.04E+07	8.70E+06	/		/	
			MIN fsweep	MAX fsweep	MIN fsweep	MAX fsweep
Δf <sub>total</sub> = Δp/p x f <sub>trav</sub> x η x h [Hz]	6.25E+04	7.16E+04	1.04E+04	6.25E+04	1.19E+04	7.16E+04
ΔWtotal [eV]	6.34E+04	6.89E+05	6.34E+04		6.89E+05	
ΔWfsweep [eV]	1703	2.57E+04	1703		25741	
numberofsweeps	35	26	35		26	
Tsweep [μs]	6017	8213	1002	6017	1369	8213
Tmicropulse [μs]	782	1026	782		1026	
Tsplit [ms]	216	213	216		213	
Δp/p of extracted beam[%]	0.1	0.1	0.1		0.1	

**TENTATIVE CHOICES FOR A MICROBUCKETS ACCELERATION TO FEED THE RESONANCE (h=100, proton case considered)**

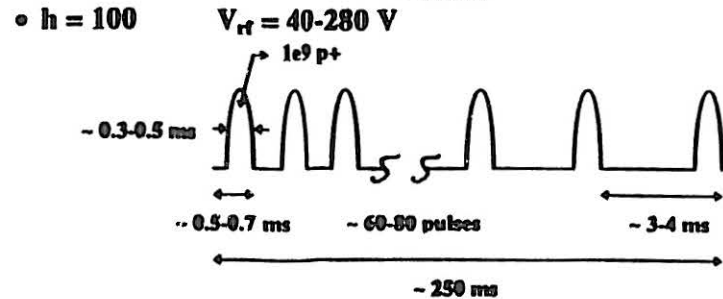
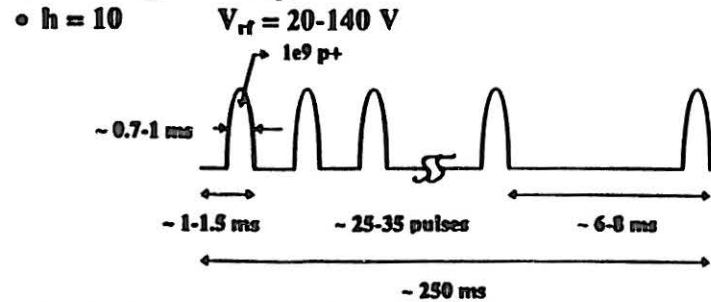
ACCELERATION FROM THE BOTTOM OF THE STACK			ACCELERATION FROM THE TOP OF THE STACK			
kinetic energy	60MeV p <sup>+</sup>	300MeV p <sup>+</sup>	60MeV p <sup>+</sup>		300MeV p <sup>+</sup>	
totalparticles	1.00E+11	1.00E+11	1.00E+11		1.00E+11	
nparticlespersweep	>1e9	>1e9	>1e9		>1e9	
h	100	100	100		100	
φ <sub>s</sub> [deg]	15	15	15		15	
V <sub>n</sub> [V]	40	260	40		260	
F <sub>n</sub> [Hz]	1.35E+08	2.59E+08	1.35E+08		2.59E+08	
Δp/p incr. due to trav. bucket[%]	1.47E-06	9.05E-06	/		/	
Synchrotron Frequency [Hz]	2.80E+04	2.57E+04	2.80E+04		2.57E+04	
maxspeedofsweep[Hz/s]	2.08E+08	1.74E+08	/		/	
			MIN fsweep	MAX fsweep	MIN fsweep	MAX fsweep
Δf <sub>total</sub> = Δp/p x f <sub>trav</sub> x η x h [Hz]	6.25E+05	7.16E+05	1.04E+05	6.25E+05	1.19E+05	7.16E+05
ΔWtotal [eV]	6.34E+04	6.89E+05	6.34E+04		6.89E+05	
ΔWfsweep [eV]	783	1.15E+04	783		11511	
numberofsweeps	80	89	80		89	
Tsweep [μs]	3003	4183	601	3003	694	4183
Tmicropulse [μs]	376	513	376		513	
Tsplit [ms]	242	223	242		223	
Δp/p of extracted beam[%]	0.1	0.1	0.1		0.1	

**BEAM PULSE STRUCTURE (PROTONS W=60-300 MeV)**

**Phase Displacement and Unstacking from Bottom.**

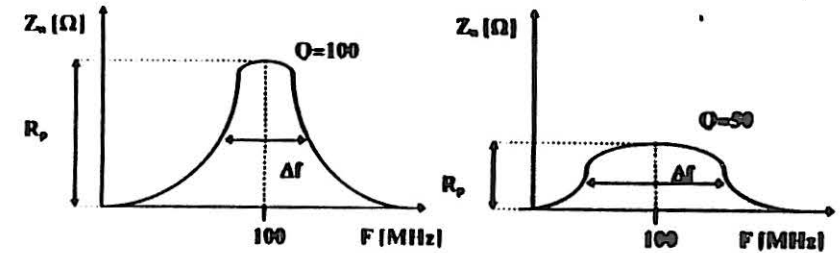


**Unstacking from Top.**



**RF SYSTEM ( $h = 100$ )**

$F_{rf} = 100$  MHz       $\Delta f \sim 1$  MHz       $\Rightarrow Q = F_{rf}/\Delta f = 100$



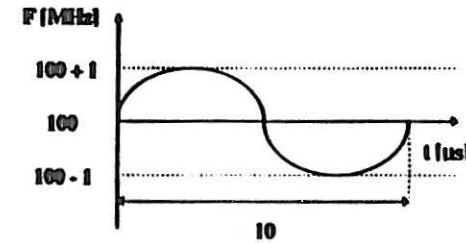
If we decrease the Q factor we can do the  $\Delta f$  swing without tuner.

$Q = 50$        $Z_n = R_p/Q \sim 100 \Omega$        $\Rightarrow R_p = 5$  k $\Omega$

$V_{rf} \sim 1000$  V

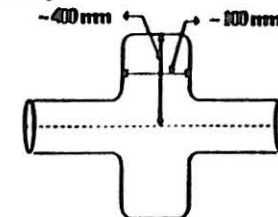
$P = V_{rf}^2 / (2\pi R_p) = 100$  W  $\Rightarrow$  small power to handle.

$\tau = Q/\pi \times 1/f \sim 160$  ns  $\Rightarrow$  the cavity will rapidly follow the swing.



$\lambda = c/F_{rf} = 3$  m

Example: a pill-box cavity.



Small beam pipe dimensions.  
Low dispersion region needed.

---

**CONCLUSION****POINTS IN FAVOUR**

- very few parameters to vary: RF voltage, frequency swing.
- unstacking from the top good estimation of the number of particles extracted per micropulse (+  $A_h$ ).
- pulsed extraction (possible treatment with voxel scanning?)
- easy and quick to stop: RF power off.

**POINTS NOT IN FAVOUR**

- slow micropulse extraction (hundreds of microseconds).
  - not continuous beam pulse extraction (not possible treatment with raster scanning?).
  - if high harmonic number a "small" dedicated RF system is needed.
  - lattice constraints: additional ~ 0.2/0.3 m needed for the additional cavity in a low dispersion region.
- 

---

**REFERENCES:**

- 1) E.J.N. Wilson, Proton Synchrotron Accelerator Theory, CERN 77/07.
  - 2) E. Ciapala, Stacking and Phase Displacement Acceleration, CERN 85/19 CAS.
  - 3) C. Bovei et al., A Selection of Formulae and Data Useful for the Design of Alternating Gradient Synchrotrons, CERN MPS-SI, Int. DL/70/4.
  - 4) P. Bryant, E. Ciapala, W. Pirkl, private communications.
-

---

**BETATRON ACCELERATION  
DURING EXTRACTION**

presented by  
C. Steinbach

February 13th and 14th 1996

PS, CERN

---

---

**BETATRON ACCELERATION  
DURING EXTRACTION**

**CH. STEINBACH**

There are (at least) 2 ways to control a resonant extraction during the "spill":

- sweep the resonance through the beam (by gradually changing the value of  $Q_x$ ),
- accelerate the beam through the resonance.

The second method is better, because:

- the extracted beam central energy is fixed,
- all transverse parameters stay constant.

Acceleration can be done with:

- continuous wave RF, but  $\Delta p/p$  is low, synchrotron oscillations can create problems and both high and low frequency structures are present in the extracted beam,
  - phase displacement, but the process is not continuous,
  - RF noise, but a lot of power is needed for spills of the order of a few hundreds of milliseconds,
  - betatron acceleration, which works with debunched beam and is compatible with the phase displacement ripple reduction technique.
-

## Principle of betatron acceleration

A magnetic flux  $\Phi$  is created around the circulating beam with one or several magnetic circuits (torus). Just like in a transformer, a field  $E$  appears inside, along the circumference, following the equation:

$$\int E ds = \frac{d\Phi}{dt} \quad (1)$$

If  $E$  is the mean electrical field over a revolution and  $C$  is the orbit length, this writes:

$$d\Phi = C E dt \quad (2)$$

The increase of the particle momentum due to this electrical field is:

$$dp = Z e E dt \quad (3)$$

where  $Z e$  is the particle charge.

From (2) and (3), we obtain:

$$dp = \frac{Z e}{C} d\Phi \quad (4)$$

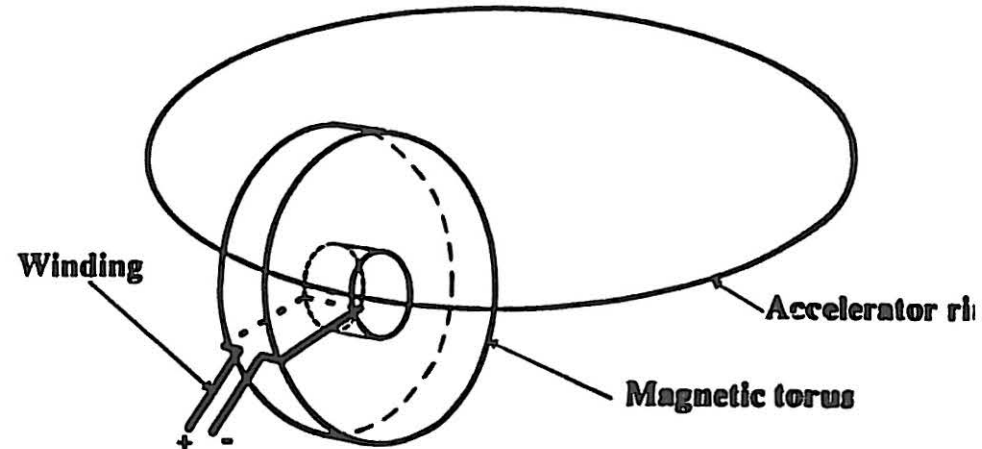
introducing the magnetic rigidity:

$$B\rho = \frac{p}{Z e} \quad (5)$$

and integrating along the time, we obtain the momentum increase due to the flux variation  $\Delta\Phi$ :

$$\frac{\Delta p}{p} = \frac{1}{C B\rho} \Delta\Phi \quad (6)$$

## Sketch of installation



## Application to TERA project (95' parameters)

If we want to accelerate by  $\Delta p/p = .3 \%$ ,

assuming  $C = 80$  m,

$B\rho = 6.3$  Tm (for high energy ions), then:

$$\frac{3}{1000} = \frac{\Delta p}{p} = \frac{1}{C B\rho} \Delta\Phi = \frac{1}{80 \times 6.3} \Delta\Phi$$

$$\Delta\Phi \cong 1.5 \text{ Tm}$$

which can be done with a section of  $.5 \text{ m}^2$  of cheap iron, and a field varying from  $-1.5$  T to  $+1.5$  T.

**Proposed characteristics (after M.Thivent, CERN PS and Heidelberg and Saclay equipments)**

**Magnetic torus (4 units):**

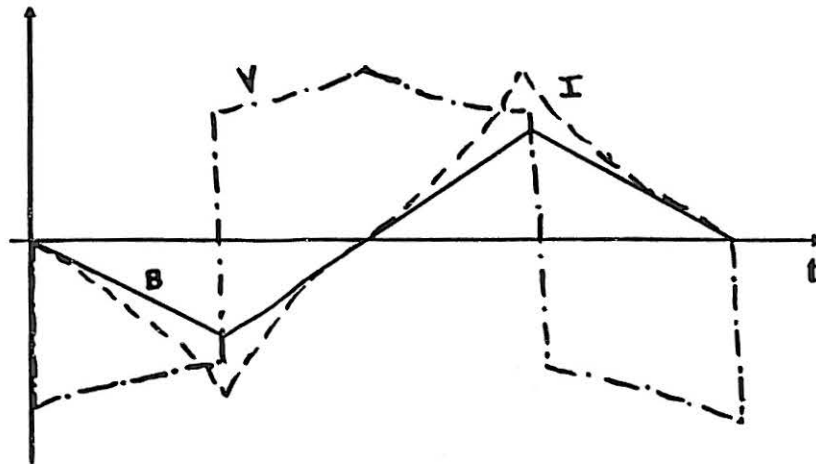
External diameter: 1000 mm  
 Internal diameter: 160 mm  
 Length: 300 mm  
 Weight: 7200 Kg (rolled iron sheet)

**Coil:**

Section: 2.5 mm<sup>2</sup>  
 Number of turns: 50  
 Resistance: 3 Ω  
 Inductance: 10 mH

**Power supply:**

Maximum current: 20 A  
 Maximum voltage: 60 V



**CONCLUSIONS**

Accelerating the beam through resonance with betatron acceleration and use of low frequency ripple reduction with RF phase displacement seems to be the most attractive scheme: it offers a constant mean energy, a small  $\Delta p/p$  of the extracted beam and a good ripple rejection.

To accelerate by  $\Delta p/p = .3\%$  (at 400 Mev/u for oxygen ions), the longitudinal space required is of the order of 1.5 m, the technology is simple and the price reasonable (as compared with RF acceleration).

**References (thanks to D. Möhl):**

An Induction Accelerator for the Heidelberg Test Storage Ring TSR, Ch. Ellert et al. MPIH-V31-1991

Le Betatron Injecteur de MIMAS, J.C. Ciret 16 mars 1998

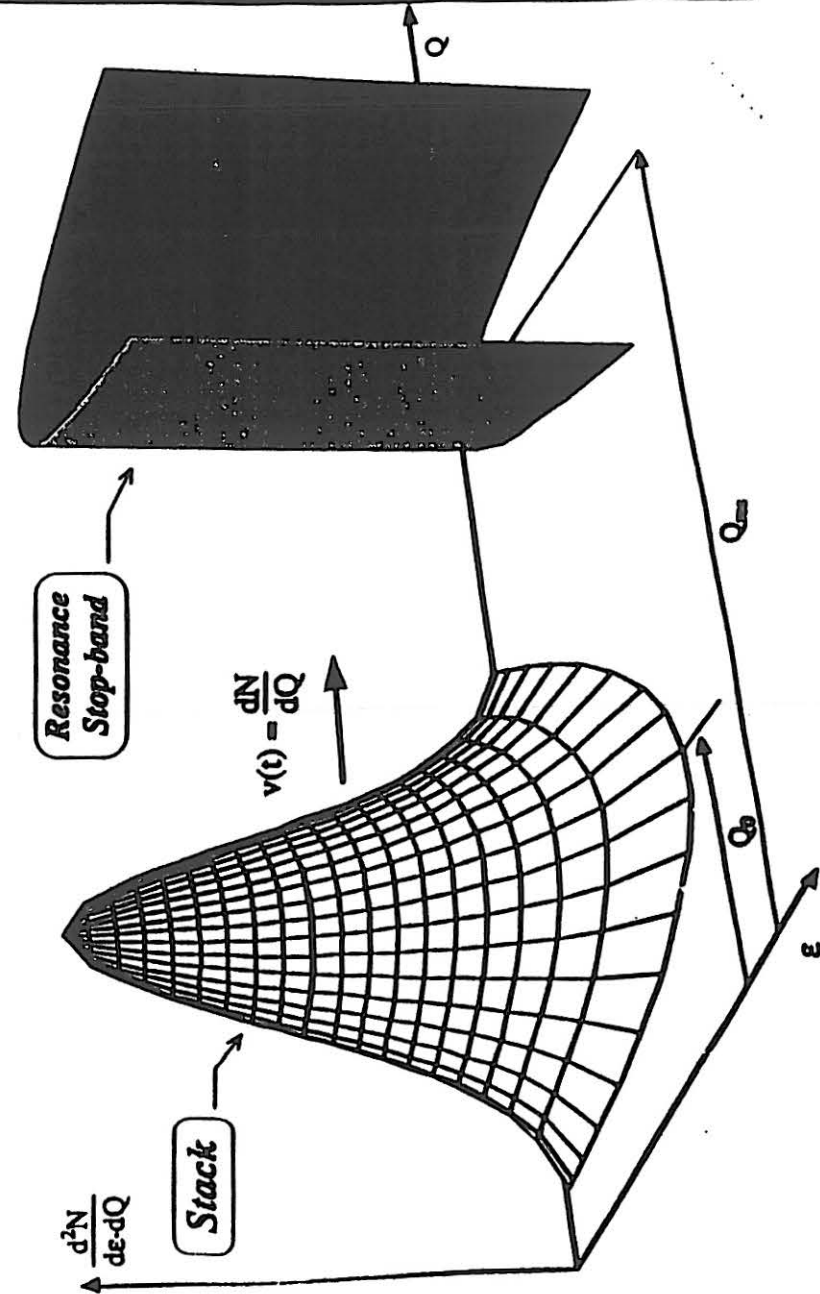
# SPS EXPERIENCE AND SPILL CONTROL

presented by  
M. Gyr, SL

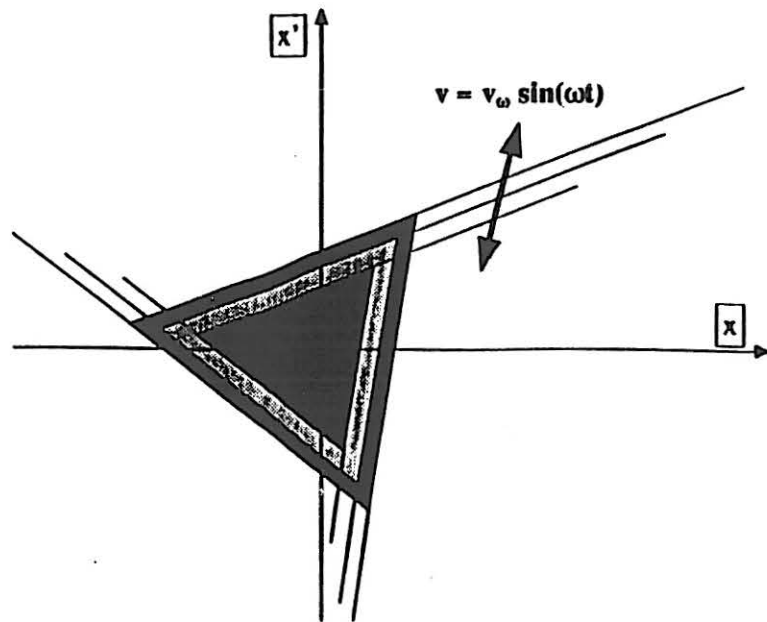
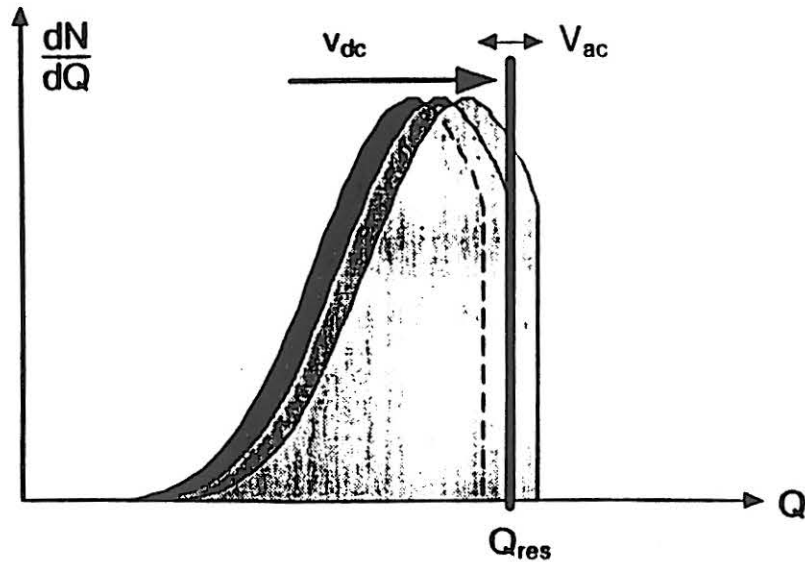
February 13th and 14th 1996

PS, CERN

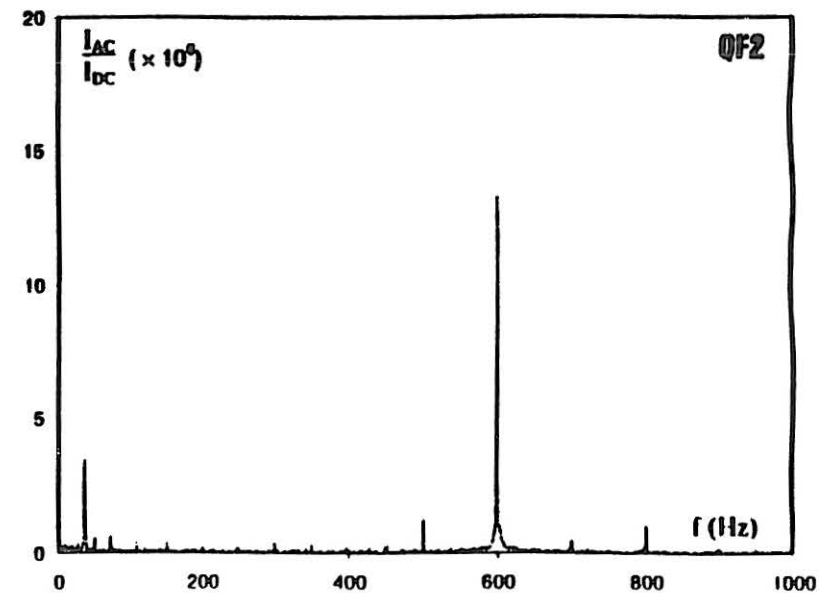
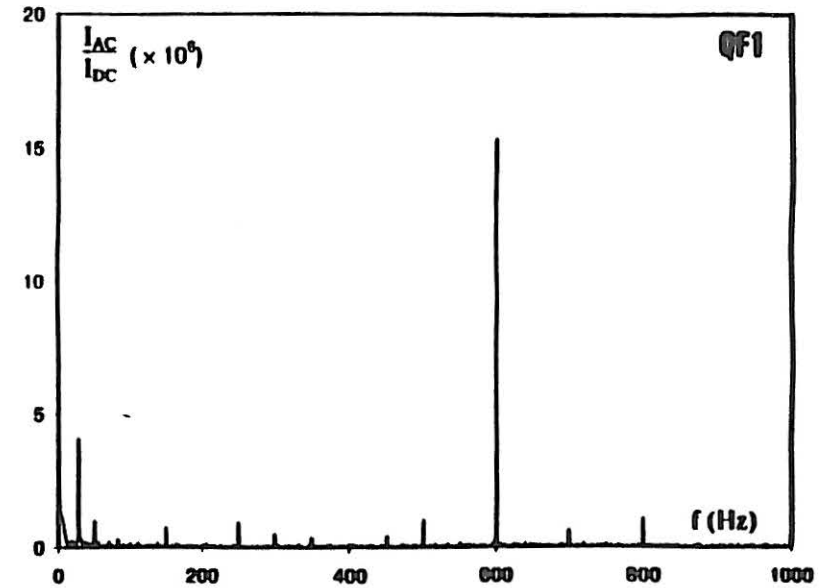
## Conventional resonant extraction in Amplitude & Momentum

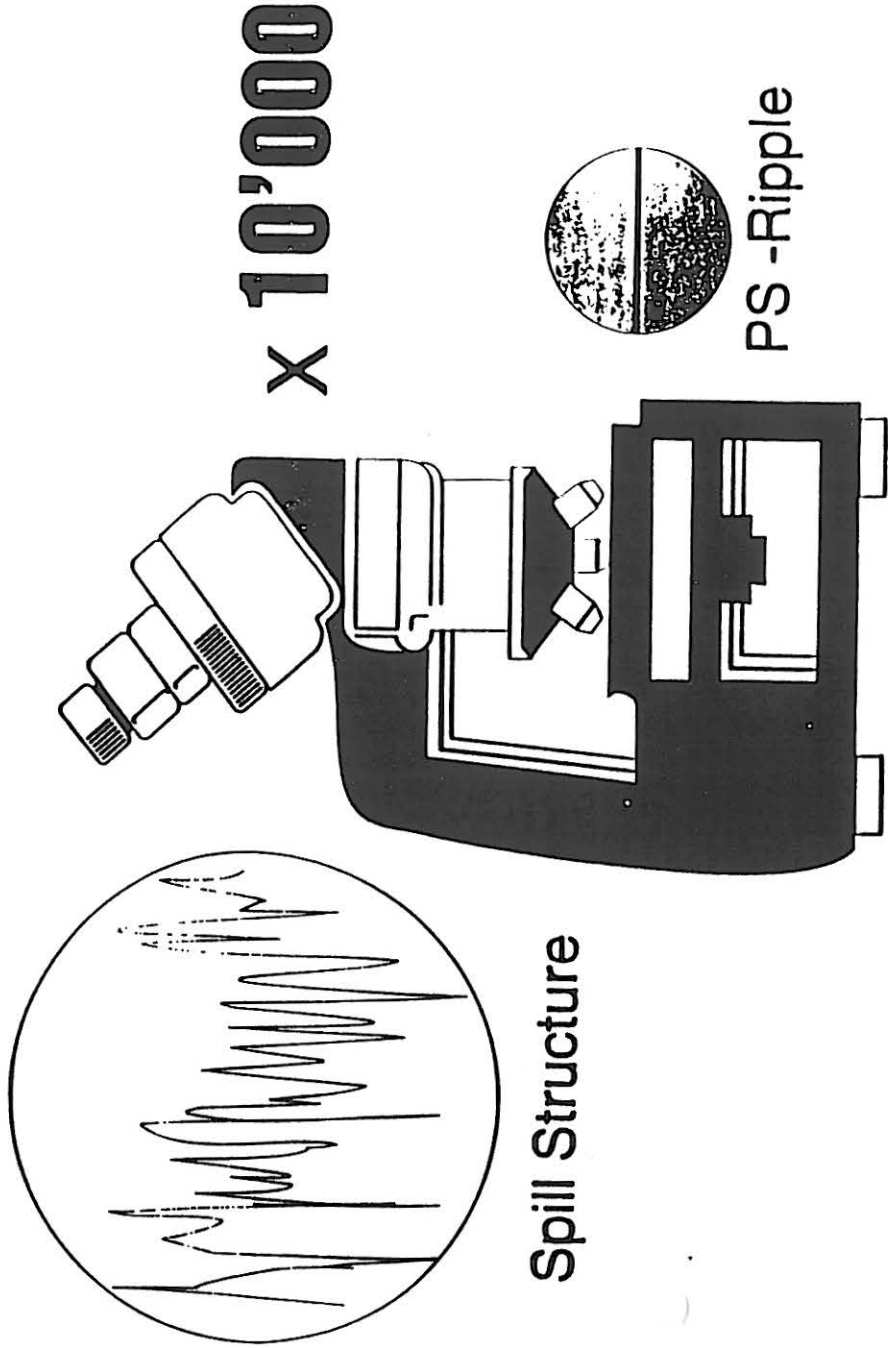


### Fluctuations at Resonance Stopband Limit in Momentum- & Phase Space

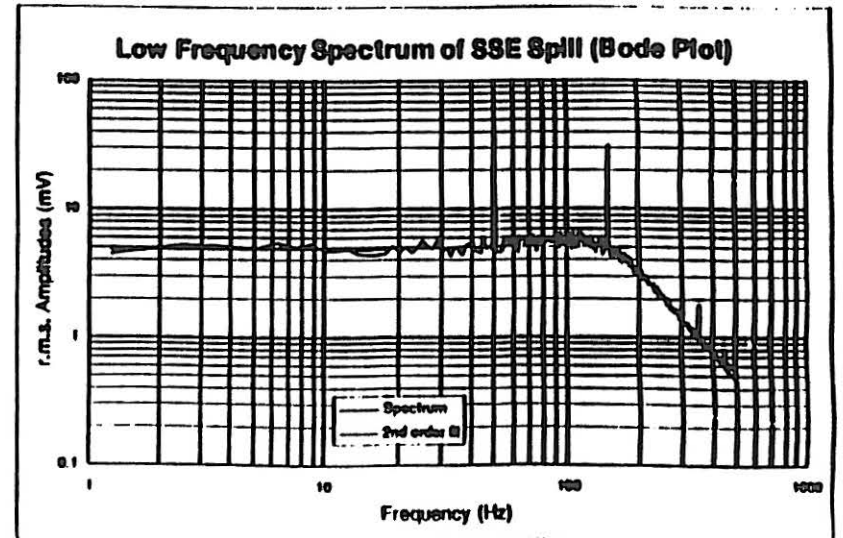
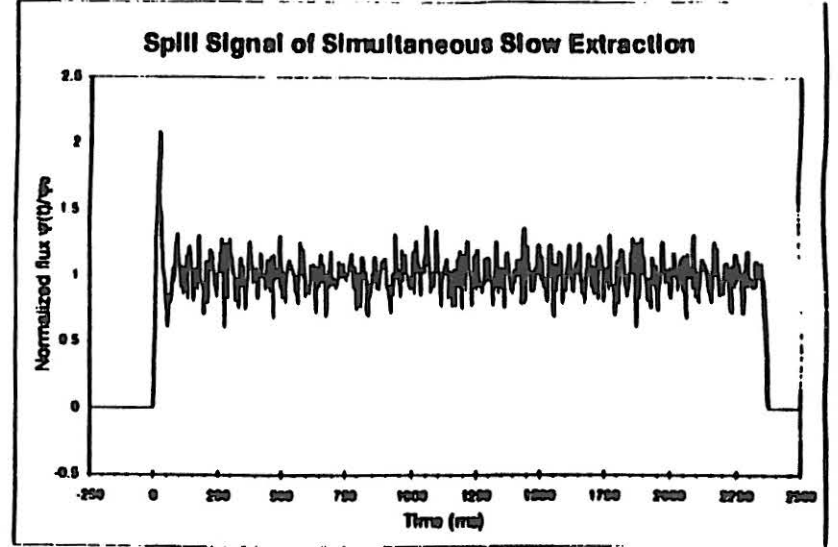


### Low frequency spectrum of current in F-quadrupoles

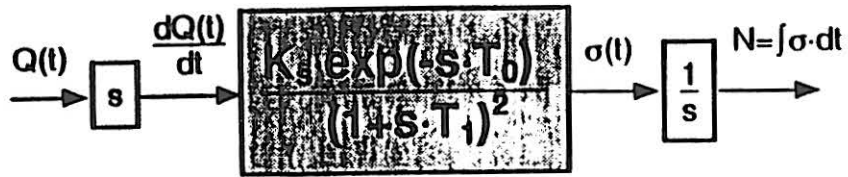




# Spill of Shared Slow Extraction



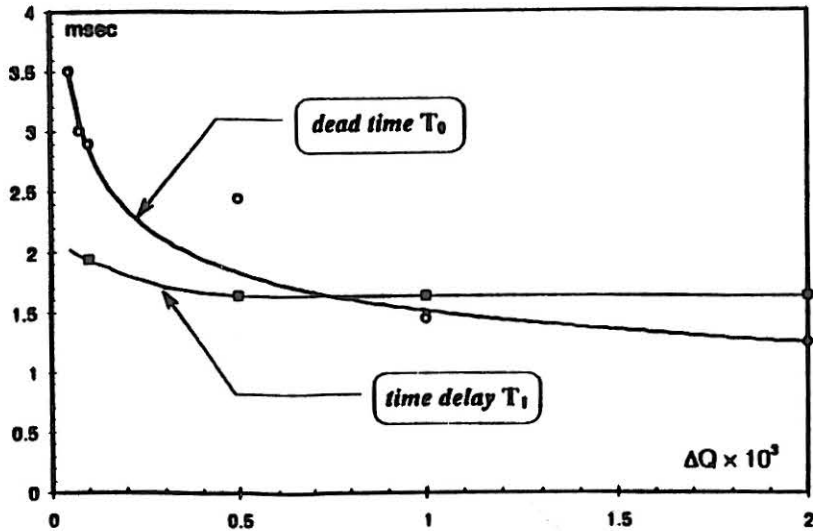
### TF G(s) of Extraction Process



obtained from unit-step response of  $N(t)$  w.r.t.  $\Delta Q(t) = u(t)$

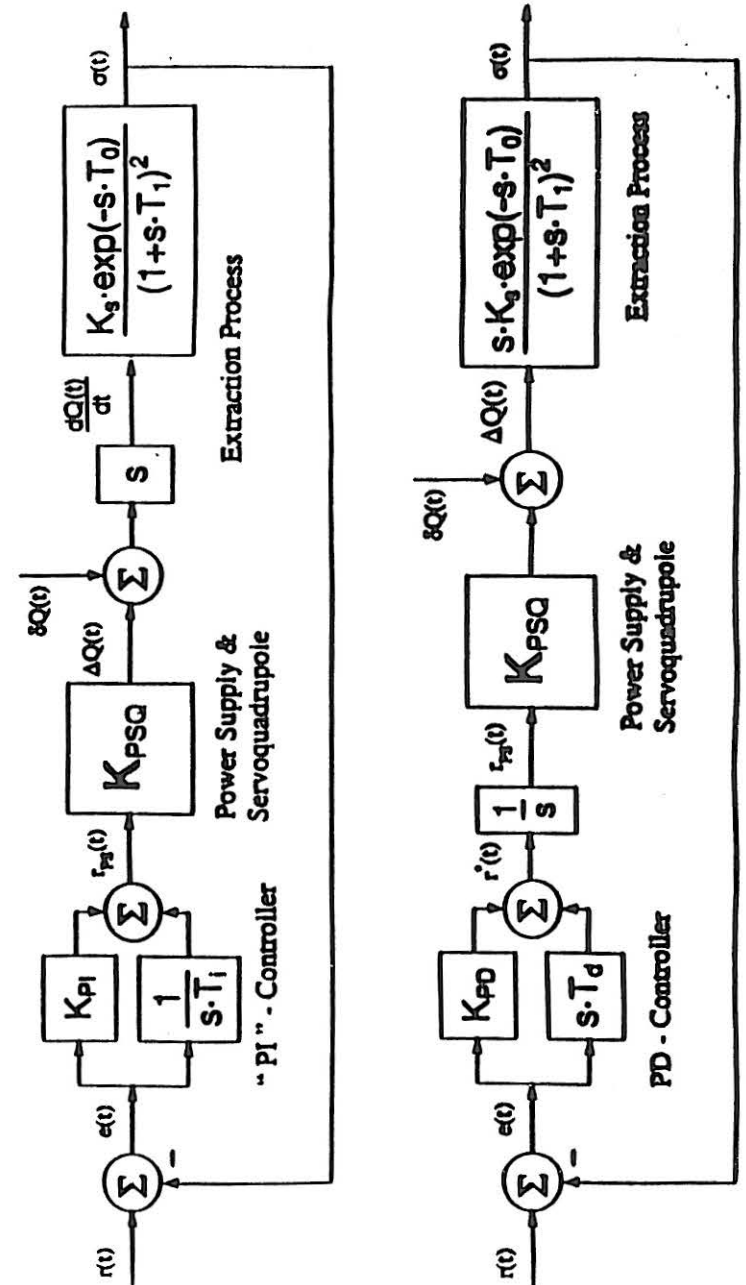
Dead time  $T_0$  due to dwell time: 60 - 100 turns  
 Time delay  $T_1$  (double pole): about 70 turns

Amplitude dependence of "Time constants"  $T_0$  and  $T_1$

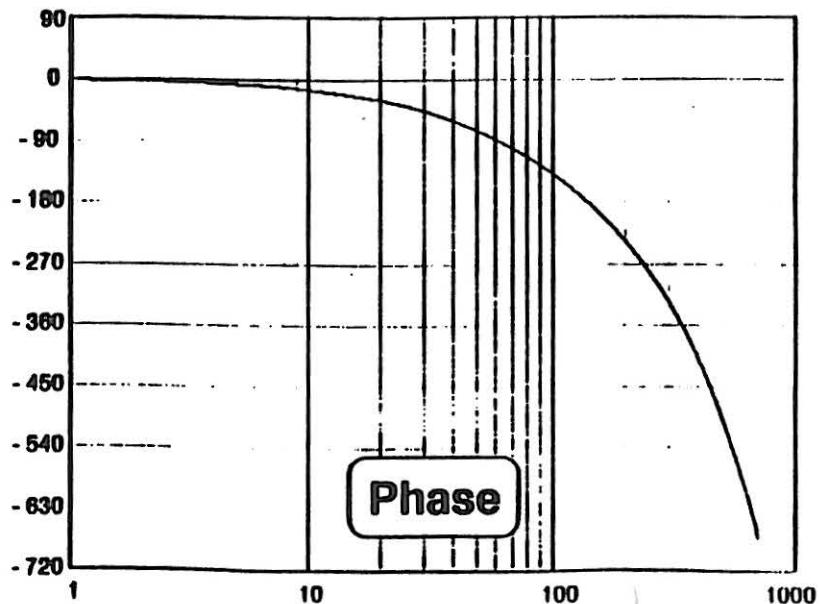
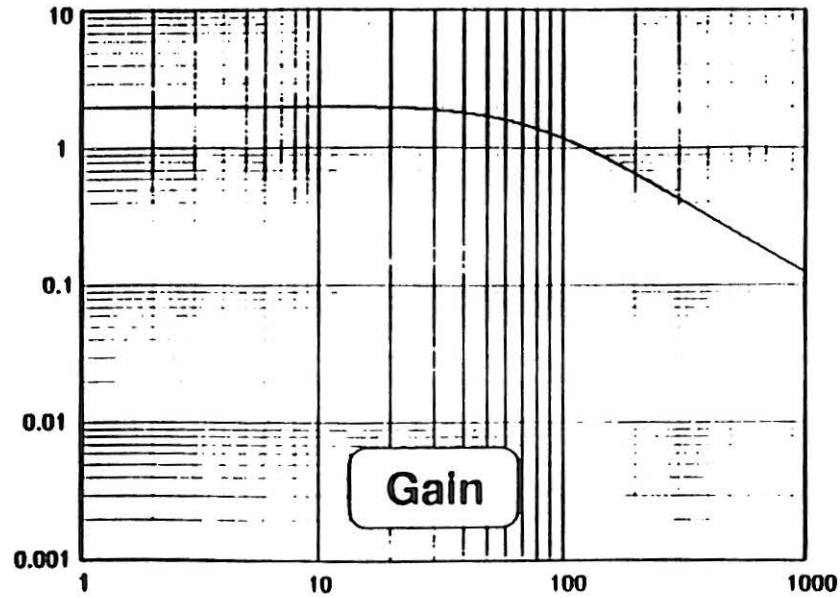


V. Rödel: *La dynamique de l'extraction lente du synchrotron à protons de 400 GeV du CERN en vue d'un asservissement* (PhD-Thesis N° 506, EPFL, 1983)

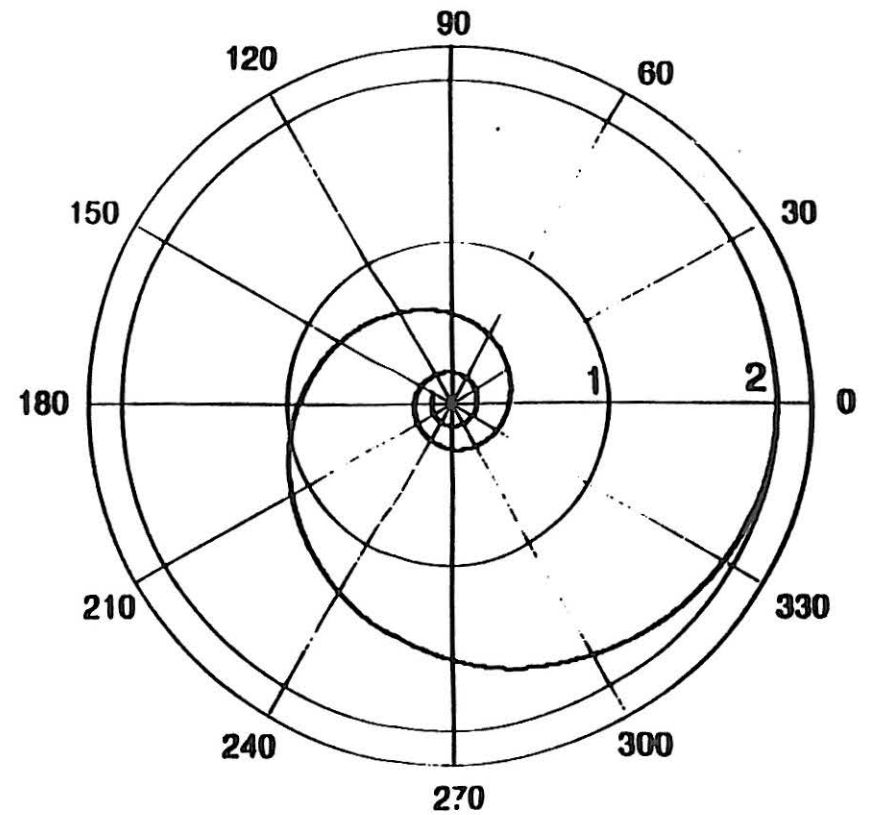
### Servo Spill Feedback System



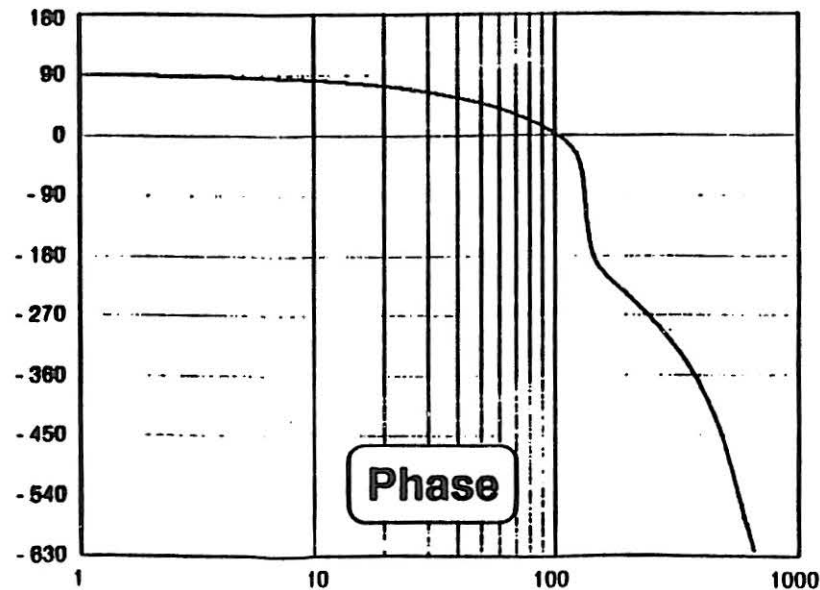
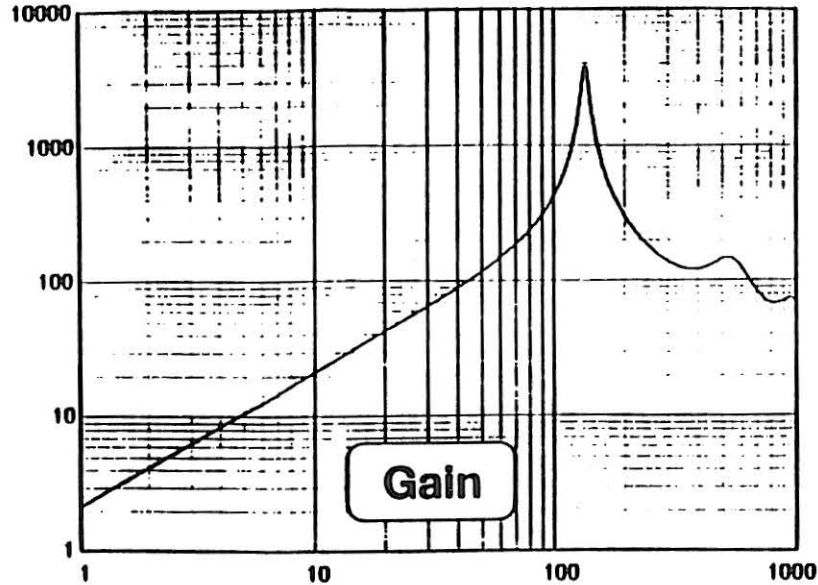
### Open loop Transfer Function



### Open loop Polar Plot: $G_0(j\omega)$



Closed loop TF:  $\delta Q(t) \rightarrow \sigma(t)$



Stochastic & "combined" extraction

Particle density:  $\Psi(\vec{r}, t) = \frac{dN}{dVol}$

Change of density due to diffusion and drift current:

$$\frac{\partial \Psi(\vec{r}, t)}{\partial t} = \text{div}(D \cdot \text{grad } \Psi(\vec{r}, t) - \vec{v} \cdot \Psi(\vec{r}, t))$$

Fokker-Planck equation

Diffusion constant D :

$$D_E = \frac{1}{2} \cdot \frac{d\langle E^2 \rangle}{dt} = \frac{1}{2W} \left( \frac{e \cdot V_{rms}}{T} \right)^2$$

p - space :  $\left( \frac{dp}{p} = \frac{1}{\beta c} \frac{dE}{E} \right) \quad D_p = \left( \frac{1}{\beta c} \right)^2 D_E$

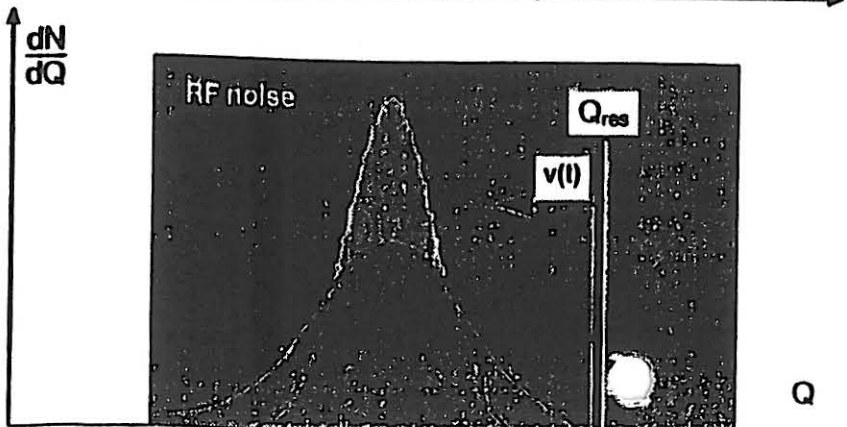
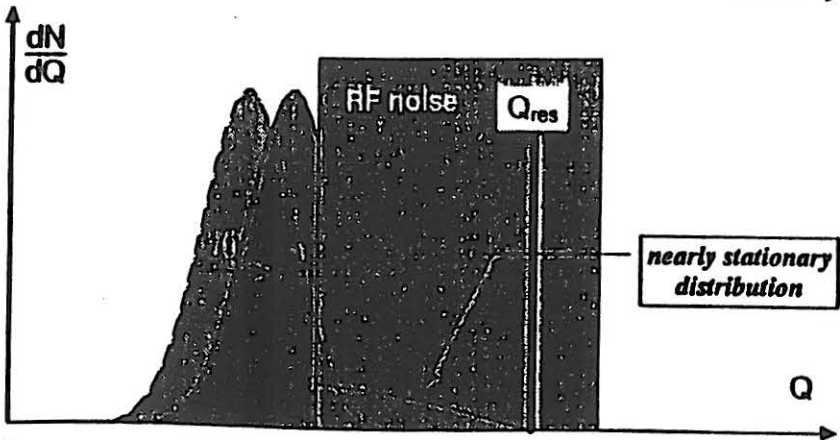
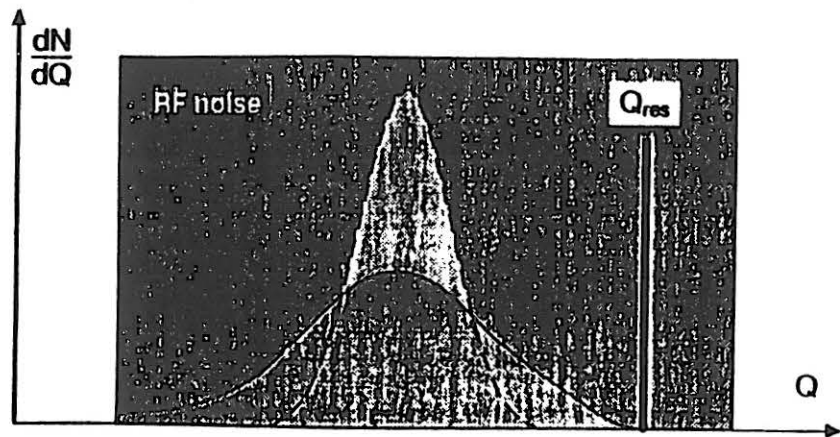
Q - space :  $\left( \frac{dQ}{Q} = \xi \frac{dp}{p} \right) \quad D_Q = \left( \frac{\xi Q}{\beta c p} \right)^2 D_E$

f - space :  $\left( \frac{df}{f_r} = \eta \frac{dp}{p} \right) \quad D_f = \left( \frac{\eta f_r}{\beta c p} \right)^2 D_E$

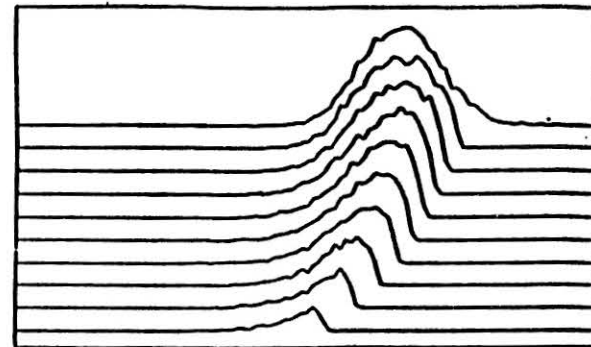
Ripple improvement factor:

$$F_\omega = \frac{\sqrt{\omega D}}{\bar{v}_o}$$

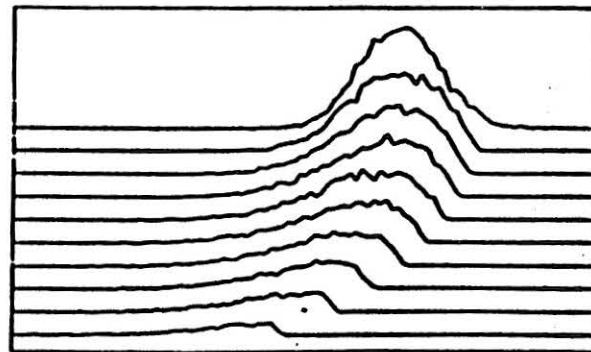
### Stochastic & Combined Extraction



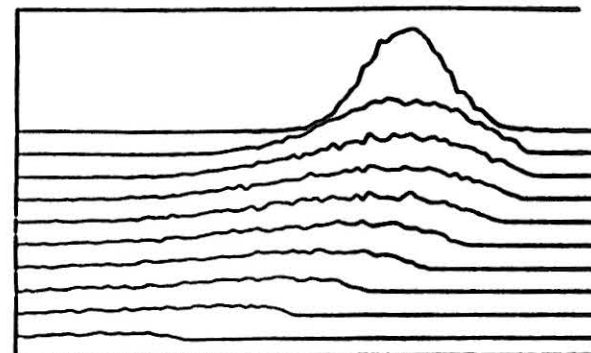
### Extraction process with RF noise



a)  $D = 1/2$



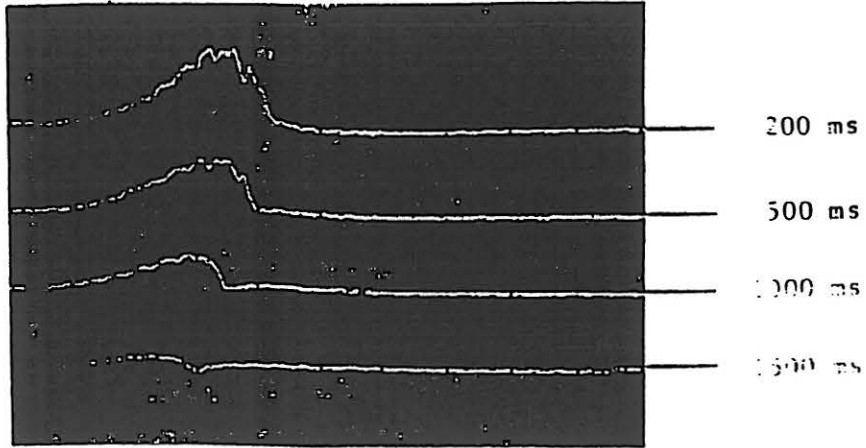
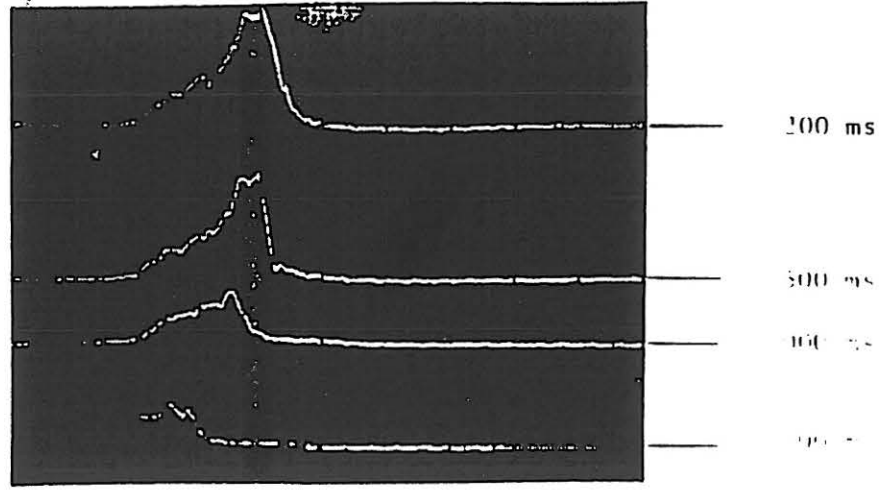
b)  $D = 1$



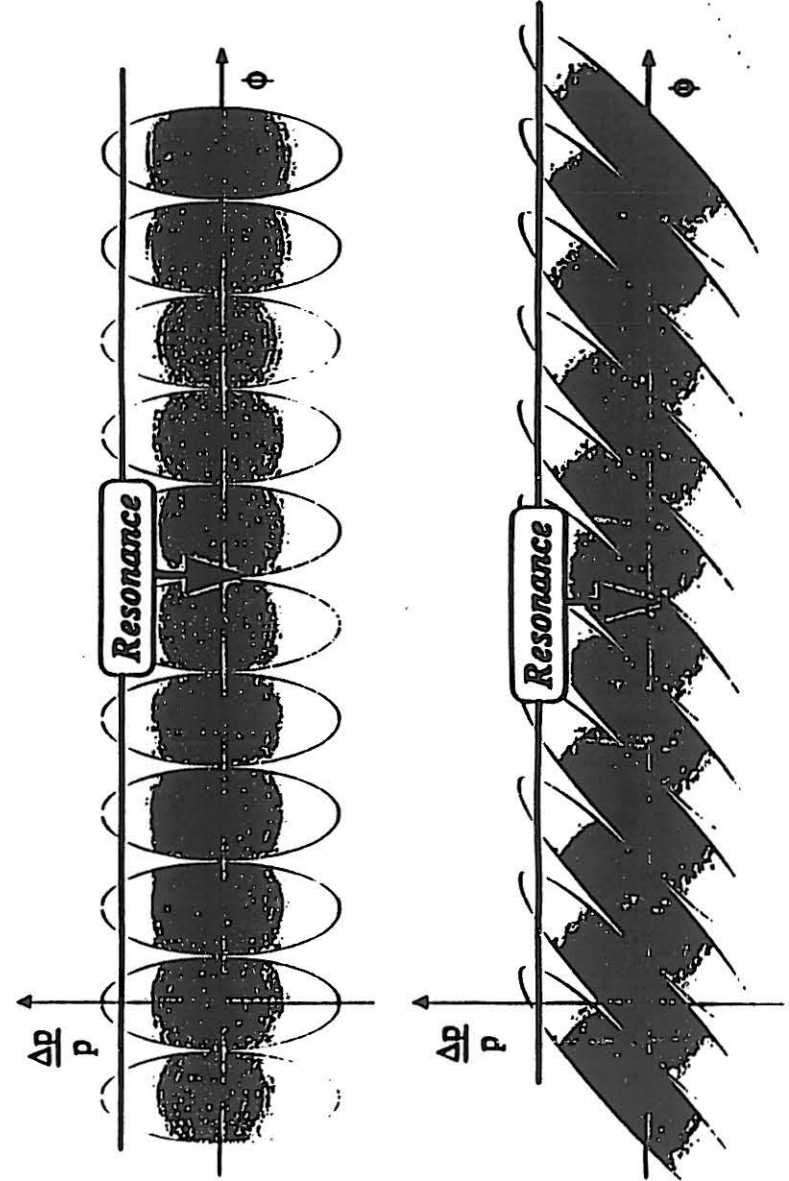
c)  $D = 1$

69480

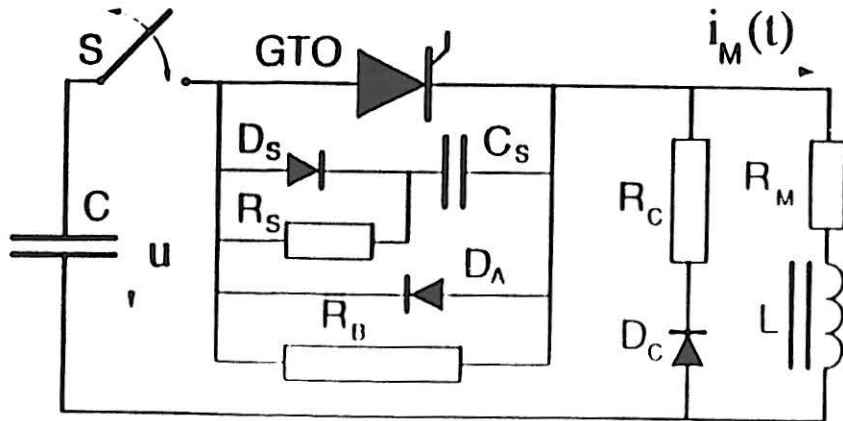
Simulation with Monte Carlo Method for different diffusion constants



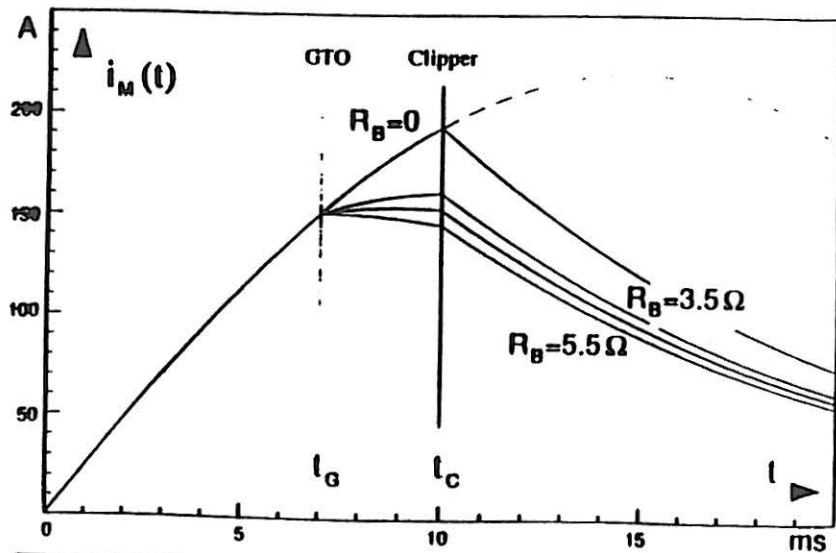
### RF-structure of "debunched" beam



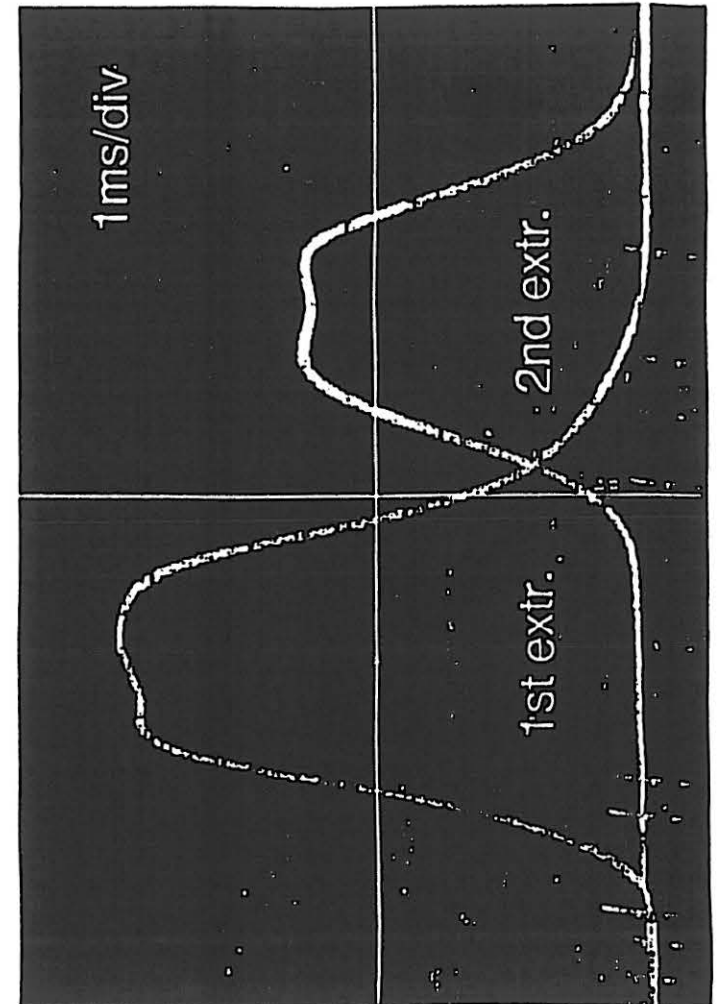
### Power Supply for "rectangular" FS-spill



### Current waveform in extraction quadrupole



### Spill Signals of FS-Extraction to Neutrino



**RESONANT  
EXTRACTION IN SPS**

presented by  
K. Cornelis, SL

**February 13th and 14th 1996**

**PS, CERN**

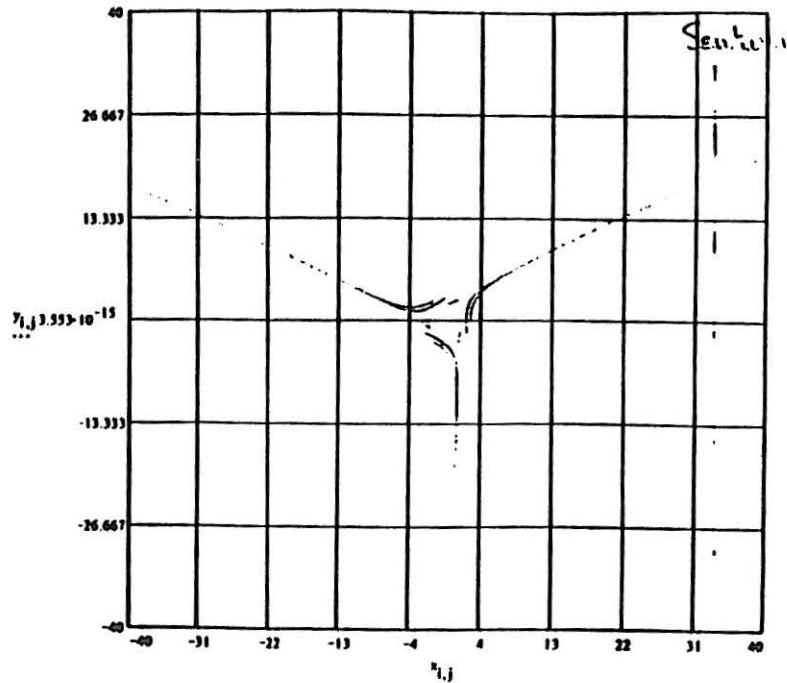
---

- Layout of the extraction channel
- Types of extractions
- The shared slow extraction 2/3
- losses on the extraction channel

**Layout of the extraction channel**

- Electrostatic septum : Voltage cannot change during the cycle. (100kV/cm)
  - Thin magnetic septum (3mm)
  - Thick magnetic septum (16mm)
  - 5 orbit correctors to make extraction bump
-





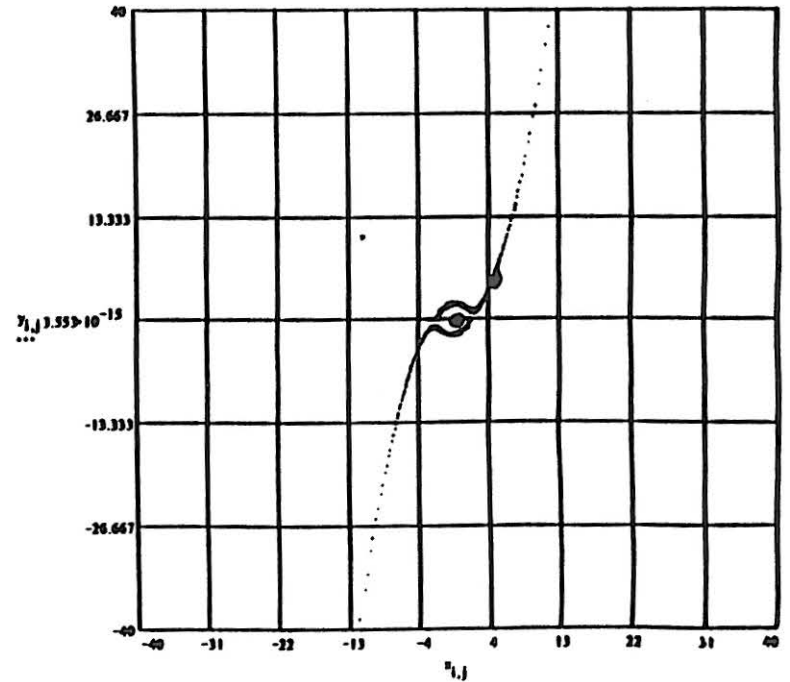
Distance to septum : 32 mm

jump : 15 mm

Beam size : 2 mm

$$D_x, D'_x = 0$$

1/2 and fast-fast slow



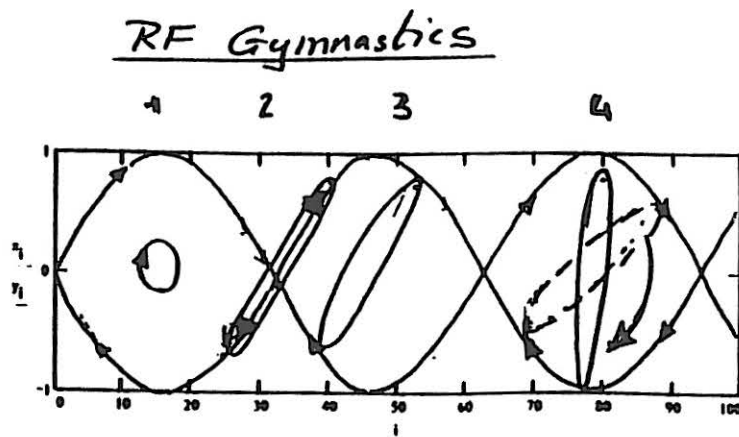
Slow extractions :

$$\xi = \frac{\frac{\Delta Q}{Q}}{\frac{\Delta P}{P}} = -1$$

i.e. a strong dependence of Q on momentum

$$Q = 26.666 - \varepsilon \quad \text{or} \quad Q = 26.500 + \varepsilon$$

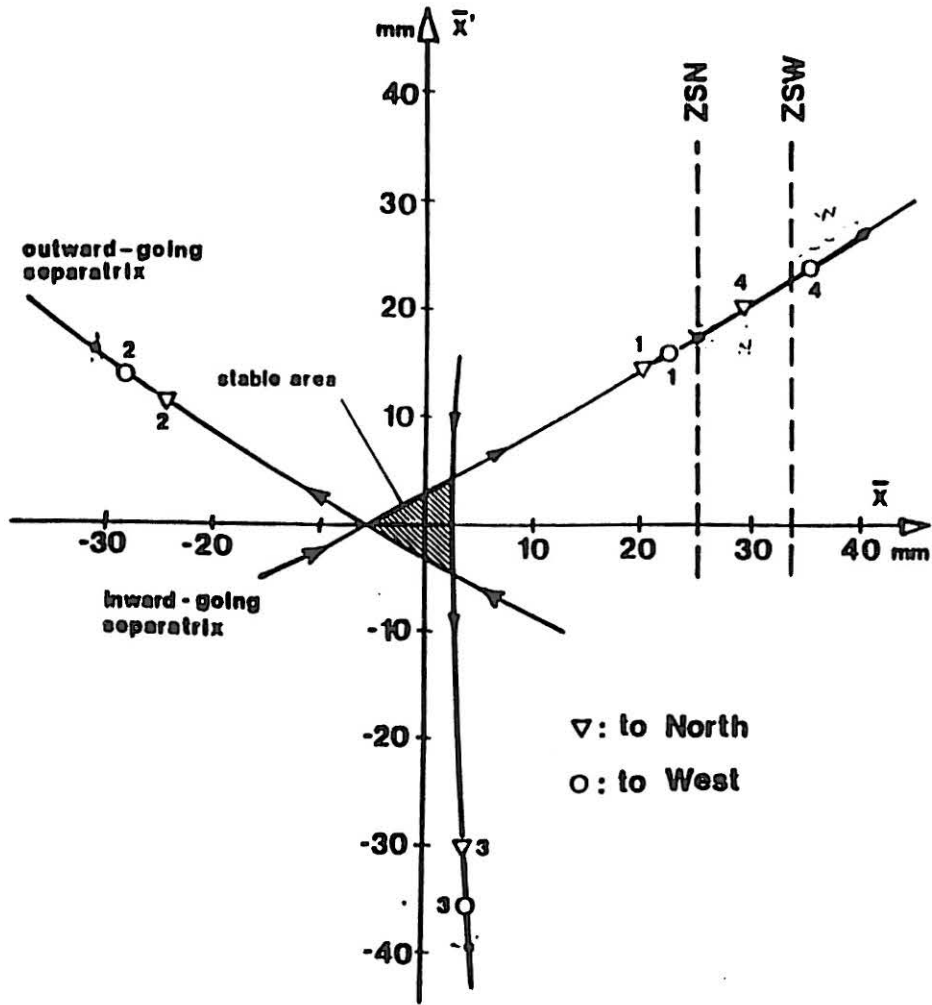
$\Delta P/P$  is maximised using RF gymnastics  $\sim 1.5 \cdot 10^{-3}$



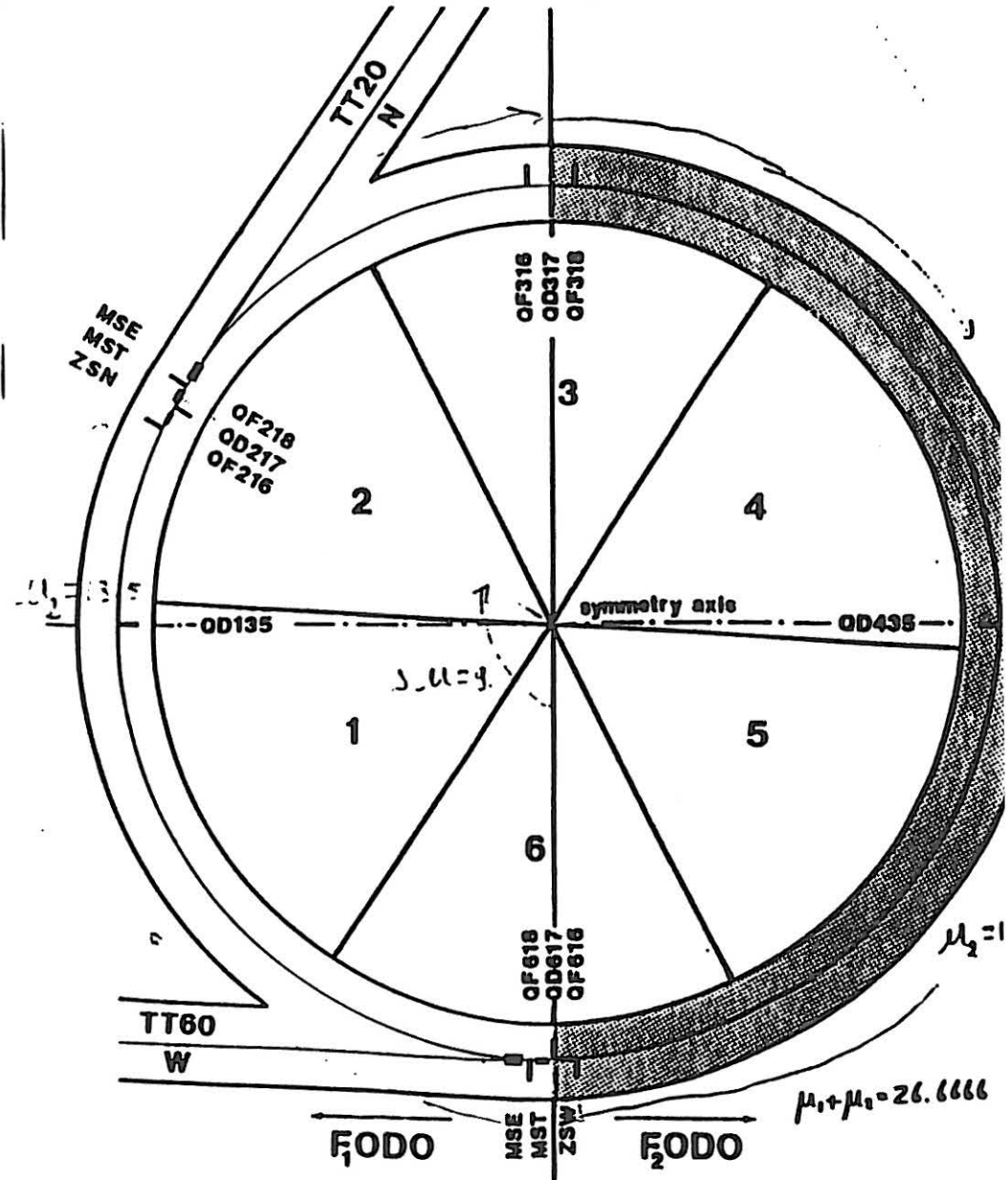
Shared slow extraction on 2/3

Simultaneous extraction in two points of the machine.

The phase advance between the two points has to be an exact integer.



▽: to North  
○: to West

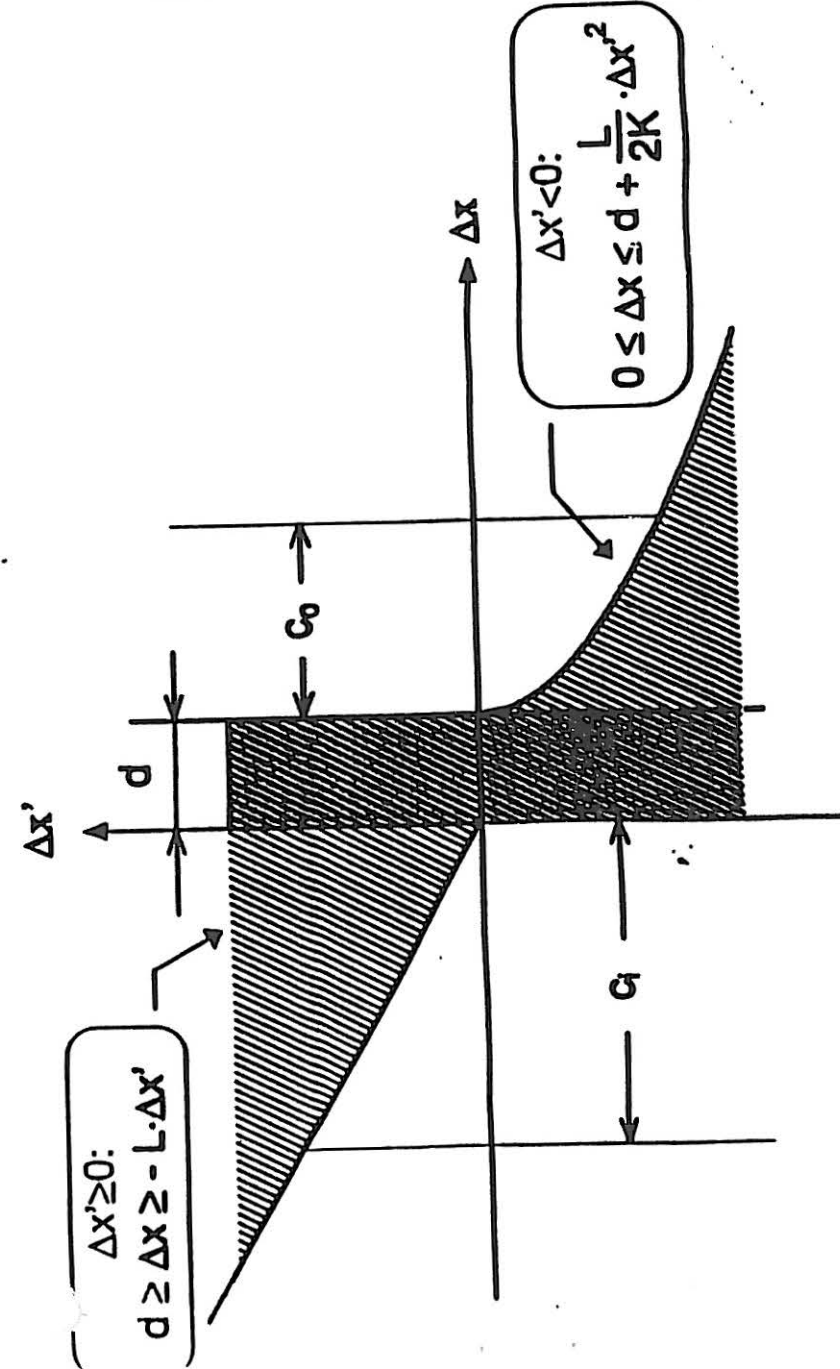


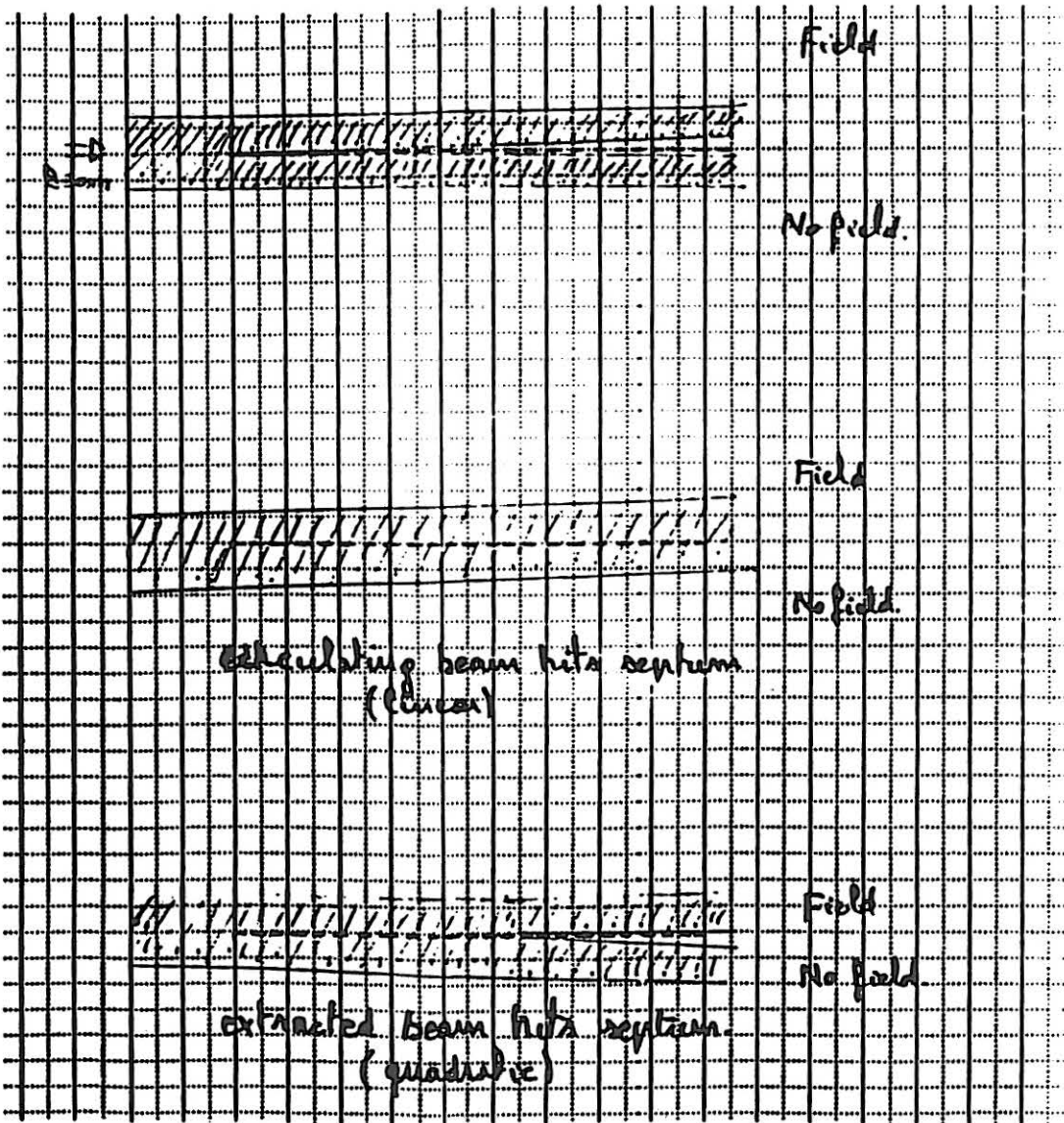
### Losses on the extraction channel

The angle at the septum has to be very well adjusted

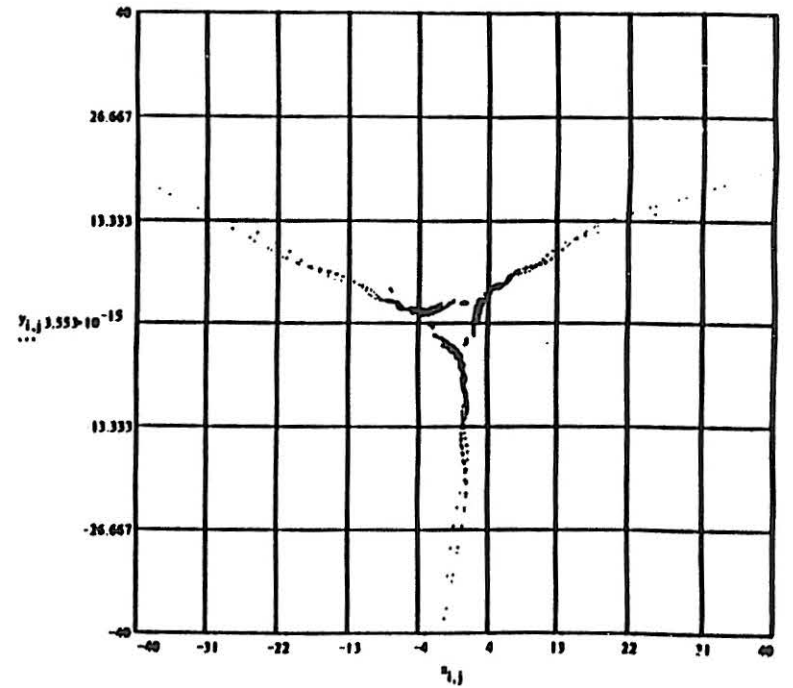
Effective septum thickness

### Effective septum thickness





The effect of time modulation.



## Tentative Medical Ring Parameters

For proton and light-ion cancer therapy

1. Relativistic parameters and constants			
Parameter	Injection	1st extraction	Top energy
<b>Protons</b>			
Kinetic energy/proton (MeV)	11	60	1.245297
$\gamma$	1.011723676	1.063947321	2.327223788
$\beta$	0.151793839	0.341460409	0.902973359
$\beta\gamma$	0.153573421	0.363295888	2.101421081
Momentum (GeV/c)	0.144093687	0.340870468	1.971705191
Magnetic rigidity (Tm)	0.480644803	1.137021493	6.576900581
Revolution time (s)	1.56E-06	.69358E-06	.26228E-06
Revolution frequency (MHz)	0.6409	1.4418	3.8127
Norm. horiz. rms emit. (pi mm mrad)	0.40	not known	not known
Norm. vert. rms emit. (pi mm mrad)	0.40	0.40	0.40
Geom. horiz. rms emit. (pi mm mrad)	2.60	not known	not known
Geom. vert. rms emit. (pi mm mrad)	2.60	1.10	0.19
Total geom. horiz. emit. (pi mm mrad)	13.02	not known	not known
Total geom. vert. emit. (pi mm mrad)	13.02	5.51	0.95
Full rel. momentum spread	0.0020	not known	not known
<b>Carbon ions</b>			
Kinetic energy/nucleon (MeV)	3	120	425
$\gamma$	1.003222625	1.12890501	1.456538576
$\beta$	0.080088875	0.464040237	0.72707388
$\beta\gamma$	0.080346971	0.523857348	1.059011154
Av. mom./nucleon (GeV/c)	0.074796446	0.48766826	0.985852596
Magnetic rigidity (Tm)	0.498988174	3.253372435	6.576900581
Revolution time (s)	2.9571E-06	.51037E-06	.32573E-06
Revolution frequency (MHz)	0.3382	1.9594	3.0700
Norm. horiz. rms emit. (pi mm mrad)	0.40	not known	not known
Norm. vert. rms emit. (pi mm mrad)	0.40	0.4	0.4
Geom. horiz. rms emit. (pi mm mrad)	4.98	not known	not known
Geom. vert. rms emit. (pi mm mrad)	4.98	0.76	0.38
Total geom. horiz. emit. (pi mm mrad)	24.89	not known	not known
Total geom. vert. emit. (pi mm mrad)	24.89	3.82	1.89
Full rel. momentum spread	0.0020	not known	not known
<b>Constants</b>			
Speed of light in vacuum	2.99792458E+08		
Equivalent proton mass (GeV)	0.9382723		
Atomic mass of H	1.0079		
Elementary charge (C)	1.6022E-19		
No. of charges (Z) for C	6		
No. of nucleons (A) for C	12		

Equiv. C mass (GeV) (approx.)	11.1710		
<b>Comments</b>			
<ul style="list-style-type: none"> <li>- The values of 'given' parameters are shown in bold. All other parameters are derived.</li> <li>- The maximum energy is set by the light-ion requirement of 425 MeV/nucleon (30cm penetr. C6+)</li> <li>- The equiv. C mass is calculated without taking account of the electrons or differences between protons and neutrons.</li> <li>- The maximum energy of the protons is a consequence of the magnetic field needed for the ions and will not be exploited.</li> <li>- The model of a parabolic beam (uniform distribution in phase space) is used, so that :  <math display="block">E \text{ (total)} = 5^{\circ} E \text{ (rms)}</math> </li> <li>- Emittances refer to the injected beam from the linac. <u>No account is yet taken of multi-turn injection or of the emittance to be expected from the resonance.</u></li> <li>- Multi-turning and the resonance will probably only affect the horizontal plane, so the vertical emittance is carried through to higher energies.</li> <li>- 1 Gray = 1 Joule per kg, which for tissue is close to 1 Joule per litre.</li> </ul>			
<b>2. Lattice and Geometry</b>			
Circumference (m)	<b>71.000000</b>		
Effective mag. lgth dipole (m)	<b>1.850000</b>		
Number of dipoles	<b>16.000000</b>		
Bending angle in dipole (rad)	<b>0.392699</b>		
Sagitta (m)	<b>0.090520</b>		
Edge focusing	Rectangular		
Nominal field for protons (T)	<b>0.1020</b>	<b>0.2414</b>	<b>1.3961</b>
Nominal field for ions (T)	<b>0.1059</b>	<b>0.6906</b>	<b>1.3961</b>
Bending radius (m)	<b>4.710986316</b>		
Effective mag. lgth quadrupole (m)	<b>0.35</b>		
Max. field gradient (T/m)	<b>3.68</b>		
Drift space for ES (m)	<b>1.7</b>		
Drift space for MS (m)	<b>3.82</b>		
Drift space for rf (m)	<b>3.82</b>		
Drift space for injection (m)	<b>3.2</b>		
<b>3. Irradiation data (approx. physical doses)</b>			
Max. dose rate for small volumes (<50 cm <sup>3</sup> )	<b>40 Gy/min</b>		
Max. dose rate for large volumes (5–2000cm <sup>3</sup> )	<b>10Gy/min</b>		
Normal dose rate	<b>5Gy/min</b>		
Parameter	1st extraction	Top extraction	
<b>Protons</b>			
Energy (MeV)	<b>60</b>	<b>220</b>	
Range (cm)	<b>3.5</b>	<b>30</b>	
No. of particle/s to deliver 40Gy/min	<b>6.93E+10</b>	<b>1.89E+10</b>	
No. of particle/s to deliver 10Gy/min	<b>1.73E+10</b>	<b>4.73E+09</b>	
No. of particle/s to deliver 5Gy/min	<b>8.67E+09</b>	<b>2.36E+09</b>	

---

Carbon Ions	120	425
Energy/nucleon (MeV)	120	425
Range (cm)	3.5	30
No. of particle/s to deliver 40Gy/min	2.89E+09	8.16E+08
No. of particle/s to deliver 10Gy/min	7.22E+08	2.04E+08
No. of particle/s to deliver 5Gy/min	3.61E+08	1.02E+08

---

---

**Index**

Achromatic arc	110-114
Aperture considerations	103
Betatron acceleration, basic theory	186
Betatron acceleration, proposed parameters	187-188
Betatron acceleration, to "feed" resonance	184-189
Betatron oscillation	8
Betatron phase	8
Bucket parameters, variations of	166
Bunch rotation	5
Chromaticity and resonance control by sextupoles, combined scheme for	23-24
Chromaticity control by sextupoles	22,115
Coupling by sextupoles	75,116
Debunching, memory of rf structure	205
Diffusion equation	131
Diffusion theory	130-142
Diffusion, in an accelerator beam	138-142
Diffusion, thermal	136
Diffusion, with perturbations	137
Distribution of the extracted beam	93-94
Duty factor, spill uniformity	128-129
Electrostatic septum, action of	61-62
Electrostatic septum, effective thickness	43-44,219-220
Electrostatic septum, gap opened by	62
Electrostatic septum, position of	103-106,115-116
Emittance	74-90
Emittance (transverse) for a continuous spill	77-78
Emittance (transverse) of the spill, global view	76-81
Emittance (transverse) with a transport mechanism	80-81
Emittance, control of	85
Emittance, effect of resonance wobble	81
Emittance, in real and normalised coordinates	10
Emittance, maximum that can be extracted	82-84
Emittance, Monte Carlo simulation	91-96
Emittance, statistical	78
Empty-bucket, channelling or stabilisation	144-145
Equilibrium orbits for off-momentum particles	39
Extraction on half-integer resonance	206-207,213
Extraction plots	122
Extraction schemes in SPS	209-221
Extraction, SPS stochastic and "combined"	201-204
Feedback on spill	196-200
Fixed points	29-30
Fixed points, motion close to	36
Gantry, relaxing the equal-emittance requirement	86-90
Hamiltonian	28,82-83

---

Hardt condition	38-56
Hardt condition, mathematical formulation	47,56
Hardt condition, reasons for	45
Hardt condition, role of the normalised dispersion	52-53,120
Homogenising the stack	5
Lattice, 'square' type	107,123-124
Lattice, arc type	107,110-119
Lattice, extended-bump type	107,125-126
Lattice, proposed	114-119
Layout of aperture	103
Leaky rf buckets, due to phase modulation	165
Losses at the electrostatic septum	43-44
$m_{13}$ and $m_{23}$ , effect of being non-zero	67-68,120
$m_{13}$ and $m_{23}$ , expressions for	60
$m_{13}$ minimisation	69-73
Magnetic septum, position of	104,115-116
Medical synchrotron, classification	98
Micro-bucket rf transfer system to "feed" the resonance	170-183
Micro-bucket transfer, tentative parameters	178-179
Micro-bucket, proposed equipment parameters	181
Momentum spread in extracted beam	99
Moving the stack or the resonance	100
Normalised coordinates	8-11
Normalised dispersion, angle of vector for Hardt condition	102,120,121
Particle energy during the passage of an empty rf bucket	157-158
Phase displacement acceleration	150-169
Phase displacement acceleration to "feed" the resonance	170-183
Phase displacement acceleration, effect of rf noise	164
Phase displacement acceleration, particle scattering during	164
Phase displacement acceleration, simulation	159-163
Phase displacement acceleration, stack profiles	167-168
Phase displacement of a stack by a single rf bucket	154
Phase displacement, proposed equipment parameters	181
Phase displacement, tentative parameters	176-177
Phase space map, of particle motion	36,212,213
Phase-space representation of a beam	39-40
Phase-space representation of the resonance	41-42
Phase-space trajectories near a stationary rf bucket	156
Phase-space trajectories round an accelerating rf bucket	155
Resonance and chromaticity control by sextupoles, combined scheme for	23-24
Resonance cancellation and reinforcement between sextupoles	22
Resonance, ideal optics for	102
Resonant extraction, diagrams	4,5,99,100,101,191
Ripple, effect on separatrices	221
Ripple, in momentum and phase	192
Ripple, low-frequency spectra	193
Ripple, types and frequency ranges	128
Rotation of dispersion vector	89

Rotation of normal mode rotation	87-89
Separatrices	29-31
Separatrix equation, expressed with its momentum dependence	46
Separatrix, action during a slow extraction	79
Separatrix, general equation	32-33
Separatrix, geometry for extraction	48-51,96
Sextupole between electrostatic and magnetic septa, effect of	71
Sextupole coefficient in MAD	16
Sextupole strength, $S$	16
Sextupole, amplitude and phase changes following a kick	17
Sextupole, equivalent virtual sextupole for a distribution	20-21
Sextupole, field	13
Sextupole, locking action	17-18
Sextupole, sign convention	14
Sextupole, simple theory for action of	25-27
Sextupole, stopband	19
Sextupole, thin-lens kick	14
Shadow regions	43-44,219-220
Size of the stable triangle, $H$ and $\delta Q$	31,56
Slow extraction with empty-bucket channelling	144-145
Slow extraction, comparison of longitudinal techniques	147
Slow extraction, from PS	143
Slow extraction, with a noisy bucket	146
Spill structure with phase-displacement and micro-buckets	180
Spill uniformity in extraction from SPS	195
Spill uniformity, duty factor	128-129
Spill uniformity, feedback	196-200
Spill uniformity, magnification of fluctuations by resonance	194
Spill, decoupling from ripple (mechanical analogy)	129
Spiral step and kick	6,27,55,56
Spot size at gantry nozzle	90
Stability of the waiting beam	54
Stable triangle	29-31
Stable triangle, at the sextupole	35
Stable triangle, emittance	31
Stable triangle, shift of origin	32,41
Stacking in coasting beam storage rings	150-152
Steinbach diagram	99
Time structure of an extracted beam	94,96
Transfer matrix for particles with a momentum deviation	59
Transfer matrix in normalised coordinates	11
Transfer matrix, in real coordinates	11,58
Transfer from electrostatic to magnetic septum	64-67
Transport mechanism	5
Uniformity of waiting stack	205
Vector potential in an accelerator magnet aperture	12

